Title
The Role of FUN in Sexual Differentiation and Leaf Development in Zea mays

Author
Vajk, Angus Hugo

Publication Date
2019

Peer reviewed|Thesis/dissertation

The Role of FUN in Sexual Differentiation and Leaf Development in *Zea mays*

By
Angus Hugo Vajk

A dissertation submitted in partial satisfaction of the
requirements for the degree of
Doctor of Philosophy
in
Plant Biology
in the
Graduate Division
of the
University of California, Berkeley

Committee in Charge:

Professor Sarah Hake, Chair
Professor Michael Freeling
Professor Barbara Baker
Professor Nicole King

Spring 2019

Abstract

The Role of FUN in Sexual Differentiation and Leaf Development in *Zea mays*

by

Angus Hugo Vajk

Doctor of Philosophy in Plant Biology

University of California, Berkeley

Professor Sarah Hake, Chair

While most angiosperms bear hermaphroditic flowers, *Zea mays* bears male and female flowers on separate inflorescences. Grasses have leaves that possess a sheath, ligule, auricle and blade. This Thesis describes a pleiotropic mutant named *fun* in *Zea mays* that bears female flowers where male flowers are expected; and deletes the auricle in adult leaves. Analysis of the interactions between *fun* and other leaf mutants allow the tentative construction of a developmental pathway including FUN. Double mutant analysis with other sex determination and leaf mutants is presented, demonstrating that the mutation is likely to be involved in multiple hormone pathways, displaying synergistic double mutant interactions with both Jasmoinc Acid and Brassinosteroid mutants. Steps towards creating an antibody to the causative gene are described, and the protein is found to be nuclear localised by YFP fusion and bioinformatic analysis. The FUN gene is found to be conserved in plants and highly conserved in the grasses.

CONTENTS

Acknowledgements

Impossible as it is to get the full scope of everyone who contributed to this, I better start with my own students. Kitae Kim, Kelatzli Mendoza, Miles Cheng and Steve You all gave up their valuable time to help with the research presented in this work. The rest of the team in the Hake Lab were likewise indispensible. Special mentions to China Lunde Shaw for making the lab run smoothly and for all her advice on how to get things done; George Chuck for starting the project and mentoring me through it; Sam Leiboff for teaching me how to talk to computers; Jazmin Abraham Juarez for her help in protein isolation and detection; Katsutoshi Tsuda for his help in RNA isolation and the building of RNA libraries; Emilio Corona for field set up and also making the lab run smoothly; my fellow Graduate Students Martin Alexander, Brianna Haining, Alyssa Anderson, and Nanticha Lutt for keeping spirits up; as well as Graduate Students Iman Sylvain, Thai Dao, Emma Kovak and Akiko Carver for doing the same outwith the lab; and of course Sarah Hake herself who believed in me when others did not and got me through and encouraged me.

I'm also indebted to the staff of the PGEC and the greenhouse without whom my work would never have gotten done. Alex in the mailroom, Lia in the greenhouse and De and Tina on the microscopes – thank you all. My friends in the Bay who supported me including Kyle Futrell, Moises Galvan, Jason Williams, the Livermores, and Katherine Yagle, youse all kept me going when I felt like it was all too much and provided distractions when it actually was too much.

My family, though they couldn't be with me while writing and working, gave support from afar and it goes without saying that I couldn't have written this work without them and their support. My parents Judith née MacDougall and Hugo Vajk always let me follow my heart, mind and soul and without that anarchistic ethic I never would have pursued this PhD. My sisters Mairi and Shona were always there for a laugh when I needed one, as were my extended family Grami Barbs and the Vajks, Auntie Mad and the Campbells, Grandpa Dave and the MacDougalls. Also I want to mention my adopted family of Ruth MacIntyre, Sarah-Anne Gowdie, Euan MacLaren, Andrew McPherson and Simone Bowie.

Finally, I'd like to thank Alexandra Elbakyan for setting up the repository SciHub to allow free access to scientific papers, which was essential for me in my research, and give a thought to Aaron Schwarz, who died for the same cause. The tyranny of private property will kill us all if we do not overthrow the parasitic landlords of the mind.

Chapter I

Sex Determination in Plants

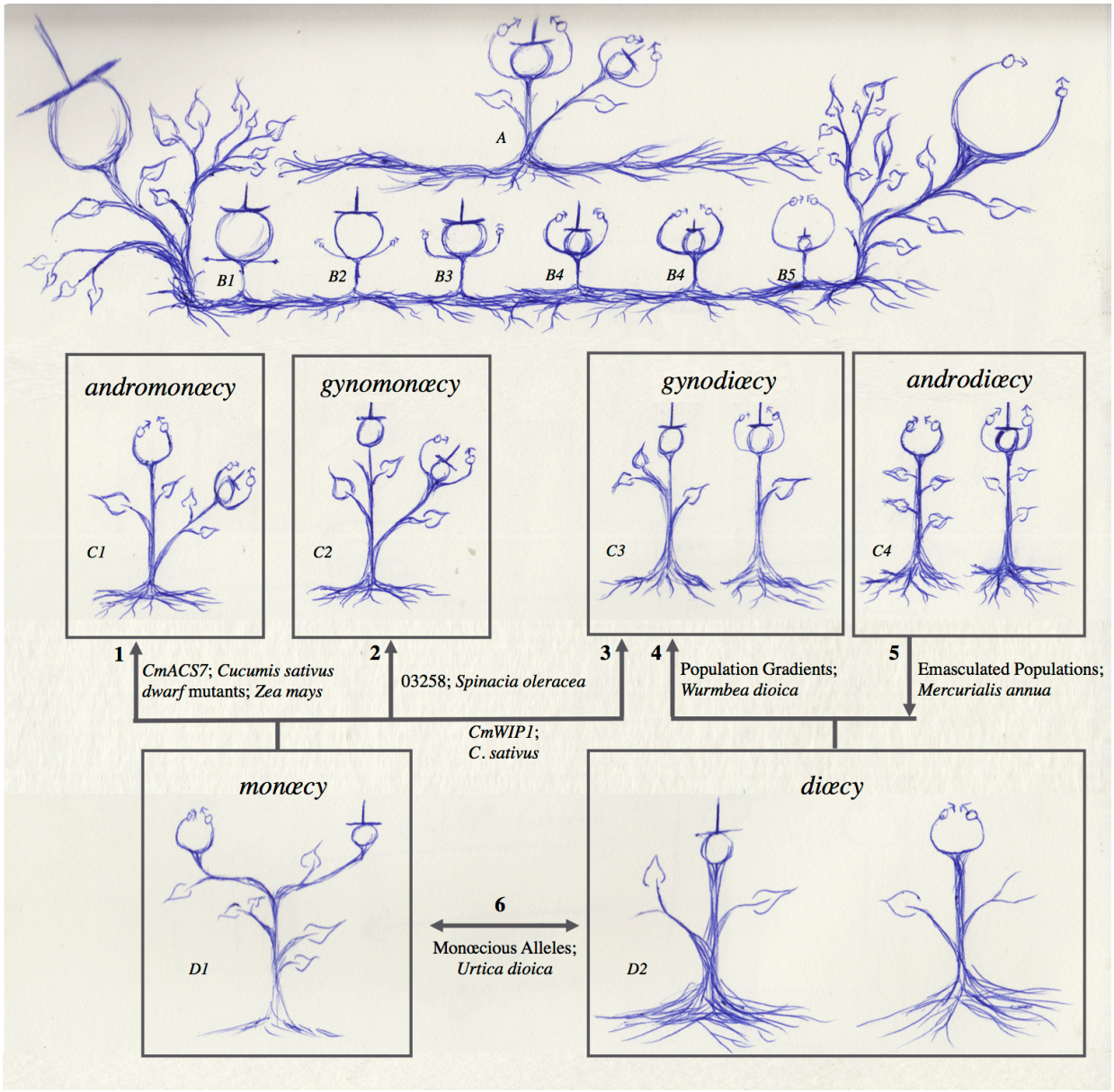

Figure 1-1: Evolution of Sexual Forms in Angiosperms

Legend for Figure 1-1

The ancestral state of angiosperms is thought to be a perfect flower (A). Through selective pressures to promote outcrossing, protandry and protogyny (B) develop. Read left to right, B shows a developmental sequence illustrating protogyny – the female form is expressed first and the stamens do not develop until later; read right to left B shows a flower displaying protandry – the stamens develop first, and the gynoecium develops later. This separation of male and female developmental pathways is theorised to allow the sexes to begin to evolve separately. C shows the primitive forms of monoecy and dioecy – C1 shows andromonoecy; C2 gynomonoecy; C3 gynodioecy; and C4 androdioecy. Over evolutionary time, a perfect flower could go through stages similar to those detailed in B to produce a single sex flower, these stages could occur stepwise as they are shown to in B, or be the result of a single mutation that deletes male or female function in some flowers on the plant (andro- or gynomonoecy) or the evolution of a segregating allele that makes half of the plants in the population produce some male or female flowers (gyno- or androdioecy). Once some flowers in the population have committed to either sex, there arises an evolutionary pressure for the remaining hermaphroditic flowers to commit to the other sex since (e.g.) a hermaphroditic flower in a gynodioecious population will struggle to compete in female function as compared to a flower that has committed all of its resources (and possibly form) to maximising seed set. Said hermaphroditic flower will thus emphasise pollen production, rendering the plant truly dioecious (D2), as has been demonstrated in *Wurmbea dioica* (arrow 3). Gyno- and andromonoecy will tend toward true monoecy in a similar fashion. Mutations and population studies have given us examples of these transitions in living angiosperms (arrows). Knockouts of *CmACS7* in *Cucumis sativa* and of *D9* in *Zea mays* (see Chapter 3) render monoecious wild type plants andromonoecious (arrow 1). The *Spinacia olearacea* cultivar 03258 is gynodioecious, while most other spinach cultivars are monoecious (arrow 2). Androdiecious *Mercurialis annua*, when relieved of the selective pressure of males in the population, enhances pollen production in hermaphroditic plants, implying the wild populations are tending toward dioecy (arrow 4). Monoecious and dioecious plants are to an extent interconvertible (arrows 5 and 6) – knockouts of *CmWIP1* in the monoecious *Cucumis sativa* (arrow 5) creates exclusively female plants producing a gynodioecious population. Some populations of dioecious *Urtica dioica* harbour sex alleles that allow the creation of monoecious plants (arrow 6), though it is unclear which would be the ancestral state, this observation makes it clear that monoecy and dioecy may interchange over evolutionary time.

Introduction

Unisexual flowers are the exception in angiosperms; the vast majority of flowering plants bear hermaphroditic (prefect, bisexual) flowers that have both pollen producing stamens and ovule-containing ovaries (Figure 1-1A). Nevertheless, a substantial number of angiosperms (between 3 and 20%, depending on the locality of the flora and sampling methods[1–3]) produce non-hermaphroditic (imperfect, unisexual) flowers. In a recent (2014) data analysis, 5-6% of plant species were found to be dioecious, but 43% of plant families were shown to contain dioecious members[4]. The rarity of dioecy at the species level, coupled with its widespread occurrence across the angiosperm lineage, shows that dioecy must have evolved multiple times. In this chapter, we will first discuss the possible benefits and costs to producing imperfect flowers, before considering the likely routes evolution has taken to produce these floral types, and the molecular mechanisms that underlie the development of imperfect flowers. Through a sequence of case studies, this chapter will detail a likely route that an ancestor bearing perfect flowers could take to arrive in the derived states of dioecy and monoecy, through the intermediary steps of protogyny and protandry; andro- and gynomonoecy; and andro- and gynodioecy (Figure 1-1).

Pros and Cons of Imperfection

A historical theory for why imperfect flowers might be beneficial was that it could promote outcrossing. Clearly a dioecious species is an obligate outcrosser, since the male and female flowers exist on separate plants. However, it is not so clear that this would be true for monoecious plants. It was hypothesised that if monoecy were to promote outcrossing inherently, monoecious plants would not have to rely on other costly mechanisms to promote outcrossing such as molecular self-incompatibility (SI). Studies have not shown this to be the case, indeed monoecy is just as common in self-compatible (SC) species as it is it in SI species[5], though of course this does not rule out the possibility that avoiding self-fertilisation could still be a factor in the evolution of imperfect flowers, especially for dioecious plants.

Instead of making a theory and trying to find data to support it, it is more fruitful to look at the natural world and make a theory to explain it. For this, we might ask: “what kinds of plants are likely to bear imperfect flowers?”. Analysis of large datasets has shown that species with imperfect flowers are likely to be viniferous or woody, wind-pollinated plants with small green flowers, and for dioecious plants, the bearing of fleshy fruits[2]. One theory proposed by Bertin to explain enrichment in wind-pollinated plants is the relatively low cost of their flowers (no need for nectar or showy petals) allows for monoecy to develop. Monoecy is more expensive than perfection because a plant with unisexual flowers will have to produce two sets of flowers where a

single perfect flower would suffice, thus Bertin argues, it is only when flowers are relatively cheap that monoecy can be permitted[5].

Bertin's theory does not explain why monoecy might be desirable, instead it merely states why it might not be punished. Since monoecy is not uncommon in plants, there must be some kind of advantage. Again, we should turn to direct observations of the natural world to explain this. As we have seen, wind pollinated plants are more likely to evolve monoecy than insect pollinated. Indeed, all gymnosperms are wind pollinated and can be thought of as dioecious or monoecious since they bear micro- and macrostrobili. When we consider the flowers of a wind pollinated angiosperm tree such as hazel, the benefit of the separation of the sexes becomes immediately apparent. The benefit is specialisation. Male hazel inflorescences hang from the branch; their primary role is in dispersal of gametes and their hanging habit allows for the efficient dispersal of pollen by the wind. On the other hand, the primary role of female flowers is the reception of gametes – female hazel flowers fulfil this end by having tentacle like protrusions that catch pollen from the air. Insect pollinated plants have no such need for specialisation – in fact they need the same insects to visit both the male and female flowers. While Bertin's theory[5] may explain how monoecy is permitted, the advantages bestowed by specialisation explains how it can become fixed.

It has further been proposed that pistils that are separated from stamens might be more effective in being pollinated because they avoid "pollen interference"[6]. Self-pollen could clog the tip of the pistil, stopping pollen from other plants from reaching into the stigma. It could also begin to grow down into the stigma and even if it is stopped at the micropyle the pollen tubes could partially or completely block the micropyle, again interfering with fertility mechanistically. This would be especially true for wind-pollinated plants that produce copious amounts of pollen that fills the surrounding environment, fitting with the observation that wind pollinated plants are more likely to have imperfect flowers. Despite the elegance of this theory, it remains to be confirmed, and studies in gynodioecious *Plantago maritima*[7] and representatives from the Lamiaceae[8] failed to find evidence for an female advantage due to lack of interference from self-pollen.

Finally, the potentially high cost of female flowers has been suggested as a driver towards imperfection[2]. Hermaphroditic flowers must produce (a) nectar, petals, sepals etc., (b) stamens, (c) ovules and (d) fruits and seeds. A male flower must produce a + b, while a female flower must produce a + c + d. Even if the fruits and seeds are aborted at some stage, there is still the cost of their inception, for example the monoecious *Cucumis spp*. make fairly large pre-fruits on their female flowers long before pollination. When fruit and seeds are especially large (recall that fleshy fruits is a predictor for dioecious plants[2]), unisexual flowers can allow a plant to produce pollen without committing large reserves of resources to ovules, fruits and seeds. As we shall see,

andromonoecy is more common than gynomonoecy, which fits with this theory.

Case Studies and the Route to Imperfection

The dogma of evolutionary theory states that change must occur by incremental mutations. If our starting point is a perfect flower as seen in most angiosperms and the basal *Amborella trichopoda* and Magnoliidae, and the unisexual flower is the derived state what are the intermediary steps from hermaphroditic flowers to a monoecious or dioecious species? Protogyny and protandry, andro- and gynomonoecy, along with andro- and gynodioecy, present themselves as intermediaries between perfection and monoecy or dioecy. Almost all of these states have been shown experimentally to be intermutatable. Once these states arise, they can remain environmentally plastic, or become fixed: in monoecy by the evolution of strict developmental pathways; and in dioecy by the evolution of autosomal sex determining loci or true (heterochromatid) sex chromosomes.

Figure 1-2: Protandry in Apiaceae. Stamens come out first in these perfect flowers (A, F, G [upper]). Small stigma can be seen emerging from the centre of the F while the stamens are fully extended. In E, the stigma are more fully extended and the stamens have fallen off, see also B. The underside of later stage flowers (C, G [lower]) have enlarged carpels which continue to grow (D), eventually to produce the fruit of this plant.

Protandry and Protogyny

One of the first steps towards unisexual flowers is thought to be the temporal separation of male and female function in hermaphroditic flowers[6,9] (see Figure 1-1B). This separation is most often thought of as a strategy for promoting outcrossing and/or reducing pollen interference[2]. The temporal separation of the sexes allows them to begin evolving as separated pathways, and can eventually lead to true unisexual flowers.

Andromonoecy – *Chaerophyllum bulbosum*

C. bulbosum is an annual from the Apiaceae common by riversides in Europe. The plants are andromonoecious – bearing both hermaphroditic and male flowers in their umbelliferous inflorescences. Andromonoecy is common in the

Apiaceae, and appears to have evolved multiple times from dioecy within this group[10]. Some Apiaceae are protandrous (see Figure 2), highlighting the role this sexual form may play in the evolution of andromonoecy. *C. bulbosum* has been shown to respond to damage and pollination restriction by increasing its ratio of hermaphroditic to male flowers in order to ensure seed set[11]. Thus, this plant is able to respond to environmental cues by changing its sex ratios to enhance reproductive success. Andromonoecy is thought to be a more common first step towards monoecy than gynomonoecy because the benefits of avoiding commitment to female flowers is more obvious, as discussed above.

Androdioecy – *Mercurialis annua*

In androdioecious populations, both hermaphroditic and male plants exist. It has been proposed that in such a situation, the population will naturally tend toward true dioecy because hermaphroditic flowers cannot compete with the high pollen production of exclusively male flowers and will therefore tend to become more female. While this has not been shown experimentally, the inverse has. By removing all male plants from a population of *M. annua*, pollen production by the hermaphroditic plants was shown to increase over 3 generations as compared to the control group[12], implying that the hermaphroditic flowers are compensating for a lack of pollen. This implies that the hermaphrodites in the wild, unmanipulated populations are restricting their pollen production and perhaps also enhancing female function as a response to the males in their population. This may mean that *M. annua* is providing us with a snapshot in evolutionary time of a species on its way towards evolving dioecy (Figure 1-1, arrow 5).

Gynomonoecy - Asteraceae

Gynomonoecy, where plants bear female and hermaphroditic flowers, is a very rare sexual state. In a survey of Occupied Palestine, Sinai and Jordan, only 0.4% of plants were listed as gynomonoecious[2]. Further, most gynomonoecious plants are of the Asteraceae, where female ray florets surround perfect disc florets. It is not likely that the femininity of these ray florets underlies their evolution and maintenance – rather it seems that these are specialised flowers that serve as pollinator attractors[13]. Overall, gynomonoecy has been understudied as a sexual system in plants, partially due to its rarity and partially because it is not thought to be important as a sexual system. Gynomonoecy does appear in domesticated species such as cultivars of *Spinacia olearacea*, which is usually monoecious[14], showing that gynomonoecy represents a possible route between sexual systems in plants (Figure 1-1, arrow 2).

Gynodioecy – *Wurmbea dioica*

Given the rarity of gynomonoecious species, it is perhaps surprising that gynodioecious species are so prevalent. Perhaps specialising as female on a separate plant is more beneficial than doing so on the same plant. Further,

gynodioecy could be useful in agriculture, for example with dates or kiwis where males must be planted alongside females for fruitset – if these crops were made gynodioecious, the pollen producers would also bear fruit. Gynodioecy, where hermaphroditic and female plants exist in a population, is thought to be an important step in the route between perfect flowers and dioecy. It has been well demonstrated that the presence of female plants in a population induces the co-occurring hermaphrodites to enhance their male function[15], further corroborating the results of the *M. annua* study[12] described above. In *Wurmbea dioica* populations sampled across the Australian continent, varying degrees along a gynodioecious to dioecious spectrum were observed[16], implying that dioecy in this species evolved via this pathway (Figure 1-1, arrow 4).

Monoecy

Monoecy in *Zea mays* is rigidly controlled with an apical male inflorescence and axillary female inflorescences. This is not simply a relic of domestication – teosinte also bears its female inflorescences laterally to its male inflorescences. Likely, this spatial separation and elevation of the male tassel enhances the specialisation of these inflorescences. Monoecy does not have to follow this strict habit though. In *Cucumis spp*. the flowers alternate unpredictably between male and female along the shoot. Another vine, *Freycinetia funiculari*, preferentially makes male flowers early in its life before switching to female flowers later in development[17]. Postponing growth of female flowers makes sense because of the greater resource investment required, especially for vines which may spend years beneath the canopy waiting for full sun.

Charlesworth and Charlesworth (1978) briefly discuss the evolution of monoecy. They argue convincingly that monoecy must evolve from hermaphroditism through a series of at least two mutations, through the intermediary steps of gyno- or andromonoecy. Charlesworth and Charlesworth further postulate that these genes would have no tendency to be linked, unlike the mutations leading to dioecy which must be linked[18]. Confirmation of this theory comes from Erin Irish's work in stacking the maize mutations of the *tasselseed* and *dwarf* class. The *tasselseed* mutants fail to abort the silk in the male tassel, rendering them female; and the *dwarf* mutants restore perfection to the female flowers. Together these two mutations change the monoecious maize plant into a plant that bears only perfect flowers[18]. Singly, the *dwarf* mutants in *Zea mays* and the *CmACS7* mutant in *Cucumis sativus* are capable of changing these monoecious plants to andromonoecious plants, showing this rote of evolution of monoecy (Figure 1-1, arrow 1). The *Cucumis sativus* mutant *CmWIP1*[19] represents a change from monoecy to gynodioecy (Figure 1-1, arrow 3) suggesting a route from monoecy to dioecy.

Monoecy is able to convert to dioecy, as shown by the high number of monoecious families containing nested dioecious species[9] but I believe it would be a mistake to consider monoecy merely a stepping stone to dioecy. Unlike

dioecy, monoecy allows plants to retain their ability to be both mothers and fathers, but allows specialisation of floral forms that is so crucial for wind pollinated plants. From a human perspective, monoecy has been a powerful tool in the genetic manipulability of *Zea mays*, allowing both hybrid crops and extensive genetic research in the modern era (and pre-historically too, no doubt).

Dioecy – the end of the road?

As we have seen, gyno- and androdioecy lead towards dioecy. When plants in a population become sex specific, there is an evolutionary pressure for hermaphrodites to specialise in the other direction thereby producing a dioecious population. Dioecy can also evolve from monoecy, as predicted by dioecious species nested within monoecious evolutionary groupings[9]. Simple dioecy is not the end of the road – it can become more and more fixed and derived as evolutionary time proceeds. It is thought that at first dioecy is characterised by simple sex determining regions (SDR) in the genome. These will often be clustered on a single autosome as is the case in *Populus balsamifera*. In this species, an SDR has been described on chromosome 19[17]. This region includes 13 genes, one of which is a paralogue of methyltransferase1 (MET1). Another gene within the region is a cytokinin signaling gene *PbRR9* and methylation of this gene (perhaps by the adjacent MET1 paralogue) is predictive of sex of the tree[21]. *P. balsamifera* is therefore a less derived dioecious species which still relies on epigenetic modifications for its sex determination loci that reside on autosomes.

Cannabis spp. on the other hand has true sex chromosomes that exist as a heterochromatic pair where XX defines female and XY defines male[22]. *Cannabis* was known in the literature to be under XY control as early as 1927[23] when female plants were damaged by having branches removed at an early stage of blooming, giving rise to male flowers, allowing the plants to be selfed. The selfed female intersexed plants gave rise to all female progeny. Similar techniques are still used today to give feminised seed[24]. The fact that simple mutilation gives rise to the development of male flowers on genetically female plants shows that each plant has the genetic capacity to produce either sex, while the XY chromosomes dictate which pathways are activated. Interestingly, damage activates maleness, perhaps because a damaged plant producing pollen still has a chance of reproduction, while a damaged plant is not likely to be able to produce healthy seed, which is costlier than pollen. Diverting to maleness can thus be thought of as an insurance policy.

The story of dioecy does not end with the evolution of sex chromosomes. *Urtica dioica* has an SDR[25], but while the name *U. dioica* implies dioecy, monoecious plants have been reported in the Netherlands and other parts of Europe[26]. Further, *U. dioica* does not always follow a 1:1 male:female ratio in its naturally occurring populations. Thus, it seems clear that *U. dioica* does not follow a simple XX/XY or ZW/ZZ mode of sex determination. It has been

proposed that there are in fact four alleles of a single sex determination locus in *U. dioica*.

Self-pollination of monoecious *U. dioica* individuals yielded a 1:2:1 ratio of male:monoecious:female individuals. This is consistent with a bi-allelic model where heterozygotes are monoecious and the two homozygotes yield male or female plants. When a true female plant is crossed with a monoecious plant, a 1:3 monoecious:female ratio is observed in the offspring. If the female were homozygous and the monoecious were heterogametic, we would expect a 1:1 monoecious to female ratio; instead partial dominance of the dioecious female allele is proposed, leading to the $A^{M}a^{D}$ plants being half female and half monoecious. When a male plant is crossed to a monoecious plant, a 3:1 male:female ratio is produced. This is consistent with the male plant being heterozygous. Further, crosses between male and female plants did not yield simple 1:1 male:female ratios, suggesting the existence of sex selection biases at some point in the developmental process[26]. Thus, dioecy is not the end of the road, and return to monoecy can occur by surprising routes (see Figure 1-1, arrow 6; and see Figure 1-2 for graphical explanation of *U. dioica* sex loci).

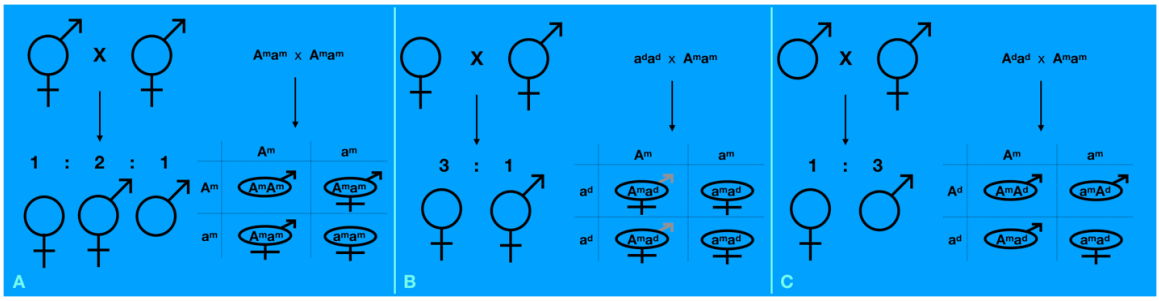

Figure 1-3: Pictorial summary of multi-allelic sex determination in *Uritica dioica*. Big A represents male allele, small a represents female allele, superscript ^{m} denotes that allele is monoecious type, superscript ^{d} denotes allele from dioecious type.

Canonical Plant Sex Hormones?

Not only has almost every plant hormone been implicated in sex determination in plants, but their roles are often not consistent across plants. While gibberellic acid (GA) promotes female inflorescence development in *Zea mays*[27] and *Cucumis spp.*[28], applications of GA are capable of masculinising female *Cannabis* plants[29]. Blocking brassinosteroids (BR) in the monoecious *Cucurbita pepo* increased male flower production[30], while BR knockouts in maize are feminised[31]. Similarly, while jasmonic acid (JA) is involved in stress induced male sterility in *Arabidopsis thaliana*[32] and *Oryza spp.*[33], it plays a vital role in gynoecium abortion in *Zea mays* to allow flowers to develop as male[34–37].

Other hormones are more conserved in their function. Ethylene has been shown to be involved in gynoecium development in the perfect flowers produced by

A. thaliana[38] and tobacco[39] and has been exhaustively shown to be involved in female flower development in the Cucurbitaceae[30,40] as well as being implicated in female flower development in *Cannabis spp*.[24]. Abscisic acid (ABA) promotes female flower development in *Cucumis spp*.[41] and has also been shown to block antheridium development (i.e. promote femaleness) in ferns[42]. Cytokinin is involved in anther development[43], and *Z. mays ZmCKX1* cytokinin biosynthetic mutants develop as male sterile[44], while in *Populus balsamifera,* methylation of a the cytokinin signalling gene *PbRR9* is associated with female trees[21].

In sum, there are two sets of sex determining hormones in plants. One set is directly involved in sex organ development, and this includes ethylene and ABA, which promote femaleness; while cytokinins represent a conserved male promoting hormone. Likely the roles of these hormones are ancient, and they provide avenues for the evolution of unisexual flowers which as we have seen occurs sporadically and frequently across angiosperms. Another set includes JA, BR and GA. These hormones are involved in growth, cell cycle regulation, cell death and cell expansion[45–47], therefore they can be co-opted to produce sex determination pathways in unisexual plants by turning on and off appropriate organ growth. Since they are not historically specific to male or female organ development, their roles as masculinising or feminising hormones are not consistent across angiosperms. The fact that some hormones are ancient and conserved regulators of sex expression and others are non-specific underlines the facts that the flowers of the common ancestor of angiosperms was perfect, but they evolved from the imperfect gymnosperms.

Summary and Conclusions

Sex determination in plants is a highly complex and varied affair. As we have seen, unisexuality has evolved multiple times in angiosperms and thus the hormonal control of this process is partially inconsistent, though consistencies exist because certain hormones are inherently tied to male or female sex organ development. Sex determination is also a highly plastic process in plants; and species that humans call “dioecious” have been observed to produce different floral forms depending on the environment. Further, single mutants can completely disrupt the monoecious or dioecious habit of plants, showing that sex determination in plants is highly labile over evolutionarily time. The presence of single mutants in maize that drastically affect sex determination pathways highlights the plasticity of sex in maize and other plants. My analysis of the pleiotropic mutant *fun* further supports this view of sex and gender fluidity that is observed in plants and animals, calling into question the traditional binary view of sex.

Chapter II

Analysis of the *fun* Phenotype

Abstract

The *feminised, upright, narrow (fun)* mutant was named after its most obvious phenotypes. The tassel is feminised, producing female flowers that produce silks and can be fertilised to produce seed. The leaves lack auricle and have an upright habit, as well as having a narrower blade than normal siblings. Here, I will describe the *fun* phenotype in as much detail as has so far been gathered.

Introduction

Unlike 95% of angiosperms, *Zea mays* is monoecious – having separate male and female flowers or inflorescences on the same plant. The male inflorescence is found at the apex of the corn plant, being the final fate of the apical meristem, and is known as the tassel. From a functional perspective, this placement makes sense as it allows the pollen from these flowers to be efficiently dispersed by the wind. The female inflorescence - or inflorescences for often there are multiple on the same plant - is known as the ear. Ears develop from axillary buds, and are found around the 5^{th}-7^{th} leaf (as counted down from the top of the plant). Along with the obvious differences between these unisexual flowers - the male flowers lack carpels, and the female flowers lack stamens - there are a number of other differences between these inflorescences. The main stem of the ear is noticeably thicker than that of the tassel, likely due to the fact that ears support kernels that are much heavier than the male flowers of the tassel; similarly the internodes subtending the ear are very short and compact, lending further support to this heavy inflorescence. A tassel, while slim, is much longer than an average ear; some of my own measurements from this study exceed half a metre for wild-type tassels – a quarter of the total height of the plant! Spikelets in the tassel bear two florets, while in the ear, the lower floret aborts. Finally a tassel bears secondary and sometimes tertiary branches from its main stem while a normal ear completely lacks branches.

The maize leaf is a fairly typical grass leaf. It has two main parts – the blade and the sheath, separated by the ligule/auricle region. The sheath is the part closest to the stem and wraps around the stem, providing support for the long blade. The ligule, a thin epidermally derived[48] fringe of tissue, exists on the adaxial side at the distal end of the sheath, and perhaps contributes to stemming the flow of water that could carry pathogens into the space between the stem and sheath. The auricle is immediately distal to the ligule consisting of two wedges of tissue that compensate for the angle at which the blade sticks out from the stem and sheath. Finally the blade, the main photosynthetic organ of the maize plant, extends from these basal supporting organs. The maize leaf is further described in Chapter 2.

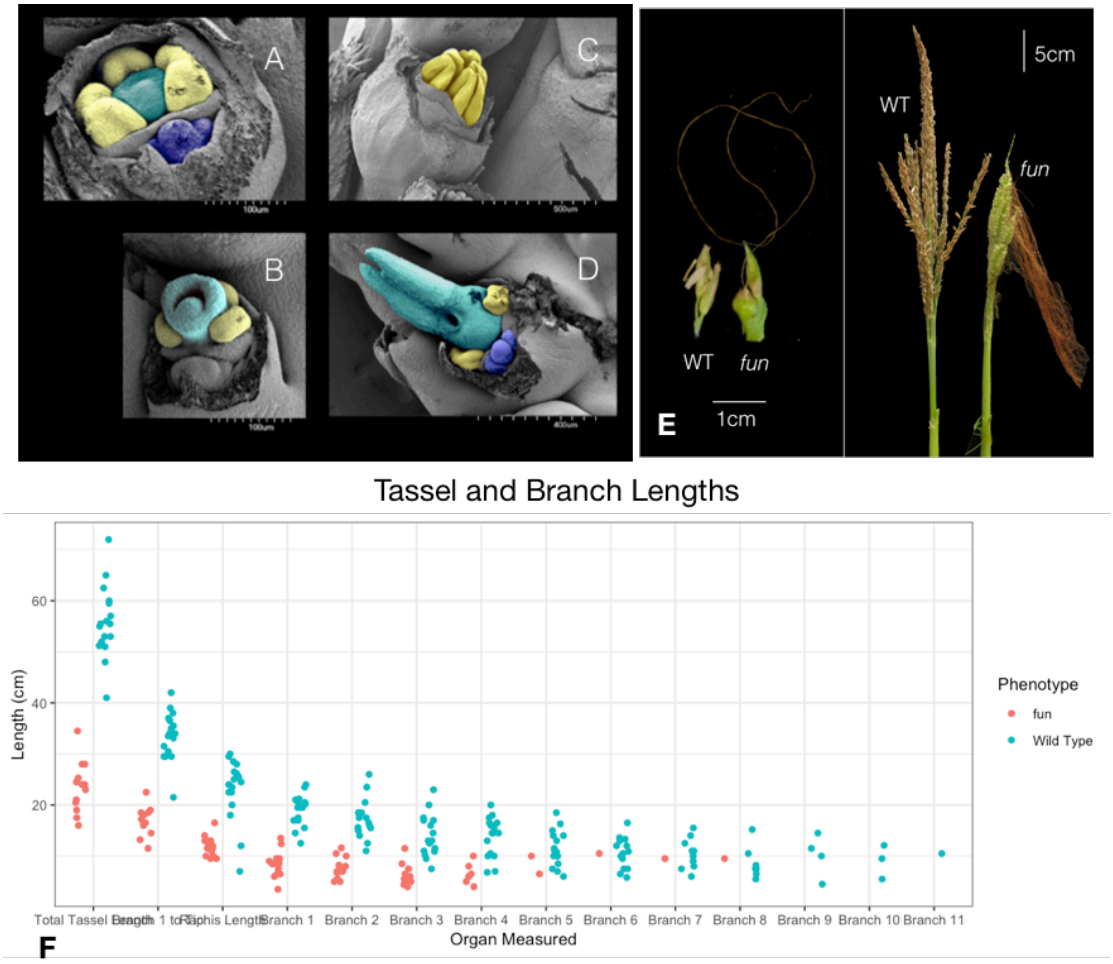

Figure 2-1: Apical Inflorescence Phenotype.
A-D: Electron Micrographs of Developing Tassel Flowers. 12mm (**A, B**) and 18mm (**C, D**) tassels were taken from wild type (**A, C**) and *fun* (**B, D**) plants. Developing flowers on them had their glumes removed in order to see the organs. Stamens have been false coloured yellow, silks in teal and secondary florets in dark blue. **E**: Left: WT and *fun* tassel spikelet pairs. Right: WT and *fun* whole tassels. **F**: Tassel and Branch Lengths. The *fun* tassel is considerably shorter than Wild Type siblings and it makes fewer, shorter branches.

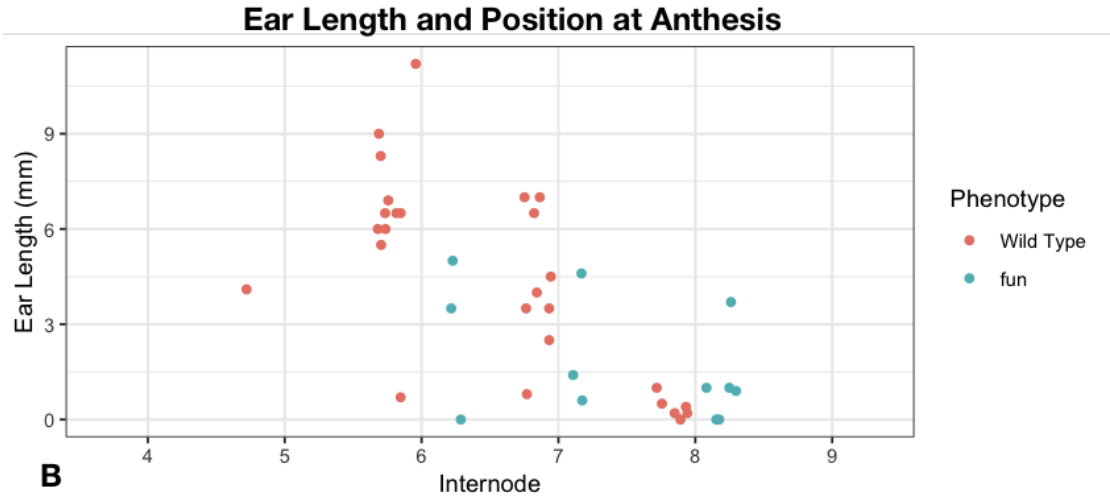

Figure 2-2: Ear Phenotypes. **A**: Open pollinated normal (3 left) and *fun* (3 right) ears harvested at the end of the season. Mutant ears are clearly smaller, but otherwise normal. **B**: Immature Ear Sizes and Location. 15 Wild Type and 15 *fun* plants were harvested when the tassels were shedding and the immature ears measured, with location recorded. WT ears are larger and more numerous – many *fun* plants showed no ears at all, while many WT plants had multiple. The *fun* plants that did have evidence of ears tended to have ears occurring lower on the stalk of the plant than WT plants.

The Feminised Tassel

The *fun* tassel has multiple traits that make it resemble a feminised inflorescence, or, an ear. Just as ears are branchless and shorter than tassels, the *fun* tassel makes half the number of branches as compared to normal siblings and is on average half the length of normal siblings (Figure 2-1F). Shortening can also be seen in the four internodes directly subtending the tassel (Figure 2-4B). Since the ear shank resembles a shortened branch made up of very compact internodes, a reasonable hypothesis would be that the feminisation of the tassel in *fun* results in a signal that causes the subtending internodes to behave as if they are supporting an ear. In support of this hypothesis, the lengths of internodes 5 and below are indistinguishable from normal siblings, implying that only those close to the feminised tassel are affected.

Flowers in the tassel and ear initiate both stamen and carpel primordia, but male flowers abort the carpel and female flowers arrest stamen growth[49,50]. The feminisation of the *fun* tassel flowers appears to arise from an early lack of abortion of the carpel and arrest of stamens, much in the way the flowers in the ear develop in normal maize plants (Figure 2-1A-D). Additionally, ears in *fun* plants progress slower than normal siblings and are displaced lower on the plant (Figure 2-2B). The *fun* ear is smaller than normal siblings (Figure 2-2A).

When considering the feminisation of the *fun* tassel, it is also important to note that it differs from the classic feminisation mutants of *tasselseed1* (*ts1*) and *ts2*. These mutants merely feminise the flowers of the tassel, leaving the branch number, architecture and floret number intact (see Chapter 3). As a result, the *ts* mutant apical inflorescences bend over from the weight of their heavier flowers. In contrast, the *fun* mutant inflorescence is able to maintain the erect form associated with a tassel since it is shortened and has fewer, shorter branches and a thickened rachis to make it more robust and able to support a feminised habit. Further, the *fun* feminised tassel flowers abort the lower floret, while in the *ts* mutants, both florets develop despite the feminisation of the tassel (See Chapter 3, Figure 2-13). When comparing these two mutants, it is possible to appreciate how *fun* is more globally feminised while *ts1;2* are more superficially feminised.

Upright, Narrow Leaves

Although adult *fun* leaves lack an auricle, they retain an obvious line of white tissue over the ligule region that can be observed on the abaxial side of the leaf

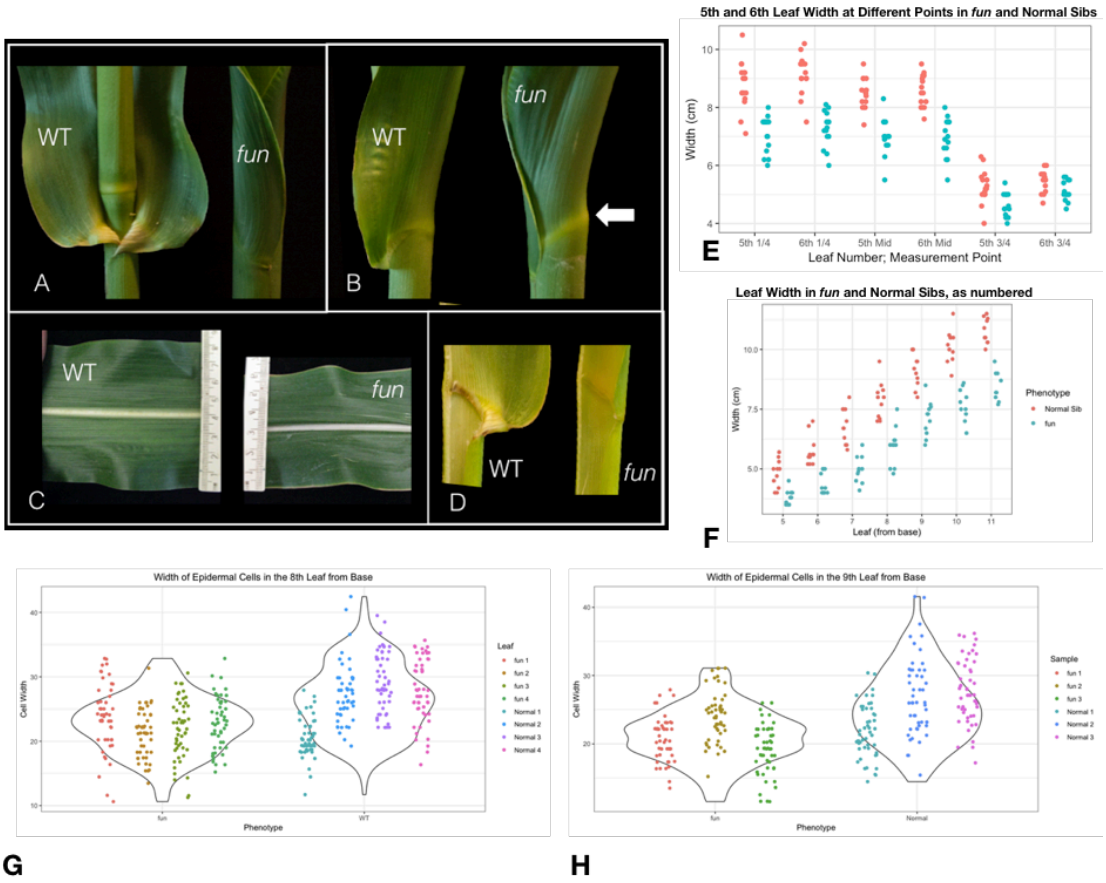
WT
fun
A
B
C
D
5th and 6th Leaf Width at Different Points in fun and Normal Sibs
Width (cm)
5th 1/4
6th 1/4
5th Mid
6th Mid
5th 3/4
6th 3/4
Leaf Number; Measurement Point
E
Leaf Width in fun and Normal Sibs, as numbered
Leaf (from base)
Phenotype
Normal Sib
F
Width of Epidermal Cells in the 8th Leaf from Base
Cell Width
Phenotype
Leaf
G
Width of Epidermal Cells in the 9th Leaf from Base
Sample
H
J
Normal
fun
K
1cm
L
M
N

Figure 2-3: The Leaf Phenotype.
A: Frontal view of ligule/auricle region to highlight the wrapping phenotype of *fun* revealing the importance of a developed auricle in opening out the leaf. **B**: Side view of ligule/auricle region to show that the boundary is still clearly visible, just not associated with auricle tissue. This image also shows the abnormality of the midrib that is wider and more diffuse in *fun* likely contributing of the uprightness of the leaf. A pronounced bump is observed where the midrib intersects the auricle ligule boundary (arrow). **C**: Width of 8th leaf from base, Normal sibling and *fun*. **D**: Adaxial side of wild type and *fun* ligule/auricle region showing that the ligule is unaffected by the *fun* mutation. **E**: Widths of leaves 5 and 6 from the top at various points. Leaves 5 and 6 clearly differ in width at ¼ of the way up the leaf and ½ way up the leaf. At the midpoint and ¼ up the leaf, the mean widths are 17-20% narrower in *fun* than in WT sibs, at the ¾ point they are only 12% and 6% different in the 5th and 6th leaf, respectively. While the difference is not as pronounced at ¾ of the way up the leaf, all these measurements are significantly different in the WT sibs *vs*. the *fun* plants under a MANOVA test at $p<0.02$. **F**: All adult leaves are affected by narrowing in the fun mutant. Measurements are taken at the midpoint. G: Cell sizes of epidermal cells in the 8th leaf. Wild-type siblings have significantly wider cells than fun mutants according to a Wilcoxon t-test ($p=2.7e-12$). The mean width of fun cells is 22.1nm, while wild-type sibs are 25.8nm, making fun cells 15% narrower than wild-type cells. H: Cell sizes of epidermal cells in the 8th leaf. Wild-type siblings have significantly wider cells than fun mutants according to a Wilcoxon t-test ($p=2.7e-12$). The mean width of fun cells is 22.1nm, while wild-type sibs are 25.8nm, making fun cells 15% narrower than wild-type cells. J: transects of the midrib region (cut point shown in **K**). As can be seen in **L**, white pith is restricted to a circular area in the middle of the midrib in wild-type, while the pith spreads out through the horseshoe shaped midrib of *fun*; **M** is an inverted version of **L** to highlight the pith and **N** shows a sketch of this image. E shows the region under light microscopy with the pith (also known as clear cells) showing these two phenotypes.

(Figure 2-3B). *fun* mutants have a leaf angle that is on average 10° steeper in the mutant than in normal siblings. Sometimes flaps of true auricle tissue appear at the margins of the leaf, but they do not seem to be associated with any bending out of the blade and instead fold outward implying that the upright habit of *fun* leaves is controlled by the distortions at the midrib. The ligule itself is unaffected (Figure 2-3D), but the region overall is subjected to a host of distortions as compared to normal siblings. At the midrib, where the blade intersects with the ligule boundary (the midrib ligular knot [MLK]), a pronounced bump is observed in the mutant (Figure 2-3B, arrow). Transects of the blade 1 cm above the ligule boundary (Figure 2-3J,L) reveal a change in shape of the midrib region from a tight triangular shape in normal leaves, to a broadened horseshoe shape that invades the blade tissue adjacent to it in mutants (Figure 2-3L). The clear cells of the midrib (Figure 2-3J) that appear as a white pith to the naked eye are also spread out in this horseshoe shape within the mutant midrib. The correlation of a lack of auricle with this broadening of the midrib may imply antagonistic signalling between these two tissue types as further up the leaf the midrib appears more like wild type. There is an overall distortion in the shape of the plant, presumably due to these auricle distortions, with the whole plant often exhibiting a curving habit not seen in wild type (not shown). Though the following observations have not been quantified, I include them for completeness: the *fun* leaves often appear to be a darker green than normal siblings, and the whole plant seems to senesce earlier at the end of the season.

The leaves of the mutant are on average 20% narrower than normal siblings (Figure 2-3E,F). At a cellular level, the cells of the epidermis are 15-17% narrower than normal siblings, implying that this defect in cell expansion results in the overall narrowing seen in the mature leaves (Figure 2-3G,H). Having smaller cells may be contributing to the darker green phenotype discussed above. Smaller cells would mean a smaller vacuole that would place the chloroplasts closer together, this proximity could lead to a greater intensity of colour, perceived at a distance as an overall darker green colour. Neither the blade nor the sheath was found to differ in length from normal siblings (not shown). All leaf phenotypes are only observed on adult leaves - that is, leaves 5-6 and onward - with juvenile plants being indistinguishable from normal siblings.

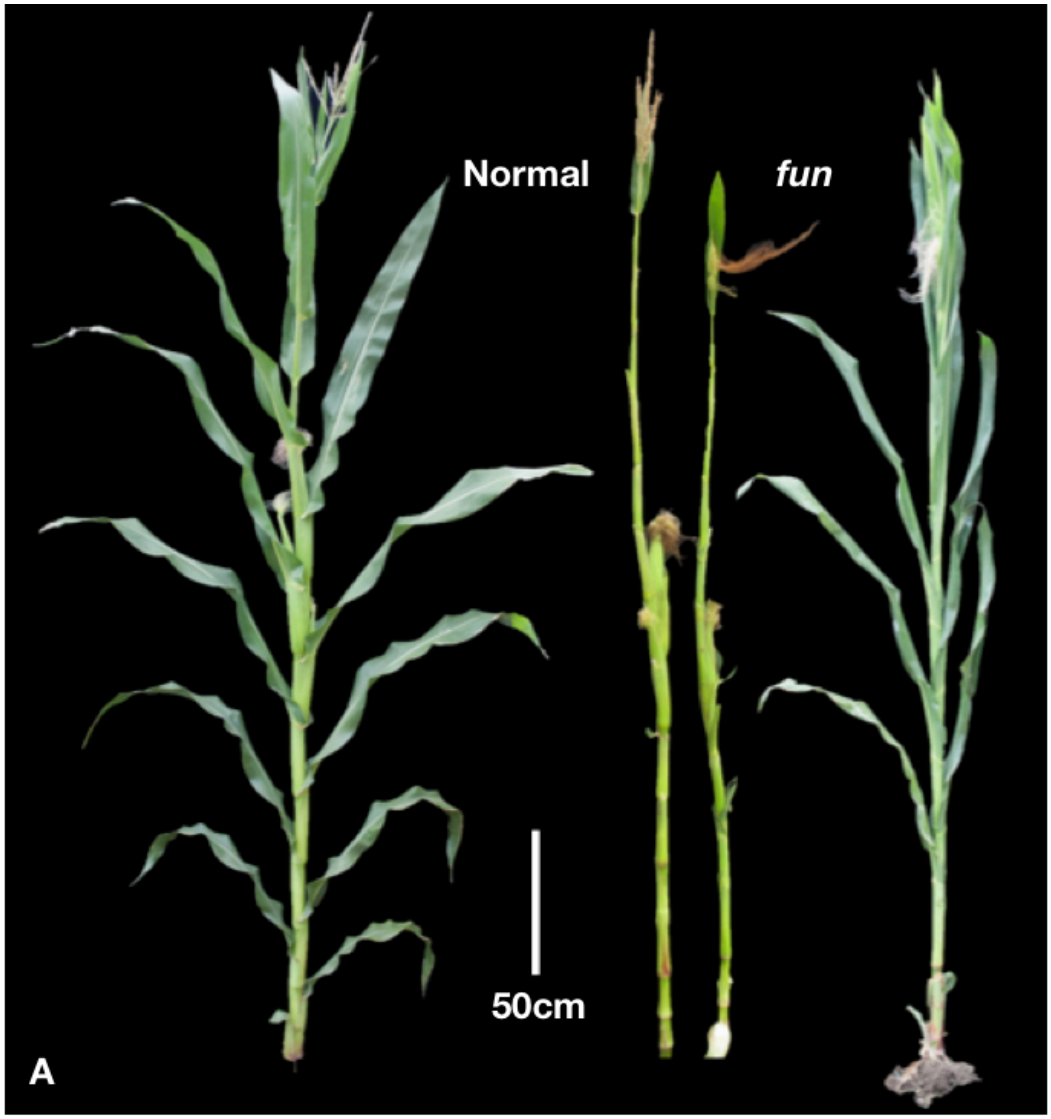

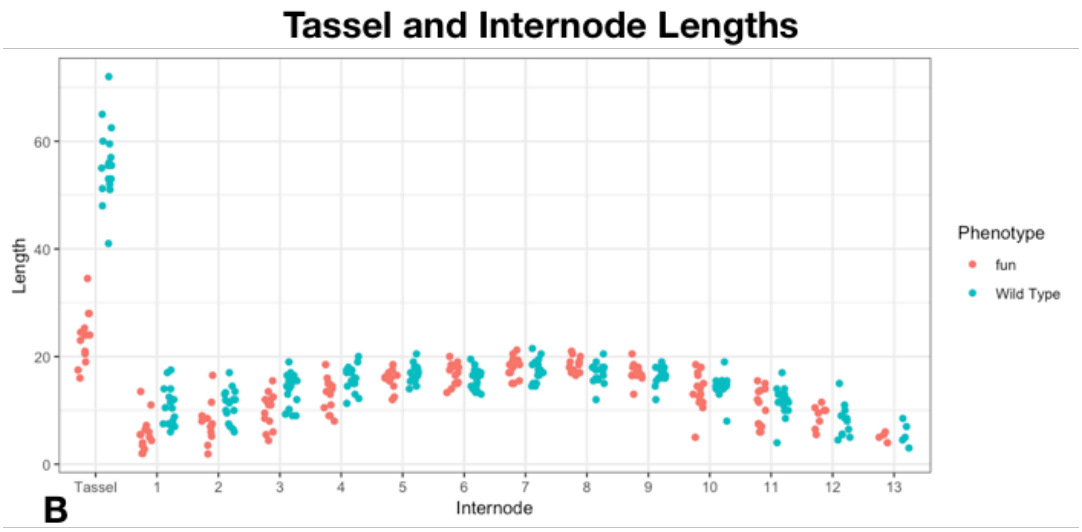

Figure 2-4: Height Phenotype.
A: Whole plant, normal left and *fun* right. Middle with leaves removed to show difference in height. **B:** Tassel and internode lengths, the tassel and subtending internodes are shorter in the mutant than in the WT sibs. Internodes 1-4 are significantly shorter in *fun* plants under a MANOVA test, at $p<0.001$.

Chapter III

Crossing *fun* to Previously Characterised Leaf Mutants

lg1, lg2 and *Wab1*

Introduction

Maize bears typical grass leaves, comprised of a sheath and a blade, which are separated by the ligule and auricle. The sheath is most proximal to the stem and wraps around it, providing support to the stem and the leaf as a whole. The ligule is immediately distal to the sheath and consists of a fringe of epidermal derived cells on the adaxial side of the leaf. Since the placement of the ligule forms a structural barrier between the environment and the internal spaces of the plant, it could be part of a "structural immune system". Distal to the ligule are the auricles. The auricles are two wedge-shaped structures that develop on either side of the midrib, expanding in the proximal-distal plane as they approach the margins. Auricles are derived from both epidermal and mesophyll tissue and their structural function is likely to allow the blade to bend outwards to maximise light capture. Together, the mature ligule and auricle represent the position of the blade/sheath boundary (BSB), but their position is defined by this boundary, not the other way round. The BSB is visible before ligule and auricle development and the anastomosis of intermediate veins, which also characterises the BSB, is visible in leaf mutants *liguleless1* (*lg1*) and *lg2* that lack the ligule[52,53]. As such, it is clear that the BSB is a fundamental component of the leaf upon which the ligule and auricle are elaborations.

The *lg1* mutant is a classical mutant that lacks both ligule and auricle and possesses a diffuse BSB[54]. The *lg2* mutant is similar to *lg1*, but upper leaves have partial recovery of ligule and auricle at the margins, while *lg1* does not display this partial recovery but has a slightly better defined boundary[52,53,55]. *lg1* leaves are slightly narrower than normal siblings[56]. Tassel branch number is reduced in both *lg1*[57] and *lg2*[58] and the transition to the reproductive phase is delayed in *lg2* mutants, such that they produce more leaves than normal siblings[58].

LG2 encodes a basic-leucine zipper (bZIP) protein that functions cell-non-autonomously[53]. The accumulation of LG2 mRNA precedes that of LG1 – it is observed in the meristem, while LG1 mRNA is only observed at the BSB[53]. On the other hand, LG2 mRNA is observed in the *lg1* background and LG1 mRNA is observed in the *lg2* background at the leaf margins[53], so there does not seem to be a direct "switching on" of LG1 by LG2 nor vice versa. LG1 encodes a nuclear localised protein that contains a domain with significant similarity to SQUAMOSA PROMOTER-BINDING1 (SPB1) and SBP2 proteins from *Antirrhinum majus*[54]. In contrast to LG2, LG1 functions cell-autonomously[55].

Wavy auricle in Blade1 (*Wab1)* is a dominant mutation that results in ectopic expression of the WAB1 protein in the leaf[57]. WAB1 functions in the tassel to turn on LG1, which in turn promotes branch initiation. When WAB1 is ectopically expressed in the leaf, the resulting activation of LG1 causes the distinctive over proliferation of the auricle at the ligule boundary as well as

ectopic auricle and sheath in the leaf blade[57]. At the blade sheath boundary the blade width of *Wab1* is similar to normal siblings, but distal to this, the blade quickly narrows such that *Wab1* has a very narrow blade further up the leaf. This narrowing is due to a deletion of the lateral domain of blade, as shown by analysis of the triple mutant *ns1*;*ns2*;*Wab1*, where both the marginal domain and lateral domains are lost[59]. A reduction in the number of lateral veins in the *Wab1* blade support the hypothesis that narrowing in the *Wab1* blade is due to deletion of domains rather than loss of cell expansion[59].

The disruption of the BSB in *lg1* and *lg2* made them obvious candidates for crossing to *fun*. As *Wab1* displays hypertrophy of the auricle, and *fun* displays complete loss of the auricle, we made a double mutant population to ask if FUN is required for ectopic auricle growth in the *Wab1* background.

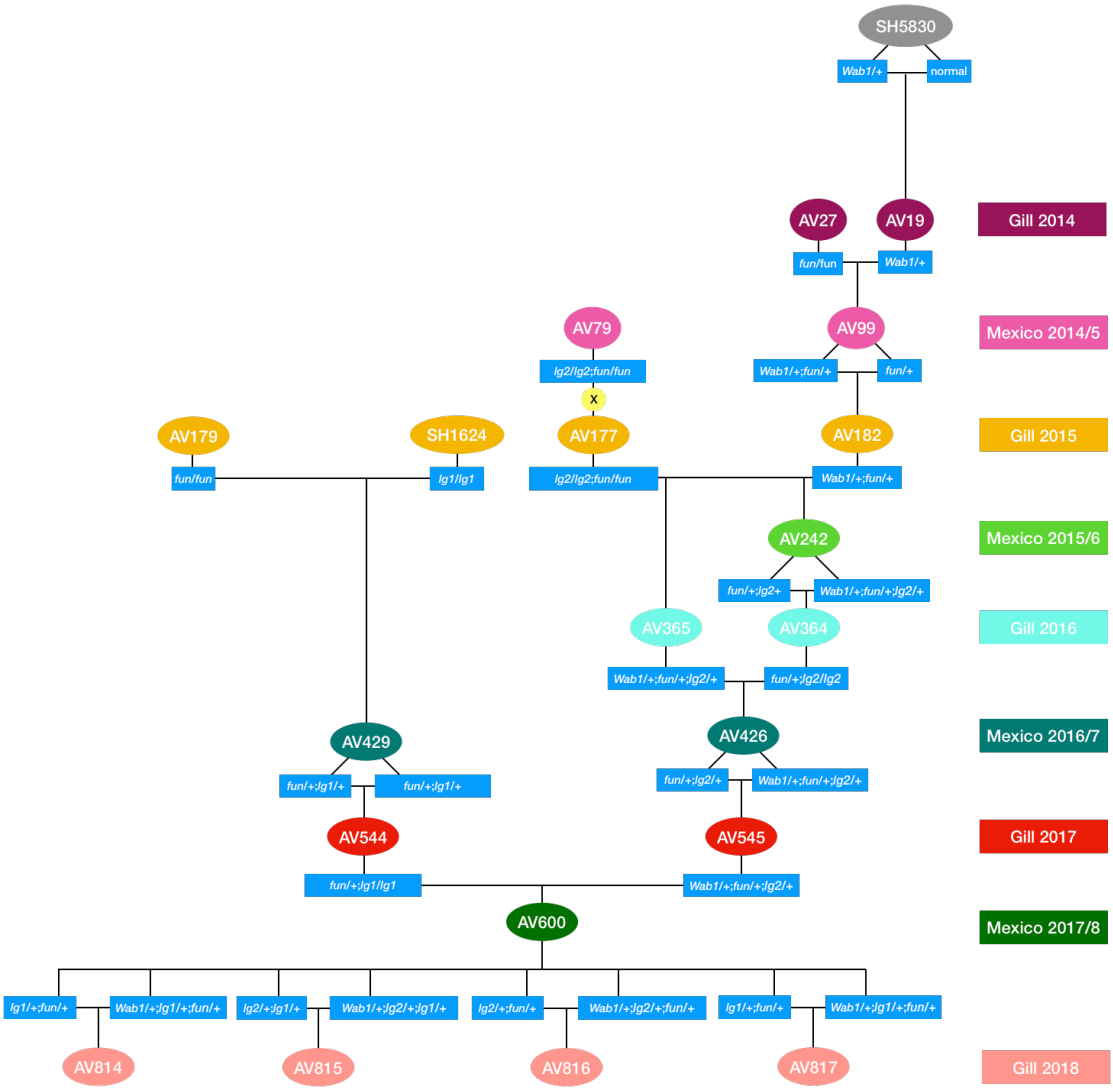

Figure 3-1: Genealogy of *Wab1*, *lg1*, *lg2* and *fun* families.

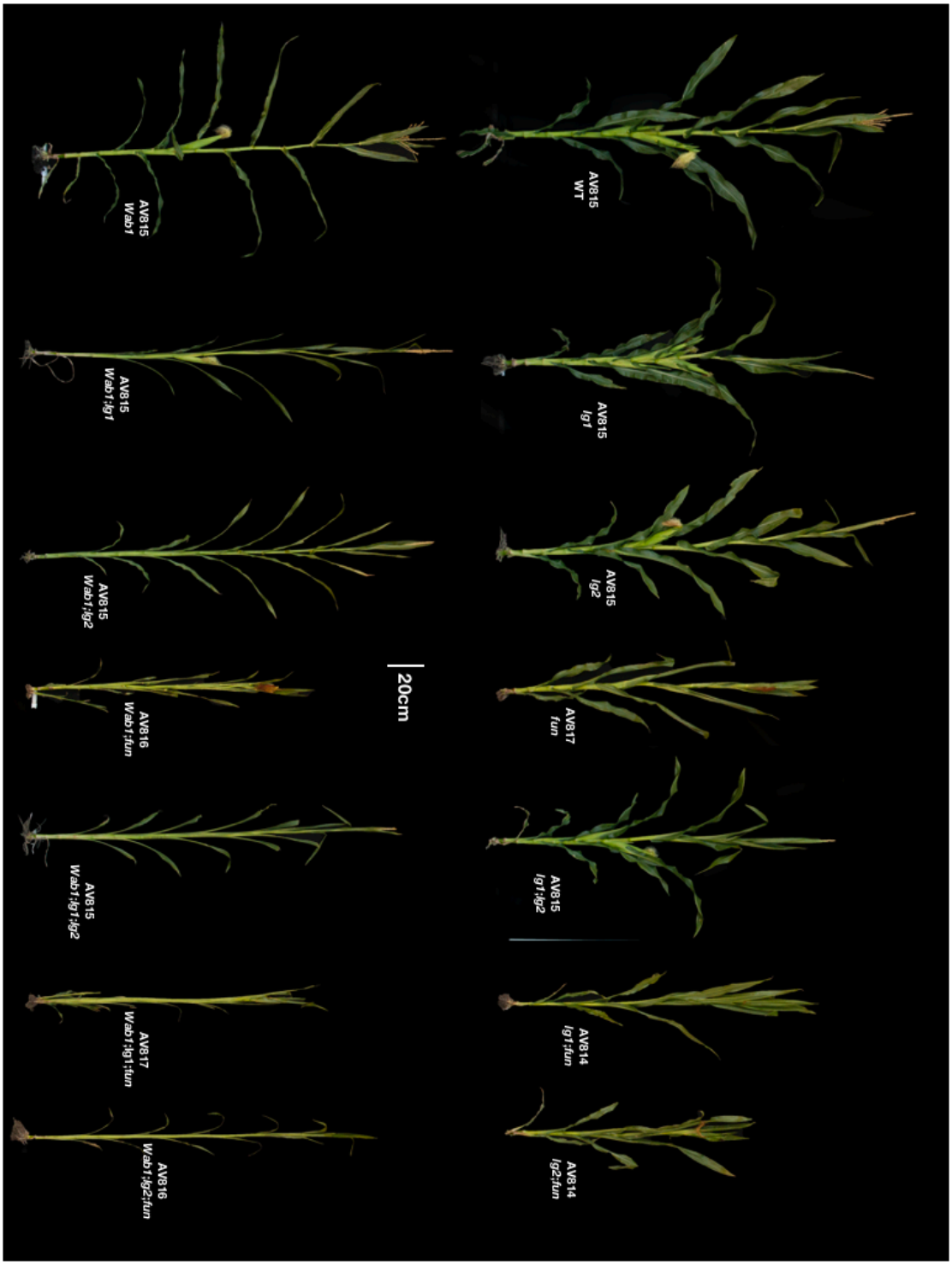

Figure 3-2: Whole Plant AV814-7. Mutant combinations shown on right of each plant, all to scale.

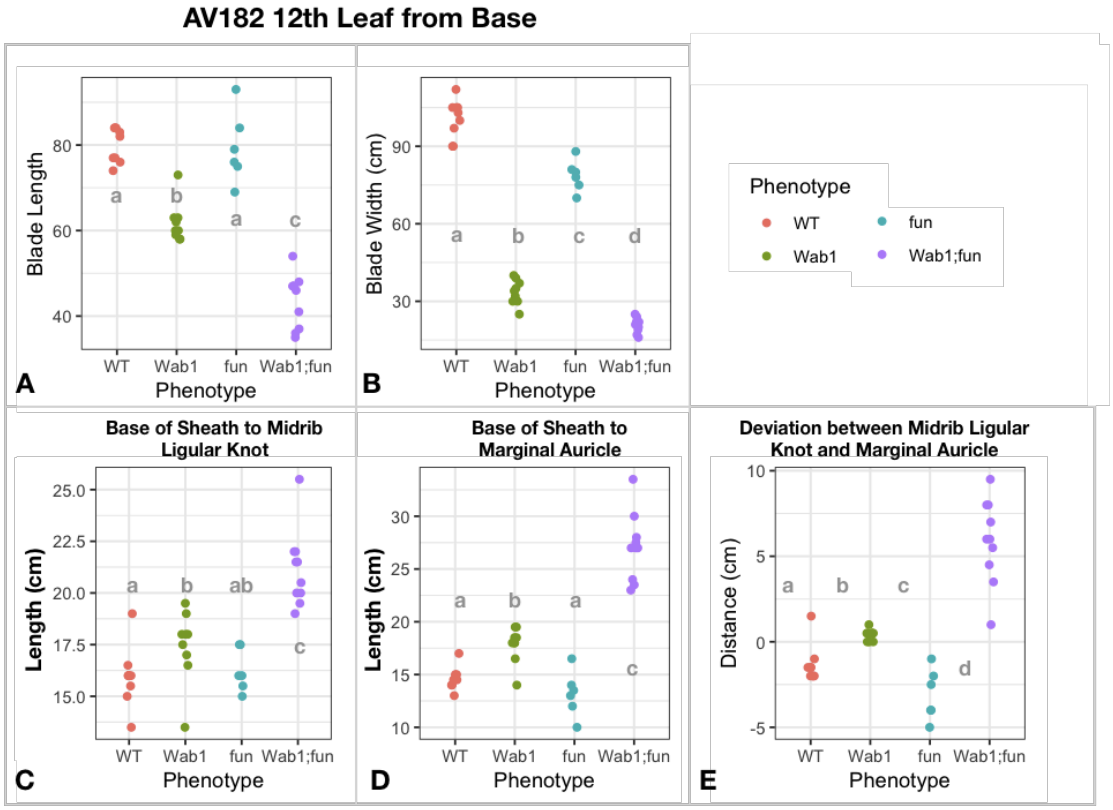

Figure 3-3: Family AV182 measurements.
Blade length (A) measured from MLK to tip of blade. Blade width (B) measured at the mid point of blade between MLK and tip of blade. Sheath length measured using MLK (C) and marginal auricle (D) as markers of end of sheath. Deviation between MLK and marginal auricle calculated from sheath length measurements, in *Wab1* these are equidistant, in normal siblings (WT) and *fun* the MLK is higher than the marginal auricle, while in *Wab1;fun*, the MLK is lower than the marginal auricle. Statistical analysis was done in R using ggpubr. A Wilcoxon method was used, and p values of lower than 0.05 were considered significant.

Methods

Families segregating for *Wab1*, *lg2*, *lg1* and *fun* were made according to the genealogy shown in Figure 3-1. Leaf width measurements were taken at blade mid point and/or 5cm above the blade/sheath boundary. Sheath lengths were measured from the base of the leaf to the MLK (see pg 37) at the midrib and/or the auricle at the margin closest to the base of the leaf. Plants were identified by their distinctive phenotypes with double mutant phenotypes from previous generations informing identification of plants as more mutations were introduced into the family. In families AV814-7, genotypes of double and triple mutants were also deduced from the presence of single mutant plants in the family.

Results

In families AV182, AV545 and AV814-7, *Wab1;fun* plants were observed (Figure 3-2). *Wab1* plants had slightly shorter blades than *fun* or normal siblings, while all three had similar sheath lengths. When *Wab1* and *fun* were combined, blade lengths were reduced and sheath length was increased (Figure

3-3A,C,D), suggesting a change in the position of the blade/sheath boundary (Figure 3-2E). The increase in sheath length did not make up for the loss of blade, resulting in a leaf that was shorter overall in the double mutant. The plants had extremely narrow leaves at the midpoint – narrower than either *Wab1* or *fun* alone (Figure 3-3B).

Wab1;*fun* double mutant plants have a disrupted BSB with both auricle and ligule displaying deviations from normal plants. While both *Wab1*[59] and *fun* have normal ligules, in the double mutant, the ligule is patchy, disrupted and displaced over a large region (Figure 3-4F). Although disruption of the BSB in the *Wab1*;*fun* double mutant is extensive, the ligule at the intersection of the BSB and the midrib is consistently present (Figure 3-4Ci) and this point is also marked on the abaxial side of the leaf as a lighter coloured area which forms a

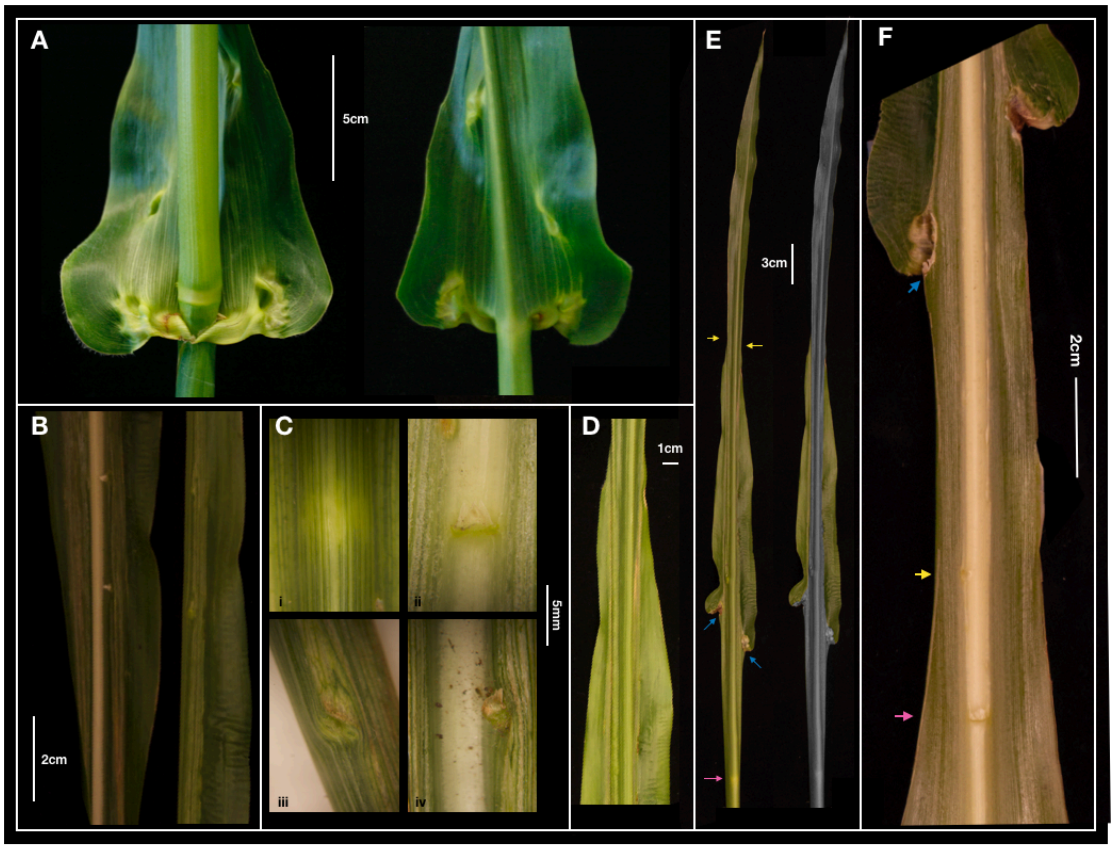

Figure 3-4: *Wab1*/+ and *Wab1*;*fun* leaf.
Adaxial (left) and abaxial (right) view of *Wab1*/+ lower leaf blade and BSB (A). Two ligular pinches shown from both the adaxial (left) and abaxial (right) sides of a *Wab*;*fun* leaf near the midpoint of the blade (B). Close up of the MLK in *Wab1*;*fun* from the abaxial (Ci) and adaxial (Cii) sides. Close up of ligule pinches in *Wab1*;*fun* midway along blade from abaxial (Ciii) and adaxial (Civ) sides. Close up of marginal wings tapering into central zone of leaf midway along blade in *Wab1*;*fun* (D). Entire *Wab1*;*fun* leaf from abaxial side (left) showing MLK (pink arrow), marginal auricle (blue arrows), point where marginal wings taper into central zone (yellow arrows), and (right) greyed out image with only marginal wings in green (E). Adaxial view of BSB zone of *Wab1*;*fun* leaf showing MLK (pink arrow), ligule pinch (yellow arrow) and ligule fringe at margin (blue arrow) with distal auricle tissue (F).

raised bump along the midrib (Figure 3-4Cii). I have termed this point the "midrib ligular knot" (MLK). In normal plants, the MLK is slightly proximal to the stem, compared to the marginal auricle, while in *Wab1* plants the MLK and marginal auricle are about equidistant. In *fun*, the MLK is displaced distally compared to normal siblings while in the *Wab1*;*fun* double, the MLK is much more proximal to the base of the leaf than the marginal auricle (Figure 3-4D,E).

Figure 3-5: BSB region of *Wab1*, *lg1*, *lg2* and *fun* combinations.
A-F show the BSB of *Wab1*;*fun*, *Wab1*;*lg1*, *Wab1*;*lg2*, *Wab1*, *Wab1*;*lg1*;*fun* and *Wab1*;*lg2*;*fun* respectively. Panel G shows *Wab1*;*fun* and *Wab1*;*lg2*;*fun*, MLK in *Wab1*;*fun* shown by pink arrow.

Wab1;*fun* double mutants form points of ectopic ligule in the blade, reminiscent of the ectopic auricle in *Wab1* single mutants, interestingly, there is very little, if any, ligule associated with the ectopic auricle in *Wab1*, while the double shows clear ectopic ligule (Figure 3-4). The *Wab1*;*fun* double mutant often retains some auricle at the margins of the leaf, and this is associated with "wings" of marginal tissue that extend a relatively short distance along the blade (Figure 3-4D,E). The tassel of *Wab1*;*fun* plants resembles a *fun* tassel (not shown).

Combining the *Wab1* mutant with *lg1* resulted in total loss of both the marginal auricle and MLK, though the boundary was still detectable by the commencement of the midrib (Figure 3-5B). When *Wab1* was combined with *lg2*, the MLK was lost but the marginal auricle was increased as in a *Wab1* plant (Figure 3-5C). In family AV545, the blade width at the midpoint was slightly reduced in *lg2* plants (Figure 3-6) but there was no evidence of an

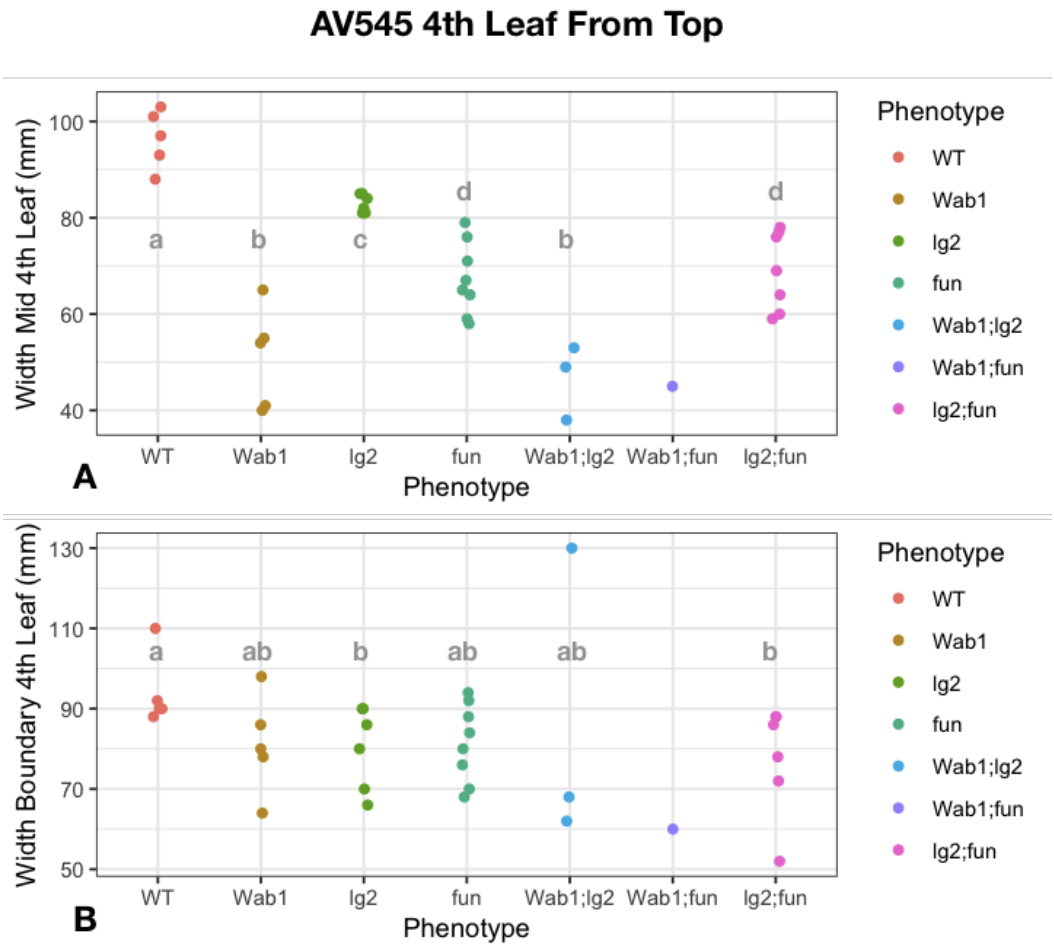

Figure 3-6: Leaf measurements from family AV545.
Blade width (A) measured at the mid point of blade between MLK and tip of blade. Blade width (B) measured 3cm above the MLK. Statistical analysis was done in R using ggpubr. A Wilcoxon method was used, and p values of lower than 0.05 were considered significant.

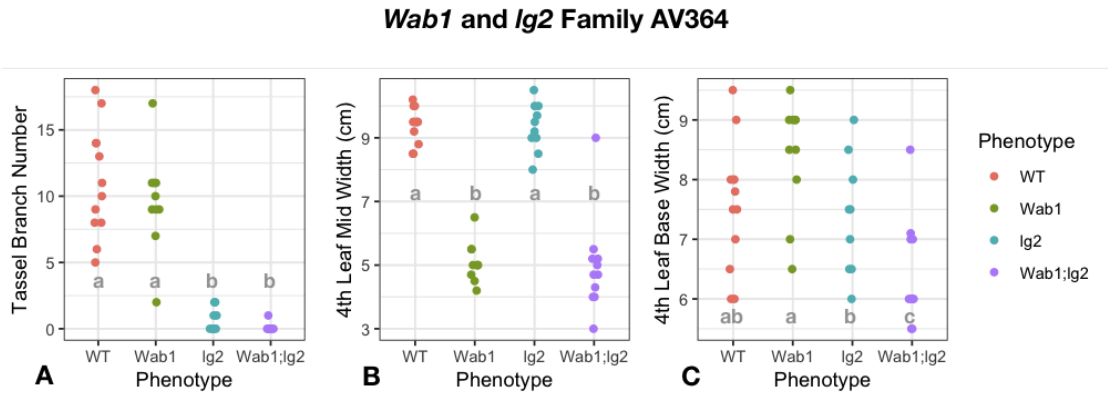

Figure 3-7: Tassel Branch Number
Epistasis of *fun* by *lg2* (A). Blade width (B) measured at the mid point of blade between MLK and tip of blade. Blade width (C) measured 3cm above the MLK. Tapered leaf width is evident in *Wab1* and *Wab1*;*lg2*, but not in normal siblings (WT) nor *lg2* (B and C). Statistical analysis was done in R using ggpubr. A Wilcoxon method was used, and p values of lower than 0.05 were considered significant.

additive effect of narrowing in the *Wab1*;*lg2* double mutant plants in family AV364 (Figure 3-7B). A Wilcoxon t-test detected a reduction in width at the base of the leaf in *Wab1;lg2* plants, though reference to the scatter plot (Figure 3-7C) reveals that the data are so scattered that the Wilcoxon t-test is misleading – rather I would argue that there is no difference in the width at the boundary between any of these mutant backgrounds. Tassel branch number is reduced to *lg2* levels in the *Wab1*;*lg2* double mutant (Figure 3-7A). The *Wab1*;*lg2*;*fun* triple mutant showed loss of the extended marginal auricle seen in *Wab1*;*lg2* as well as loss of the MLK seen in *Wab1*;*fun* (Figure 3-5).

In the *lg2*;*fun* double, mutant, the line of the BSB is still visible as a faint line of paler green on the abaxial side (Figure 3-8B), but the ligule is reduced to that of a *lg2* single mutant (Figure 3-8F) and there is no marginal auricle (Figure 3-8B).

The MLK is lost in the *lg2*;*fun* double mutant (Figure 3-8B). *lg2*;*fun* leaves are the same width as *fun* single leaves when measured at the midpoint (Figure 3-6A) and no tassel branches were observed in the 5 tassels examined from family AV545 though internodes were visible (representative tassel shown in Figure 3-8C). The *lg2*;*fun* tassel had a thick rachis in comparison to the *fun* single plant and was completely feminised (Figure 3-8A,C).

When *lg1* is combined with *fun*, the entire ligule and auricle is lost, which is similar to the *lg1* mutant alone. The small amount of ligule that appears in the upper leaves in *lg1* is also lost in the *lg1*;*fun* double mutant (Figure 3-9). Feminisation occurs in the tassel.

The extreme leaf phenotype of the *Wab1*;*lg1* double mutant is mirrored in the *Wab1*;*lg2*;*fun* triple mutant. The marginal auricle is almost completely lost (Figure 3-5F) and the MLK is lost. The *Wab1*;*lg1*;*fun* triple mutant has no visible BSB (Figure 3-5E) but there is still transition between sheath like tissue and blade like tissue, so the BSB has not been abolished.

Discussion

Both *Wab1* and *fun* lead to narrowing of the leaf blade. Since narrowing in the leaf blade of *Wab1* is due to a deletion of the lateral domain of the leaf[59], and narrowing in *fun* is associated with narrow cells (see Chapter 1), an additive interaction in the double mutant is not surprising. The lack of narrowing in *lg2* and the epistatic narrowing observed in the *lg2*;*fun* double mutants (Figure 3-6A) implies that lateral expansion of the blade is associated with elaboration of the auricle but not definition of the MLK or the ligule itself. The partial recovery of blade width close to the BSB (Figure 3-6C) in the *Wab1* mutant where there is extensive auricle supports this hypothesis.

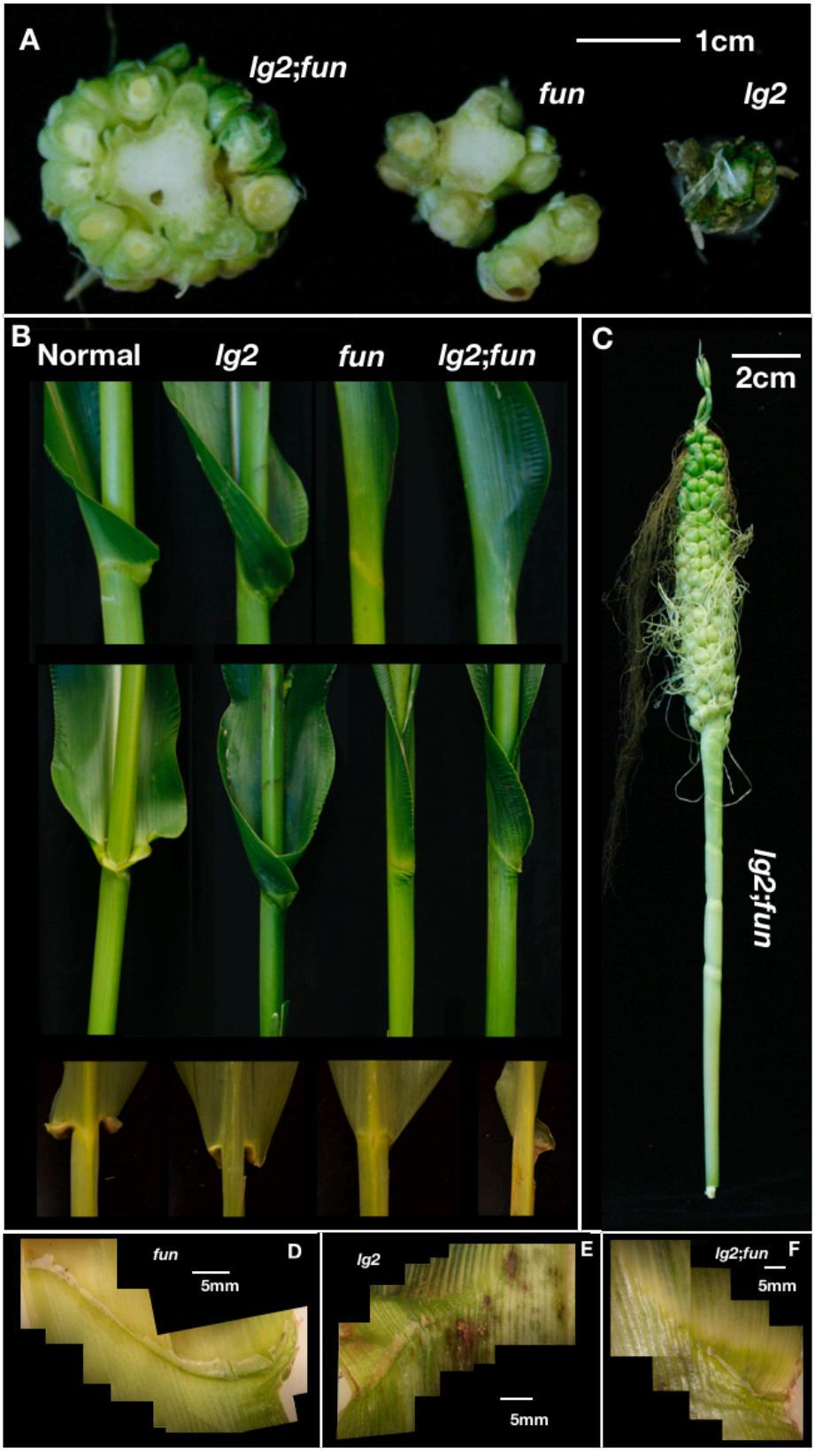

Figure 3-8: *lg2* and *fun* single and double mutants.
Tassel cut at midpoint to show width of tassel in cross section (A). Normal, *lg2*, *fun*, and *lg2*;*fun* leaves shown from side, front and back (B). Whole *lg2*;*fun* tassel from cut at flag leaf (C). D-F show BSB of *fun*, *lg2* and *lg2*;*fun* respectively.

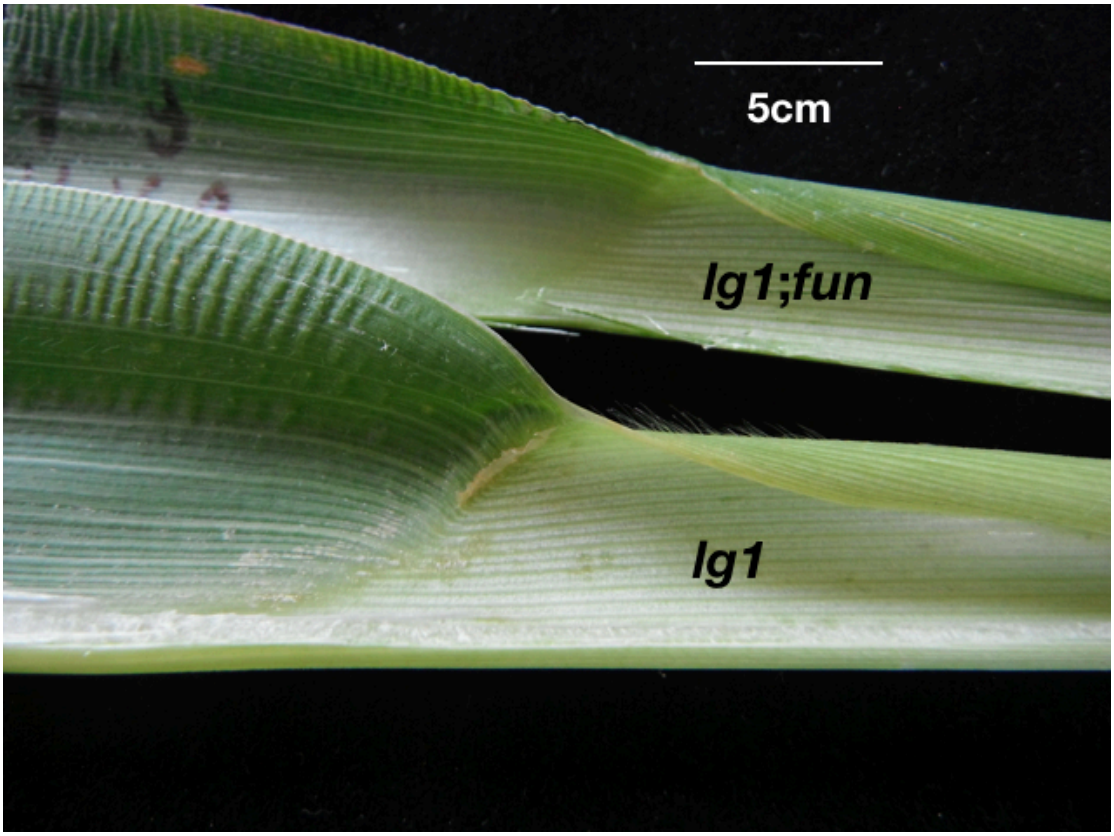

Figure 3-9: *lg1* and *lg1*;*fun* double upper leaves, adaxial side.
Complete loss of ligule in the double mutant (upper); small marginal ligule retained in *lg1* single mutant.

Although *Wab1* leaf blades are slightly shorter than normal siblings, the extreme shortening of *Wab1*;*fun* double mutant blades was surprising since *fun* blades are of normal length (Figure 3-3A). Furthermore, though *Wab1* displays almost no displacement of the MLK and marginal auricle location as compared to normal siblings, and *fun* displays a slight distal displacement of the MLK, the *Wab1*;*fun* double mutant MLK is extremely proximal to the stem as compared to the marginal auricle (Figure 3-3E, 3-4F). This extensive synergistic interaction is mirrored in the *Wab1*;*lg1* double but not the *Wab1*;*lg2* double mutant. Since *Wab1* is known to activate LG1[57] but not LG2 (Lewis, unpublished), these interactions would place FUN downstream of LG1.

The additive interaction between *lg2* and *fun* resulting in a loss of ligule at the midrib as well as loss of auricle at the margins (Figure 3-8B) shows that these genes function in different zones and pathways to elaborate the BSB. It seems likely that LG2 is responsible for elaborating the boundary at the midrib, while FUN elaborates the auricle at the margins. The different zones of action are underlined by the double mutants with *Wab1* – loss of LG2 does not affect the elaboration of marginal auricle in the *Wab1*;*lg2* double mutant (Figure 3-5C), while the *Wab1*;*fun* double retains the MLK but loses the marginal auricle. In the *Wab1*;*lg2*;*fun* triple mutant both the marginal auricle is reduced, and the MLK is lost, as would be expected if LG2 and FUN work in different domains. It is possible that LG2 and FUN have a common upstream element and

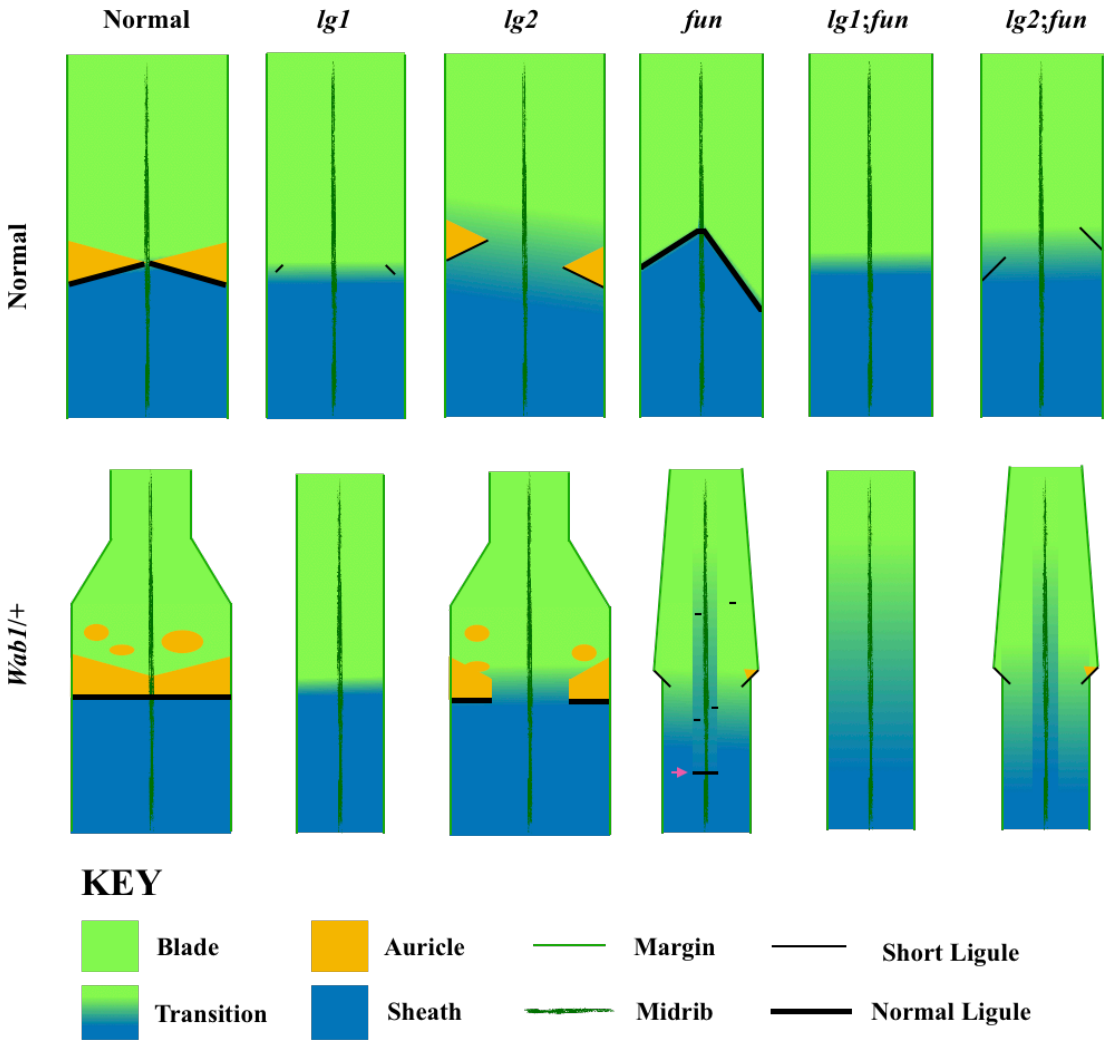

Figure 3-10: Summary of Leaf Phenotypes observed in families AV182, AV545 and AV814-7.

Legend for Figure 3-10

Normal maize plants, like most grasses, have four well-defined, distinct leaf sheath, ligule, auricle and blade (listed in proximal to distal order). In *lg1*, the ligule and auricle are all but lost (on a few upper leaves small patches of short ligule can sometimes be observed), but the BSB still exists and anastomosis occurs as normal. The *lg1* blade is narrower than normal siblings. In *lg2*, ligule and auricle both exist at the margins, but are displaced and there is never ligule at the midrib. The BSB is slightly more diffuse in *lg2* than *lg1*, but still present. In *fun*, the ligule and underlying BSB is displaced but distinct while the auricle is absent, though sometimes a little auricle remains. The *fun* blade is narrower than normal siblings. The *lg1*;*fun* double mutant removes even the small amount of ligule that remains in the *lg1* single mutant, but otherwise resembles the *lg1* single mutant. Width measurements have not been taken for the *lg1*;*fun* double mutant and would be helpful in our understanding of this interaction. In the *lg2*;*fun* double mutant, the marginal auricle observed in *lg2* is removed, but the short ligule remains; the blade is narrow as in *fun*.

In the dominant *Wab1*/+ background, the point of intersection of the ligule and the midrib is level with that of the ligule's intersection with the margin. This is in contrast to normal siblings where the midrib-ligule intersection is slightly distal to the margin-ligule intersection. Above the ligule, the auricle is expanded, and ectopic auricle invades the blade. Distal to the BSB and immediately distal tissue, the blade narrows dramatically. In the *Wab1*;*lg1* double mutant, the BSB remains but ligule and auricle are lost. The widening of the blade close to the BSB observed in *Wab1*/+ is lost and the entire blade is very narrow. In the *Wab1*;*lg2* double mutant, the enlarged and ectopic auricle persists, and the blade width is thus fairly normal close to the BSB. Like the *Wab1*/+ single mutant, the *Wab1*;*lg2* leaf is very narrow distal to the BSB and like the *lg2* mutant, ligule is not observed at the midrib. In the *Wab1*;*fun* double mutant, ligule exists at a point in the midrib, but is cut off abruptly at the edge of the midrib. Small points of ligule are visible at points along an imagined line that connects the MLK (pink arrow) with the proximal edge of "wings" that protrude from the midrib backbone. Small patches of auricle are often observed at the base of these wings, and ectopic ligule is also formed blade. In the *Wab1*;*lg1*;*fun* triple mutant, the presence of a defined BSB is highly questionable and no ligule or auricle remain. The *Wab1*;*lg1*;*fun* leaf resembles a *Wab1*;*lg1* leaf but with less definition of BSB. In the *Wab1*;*lg2*;*fun* triple mutant, the leaf resembles the *Wab1*;*fun* double mutant, but loses the MLK.

represent forks in a pathway defining and elaborating the BSB. This upstream element could be LG1, since the *lg1*;*fun* double mutant shows epistasis of the *lg1* phenotype, the *lg1*;*lg2* double mutant shows partial synergy[60], and the *lg1* phenotype is more severe than either the *lg2* or *fun* phenotypes. Figure 3-11 shows a tentative pathway for ligular region development that includes FUN.

The *lg2*;*fun* tassel has no branches and the rachis is thickened, similar to the female inflorescence. This phenotype could be considered additive, with both *lg2* and *fun* removing branches, but for different reasons (Figure 3-8C). This analysis also underlines the idea that reduction in inflorescence branching is a female trait in maize inflorescences and that LG2 may function in promoting the masculine trait of branch initiation.

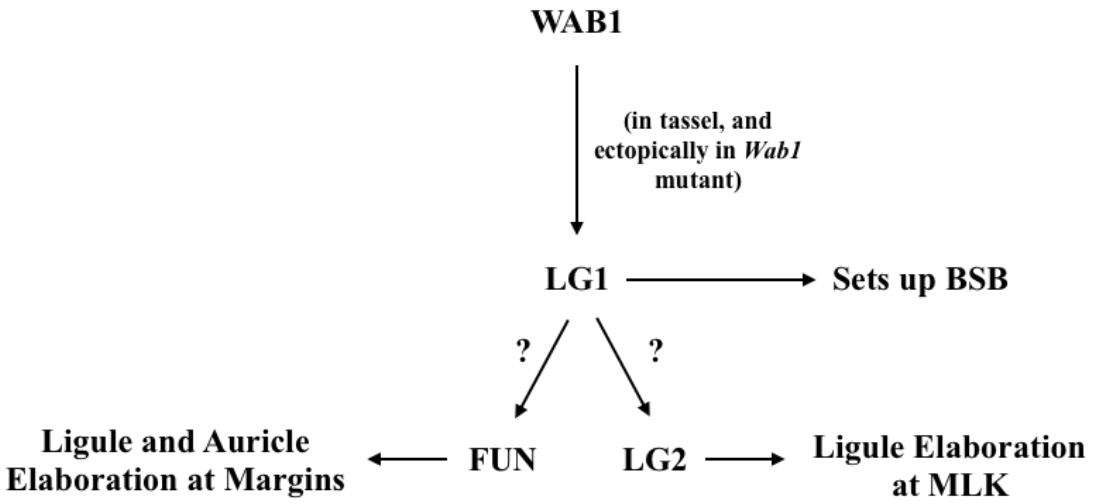

Figure 3-11: Genetic Pathway of Ligule Region Development. WAB1 is known to turn on LG1 in the tassel (Lewis, unpublished data) and loss of LG1 causes elaboration of the BSB to halt at an early stage leaving only the anastomosis of veins in the mature leaf but no ligule or auricle[52,55]. Though LG1 does not directly turn on LG2, LG2 is placed downstream here in a temporal sense. FUN's placement downstream of LG1 is to be viewed in a similar sense, though direct activation of FUN by LG1 is possible. Analysis of the *Wab1;lg2* and *Wab1;fun* double mutants showed the differing zones of action of these two genes in elaboration of the ligular region

eta1

Introduction

extended auricle1 (*eta1*) is characterised by larger than normal auricle, a diffuse BSB, disrupted ligule, and short internodes leading to an overall shorter plant. *eta1* interacts synergistically with *lg1* and *lg2* in a does dependent manner[61]. Since *fun* is also short and has BSB disruptions, a family segregating for both mutant alleles was created and double mutants examined.

Results

The *eta1*;*fun* double mutant was shorter than either of its single mutant siblings, and the auricle was absent (Figure 3-11).

Discussion

The epistasis of the auricleless phenotype of *fun* along with the additivity of the height phenotype suggests that FUN works in a different pathway that is temporally downstream of ETA1. This would support a hypothesis that FUN is required to directly make auricle, while ETA1, like ectopic *Wab1*, turns on this pathway, in the *fun* background no actual auricle is made.

Figure 3-11: *eta1* and *eta1*;*fun* double mutant.
Large auricle are in *eta1* are completely absent in the double mutant.

Chapter IV

Crossing *fun* to Hormone Mutants and Hormone Applications

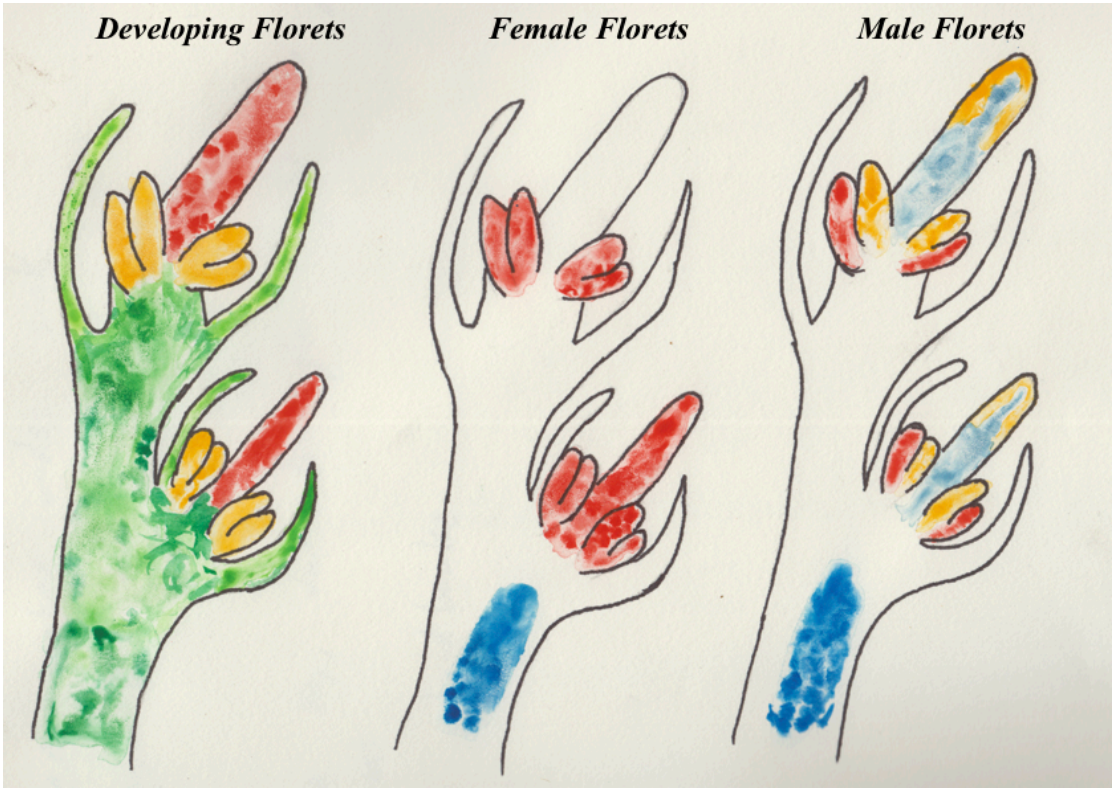

Figure 4-1: Gene and Hormone Localisation Patterns in Developing Florets

Left: sketch of a developing pair of maize florets. Glumes (green) enclose stamens (yellow) that surround a silk (red).
Middle: sketch of florets developing on a female inflorescence (ear). GA biosynthetic gene, *Dwarf1* (red), accumulates in stamens in the upper floret and the entire lower floret. These organs are all destined to abort. JA biosynthesis gene, *Tasselseed1* (blue), accumulates along the base of the pedicel. Red can also be interpreted as GA localisation, dark blue as JA localisation.
Right: sketch of florets developing on a male inflorescence (tassel). D1 (red) and BR biosynthetic gene NANA1 (umber) accumulate in stamens of both the upper and lower floret. TS2 (light blue) accumulates in the silk of the upper floret and entire lower floret; these organs are destined to abort. TS1 (dark blue) accumulates along the base of the pedicel. Red can also be interpreted as GA localisation, blues as JA localisation, and yellow as BR localisation

Notes

Placement of NA1[62], TS1[35] and TS2[36] are based on *in situ*, D1 on antibody[63].

No data has been recorded in the literature for placement of either TS2 or NA1 in the female floret.

SK1 not shown, but RNAseq suggests it accumulates in anthers and it has also been suggested to accumulate in the silk, though *in situs* are reported to have failed due to low abundance or transcript.
Though D1 is present in male stamens, it is thought not to produce as much GA as in female as per the observations of Nickerson *et al*. that GA is lower in the tassel than in the ear. Alternatively (and/or additionally) the interaction with BR produced by NA1 may be countering its effects.

Hormone Control of Sex Determination in Maize

- in a nutshell -

Three major hormones have been implicated in the sex determination pathway of *Zea mays*: brassinosteroids (BR)[31,62], jasmonic acid (JA)[35,37,64] and gibberellic acid (GA)[27,63,65,66]. BR accumulates in the developing stamens of male flowers[62], while JA accumulates in the silks[36] which abort[67]. In flowers destined to become female, GA accumulates in the anthers[63] which arrest[67], and the JA that accumulates in the silk is degraded by SILKLESS1, protecting them from abortion[37]. Overall, it can be argued that in maize GA is a feminising agent, while BR and JA are masculinising agents. In order to understand the feminisation of *fun,* I made crosses with different hormone mutants and assessed the double mutant phenotypes.

Brassinosteroids

Introduction

Two characterised mutants that are defective in the synthesis of brassinosteroids (BR) in maize are *nana1* and *nana2*. The maize mutant *nana1* was isolated from the F2 of a plant with active *Mutator* transposons. PCR revealed a 497-bp insertion in a gene homologous to *DE-ETIOLATED2* (*DET2*) in *A. thaliana*[62]. *DET2* is a steroid 5α-reductase[68] known to catalyse a step in the BR synthesis pathway in *A. thaliana*[69]. The knockout *det2* phenotype can be rescued by addition of active brassinolide[70] and is characterised in *A. thaliana* by extreme dwarfism as well as increased male sterility, dark green leaves, and repression of hypocotyl etiolation in the dark[71]. In the maize *na1* plant, levels of the substrate of the DET2 enzyme, (*24R*)-24-methylcholest-4-en-3-one, accumulated to 475% that of normal sibs, while downstream intermediates were reduced (actual active BR was not measured)[62]. While rescue by addition of brassinolide was not reported, addition of the BR inhibitor propiconazole (PCZ) to wild-type maize plants caused them to phenocopy the *nana1* phenotypes of greatly shortened stature and feminised tassels[62]. Since NA1 transcript was shown by *in situ* to accumulate in developing anthers[62], the role of BR in development of masculine flowers is supported.

Five years after the publication of the causative mutation of the *nana1* plant, the classical mutant *nana2* was cloned[31]. Like *na1*, *na2* is of greatly reduced height and has a feminised tassel. Since the *na2* phenotype was so similar to *na1*, it was not surprising that a mutation was found in the maize orthologue of the *A. thaliana DWF1* gene[31]. *At*DWF1 is a Δ4-sterol reductase[72] and *dwf1* mutants accumulate its substrate 24-methylenecholesterol and have low levels of campestrol indicating a block in the BR pathway[73]. The *dwf1* phenotype, like *det2*, can be rescued by application of brassinolide[73] in *A. thaliana*. The maize

na2 plant was also shown to have low campestrol and later intermediates implying a similar block in the BR biosynthesis pathway[31]. The overall *na2* phenotype is similar to *na1*: short stature, feminised tassel and suppressed tillering.

NA2 transcript is expressed in many tissue types including seedlings, mature and growing leaves, and immature ears and tassels with the highest expression detected in developing leaf collars, which is the position of ligule and auricle[31]. Older tissues tend to have lower expression of NA2, supporting a role for BR in expansion and growth. Crosses with GA deficient mutants (such as *dwarf5* [*d5*]) and application of GA to developing *na2* plants has shown an interaction between these two hormone pathways in regulating growth and defining sex in *Zea mays*. GA and BR are thought to have independent roles in defining the absolute height of a plant, since the *na2;d5* double mutant was shorter than either single mutant[31]. Masculine inflorescence development requires GA and BR to work together – the feminised tassel of *na2* is abolished in the double mutant, implying that GA is needed for BR deficiency dependent feminisation. This hierarchy is mirrored in the ear: the anther ear phenotype of *d5* is not abolished in the *na2;d5* double mutant. Together these results show that BR is not essential for the masculinisation of inflorescences, while GA is essential for emasculation[31]. Application of GA to developing *na2* tassels enhanced their feminisation, supporting this hypothesis.

In *Arabidopsis thaliana, BRASSINOSTEROID INSENSITIVE1* (*BRI1*) encodes a membrane-bound leucine-rich repeat (LRR) receptor kinase (RK) that binds BR and sets up a signal cascade ultimately leading to BR response[74]. BRI1 homologs in maize are ZmBRI1a and ZmBRI1b, along with other members of the family BRASSINOSTEROID INSENSITIVE1-LIKE RECEPTOR KINASE (BRL1-3)[75]. The RNAi based transgenic knockdown based on the ZmBRI1a sequence, was shown by qRT-PCR to have reduced levels of all five of these predicted BR receptors in 8-week-old shoot apices[75]. Reduced response to BR in the knockdown line was confirmed by analysis of expression of BR marker genes *constitutive photomorphogenic dwarf* (*cpd*) and *brassinosteroid dependent1* (*brd1*) and a BR root growth inhibition assay. In addition, a cross with the BRASSINOSTEROID INSENSITIVE1-ETHYL METHANESULFONATESUPPRESSOR1 (BES1)-YFP line showed a change in localization pattern. In wild-type plants, BES1 is in the nucleus in a BR inducible manner. When crossed to the *bri1*::*RNAi* line, the localization is no longer nuclear[75]. BR insensitivity in this RNAi line was further supported by the presence of BR deficient phenotypes such as short, thickened leaves, shortened stature[31,62,69], and decreased auricle, phenotypes that were observed in *Oryza sativa bri* mutants[76,77,78]. The *bri1*::*RNAi* line was also observed to have shortened internodes, especially those between the ear and tassel, and twisting in the leaves. The twisting was sometimes so extreme that leaves had to be removed to access the tassel since they clasped it and prevented it from growing out[75].

Mutants in BIN2 were first identified in *Arabidopsis thaliana* as semi-dwarf plants that were not rescued by exogenous BR[79,80]. The *bin2* mutant phenocopied classical BR knockout mutants, but was found to contain a gain-of-function mutation in the causative gene, rather than a loss of function like *bri1*[81] or *deetiolated1*[69]. Loss of function in BIN2 gives a constitutive response to BR, which manifests in *A. thaliana* as long wavy petioles and narrow leaves[79,82]. BIN2 is a serine /threonine kinase of the Glycogen Synthase Kinase-3 (GSK3) family[79] that phosphorylates BR transcription factors to tag them for degradation in the absence of BR. Thus, when BIN2 is knocked down, the plant is unable to degrade BR transcription factors in the absence of BR and therefore constitutively responds to BR.

Maize has at least 10 GSK3 like kinases that were identified by BLAST, 8 of which are expressed in leaf tissue. All 8 of the GSK3 like kinases expressed in leaf tissue were knocked down by the RNAi line created by Dr Kir[83], so despite the possibility of functional redundancy among these genes, the knockdown of BIN2 activity is likely to be real. While BR knockouts are usually associated with shorter plants[31,69,73,75,84], the constitutively BR responding *bin2*::*RNAi* line had an unexpectedly shorter stature than normal siblings. This shortened stature was due to shortened internodes, but the internodes of the tassel were found to be longer in the *bin2*::*RNAi* plants[83]. In concurrence with suppression of BIN2 in rice, auricles were larger in the *bin2*::*RNAi* maize line, but unlike the rice line, leaf blades were wider and longer, while the rice line had narrower, longer leaves[84]. The maize *bin2*::*RNAi* line leaves also had distinctive crenulations along their blades[83].

Methods

In order to ask if the *fun* mutant is involved in the BR pathway, double mutants were created with *na2*, *bri1::RNAi* and *bin2::RNAi* lines. Stocks of the *na2* mutant were obtained from the MaizeGDB stock centre (*na2-5* 532I) and grown in the greenhouse. A plant displaying the *na2* phenotype was crossed to a *fun-1* plant from family AV383. Resulting kernels were planted in the greenhouse to create family AV393. Individuals from family AV393, heterozygous for both mutations, were self-pollinated to create family AV829 that was grown in the Gill Tract field in the summer of 2018 and used for analysis of the double mutant. 120 plants grew to adulthood, of which 87 were normal, 12 were *na2,* 16 were *fun,* 5 were *na2;fun*. The observed phenotypes were confirmed by genotyping of both *fun* and *na2* (see Appendix 3) and the expected 9:3:3:1 ratio of 120 plants comes to 63:21:21:7 as compared to the observed 87:12:16:5. 132 kernels were planted, so disproportionate death of mutant plants could be an explanation of deviation from the expected ratio, in accordance with original observations that BR mutant plants struggle with seedling establishment[31,85].

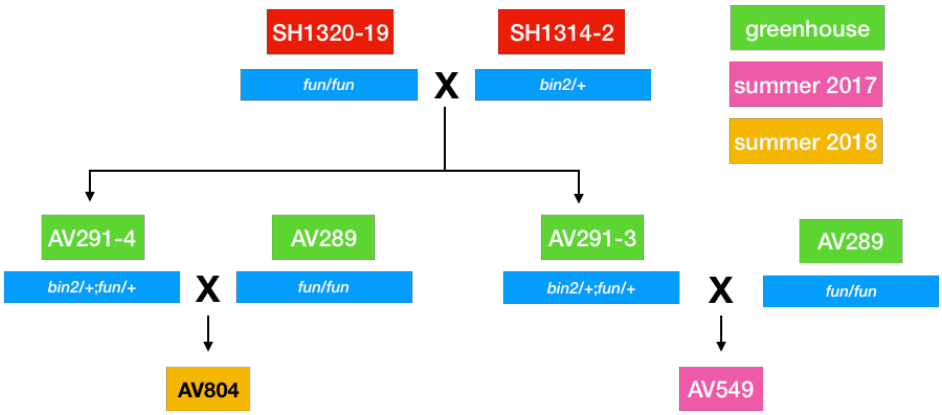

Figure 4-2: Genealogy of plants used in analysis of *bin2::RNAi* and double phenotypes.

Stocks of the *bri1*::*RNAi* mutant were obtained from Phil Becraft (Iowa State) and back-crossed 3 times to B73. Family AV802 was created by crossing a *bri1*::*RNAi*/+;*fun*/+ plant with a *fun*/+ sibling and growing the segregating family in the Oxford Tract in the summer of 2018. AV802 comprised 66 individuals, 24 of which were *bri1*::*RNAi*, 9 of which were *bri1*::*RNAi*;*fun*, 10 of which were *fun* and 23 of which were WT. This observed ratio of 24:9:10:23 closely fits a 3:1:1:3 ratio of 25:8:8:25 (rounded to nearest whole). A BASTA test was used to confirm the presence of the *bri1*::*RNAi* genotype (see Appendix 3) and *fun* plants were identified by their phenotype. In order to confirm that the transgene was not silenced, *bri1*::*RNAi* plants were backcrossed to B73 and the progeny scored for the presence of the *bri1*::*RNAi* phenotype.

Since *bri1*::*RNAi* can display a twisting habit, and feminised tassels often bend over due to their own weight, plants were measured from the ground to the tip of their tassel, which was pulled upright for measuring. Tassel length was measured from the flag leaf node to the tip of the tassel and a tassel branch was defined as a branch possessing more than two spikelet pairs arising from the main rachis. A tassel branch was counted as feminised if it possessed two or more feminised spikelet pairs. Leaf widths were measured at the midpoint of the blade and auricle was measured in length at the leaf margin.

Stocks of *bin2*::*RNAi* were obtained from Phil Becraft (Iowa State) and back-crossed twice to Mo17 before crosses to *fun* crossed once to Mo17. Family AV549 was created by crossing plant AV291-3 (*bin2*::*RNAi*/+;*fun*/+) to a *fun*/*fun* plant from family AV289. This family was grown in the Oxford Tract in the summer of 2017 and plants from this family were used for photographs. Family AV804 was created by crossing plant AV291-4 (*bin2*::*RNAi* /+;*fun*/+) to a *fun*/*fun* plant from family AV289 (Figure 4-2). This family was grown in the Oxford Tract in the summer of 2018 and plants from this family were used for measurements and statistical analysis. Family AV804 segregated 15:22:11:25 WT:*bin2*::*RNAi*:*fun*:*bin2*::*RNAi*;*fun* which deviates from the expected 1:1:1:1 segregation. A BASTA test was used to confirm the presence of the *bin2*::*RNAi* genotype (see Appendix 3) and *fun* plants were identified by

their feminisation phenotype. Backcrosses of double mutants to the inbred B73 confirmed that the transgene had not been silenced.

Results

Combining *fun* with the *na2* mutant shortened the stature of *na2* even further (Figure 4-3A). The extreme shortening appears to come from further shortening of the tassel, as well as increased shortening of internodes (Figure 4-3B). While *na2* has normal auricles (Figure 4-4A,D,G), the double mutant retains the ligule auricle boundary, but does not make normal auricle tissue (Figure 4-4B,E). Instead, the *na2;fun* double mutant produces a tough, thickened tissue that spreads from the midrib towards the blade margin, above the ligule auricle boundary (Figure 4-4G). Further, anastomosis of lateral veins occurs above the ligule auricle boundary in *na2;fun* double mutants (Figure 4-4C, F). While anastomosis of intermediate veins at the ligule auricle boundary is normal[53,55,86], lateral veins are not known to anastomose, nor do intermediate veins normally anastomose above the ligule auricle boundary.

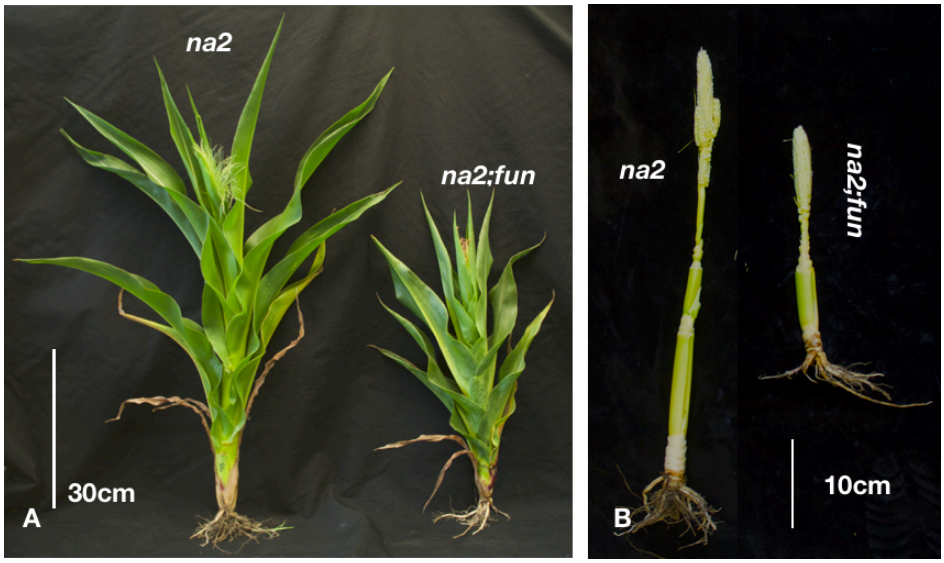

Figure 4-3: Whole plant phenotype of *na2* and *na2;fun* genotypes. Panel A shows two representative plants from family AV829 and panel B shows the same plants with all leaves removed.

Feminisation of tassels was measured by a number of metrics in family AV802. *bri1*::*RNAi* plants had more branches than normal siblings (Figure 4-5A), but these branches tended to be smaller than those of normal siblings. This trend was especially true for the upper branches, some of which consisted of only 3 or 4 spikelet pairs (Figure 4-5E). Branch number in *fun* and *bri1*::*RNAi*;*fun* plants was not significantly different from each other, but was greatly reduced as compared to normal and *bri1*::*RNAi* siblings. The length of tassel was different in each phenotypic class: normal siblings had the longest tassels, then *bri1*::*RNAi*, then *fun*, then *bri1*::*RNAi*;*fun* (Figure 4-5B). Both *fun* and *bri1*::*RNAi*;*fun* showed a high percentage of feminised branches (Figure 4-5C), and though this metric is not significantly different for *fun* and *bri1*::*RNAi*;*fun*, it can be seen from the images in Figure 4-5D,E that feminisation is more

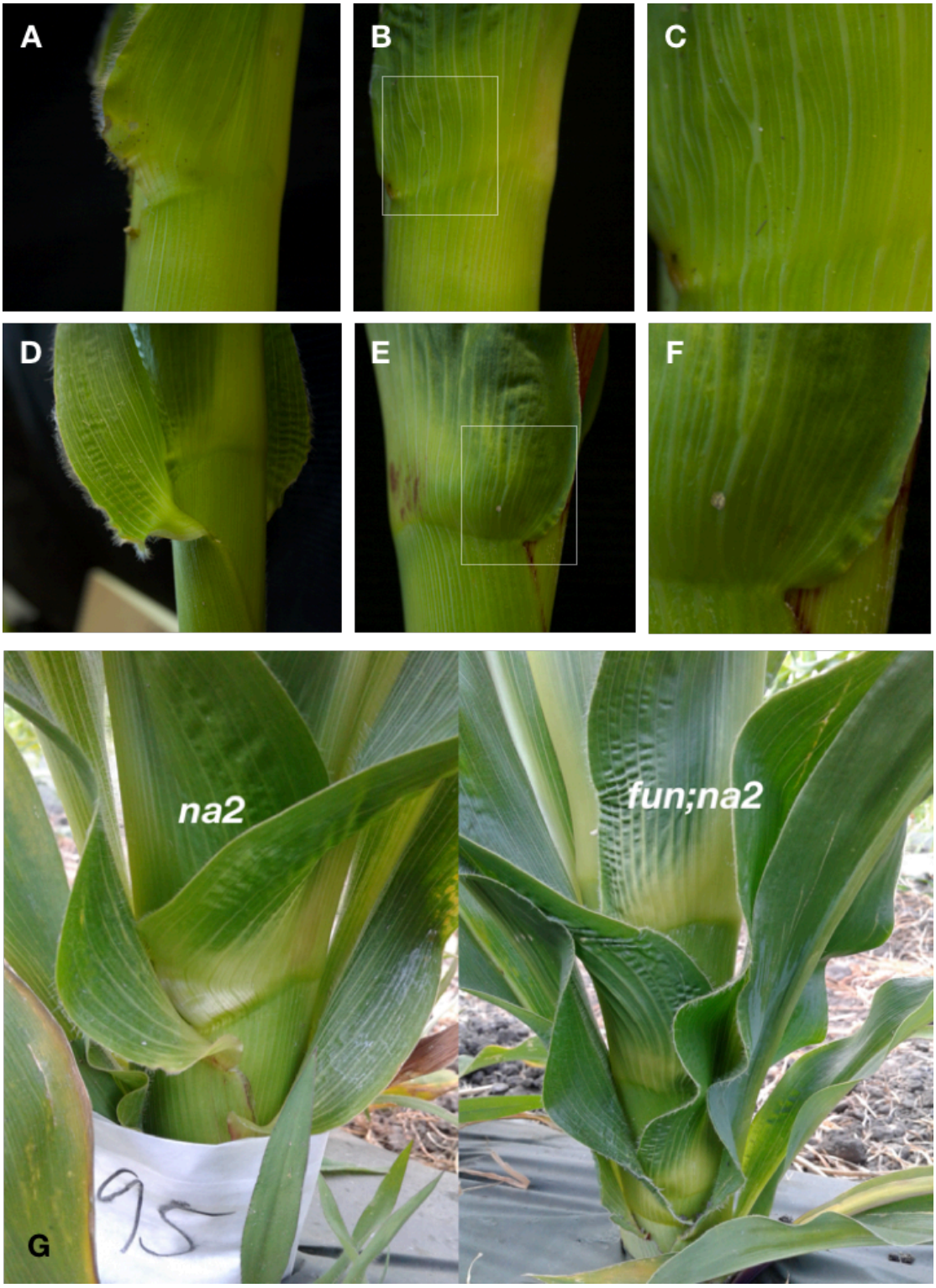

Figure 4-4: Leaf phenotype of *na2* and *na2;fun* genotypes. 9th (A,B,C) and 8th (D,E,F) leaves from top on *na2* (A,C) and *na2;fun* (B,D) plants with blow ups of highlighted region of B and D (C,F, respectively). G: Left: *na2* single mutant; right: *na2;fun* double mutant, family AV829. The double mutant lacks normal auricle tissue that can clearly be seen in the *na2* single.

Figure 4-5. Feminisation of *bri1::RNAi*, *fun* and double "mutant" plants. Graphs show branch number (A), length (B) and percentage of branches that bear female flowers (C) of mature tassels from family AV802, divided into their phenotypic classes. Panel D shows representative tassels of family AV800, including the rare *bri1::RNAi* tassels that show mild feminisation (marked with red arrows). Panel E shows these same tassels deconstructed. Statistical analysis was done in R using ggpubr. A Wilcoxon method was used, and p values of lower than 0.05 were considered significant.

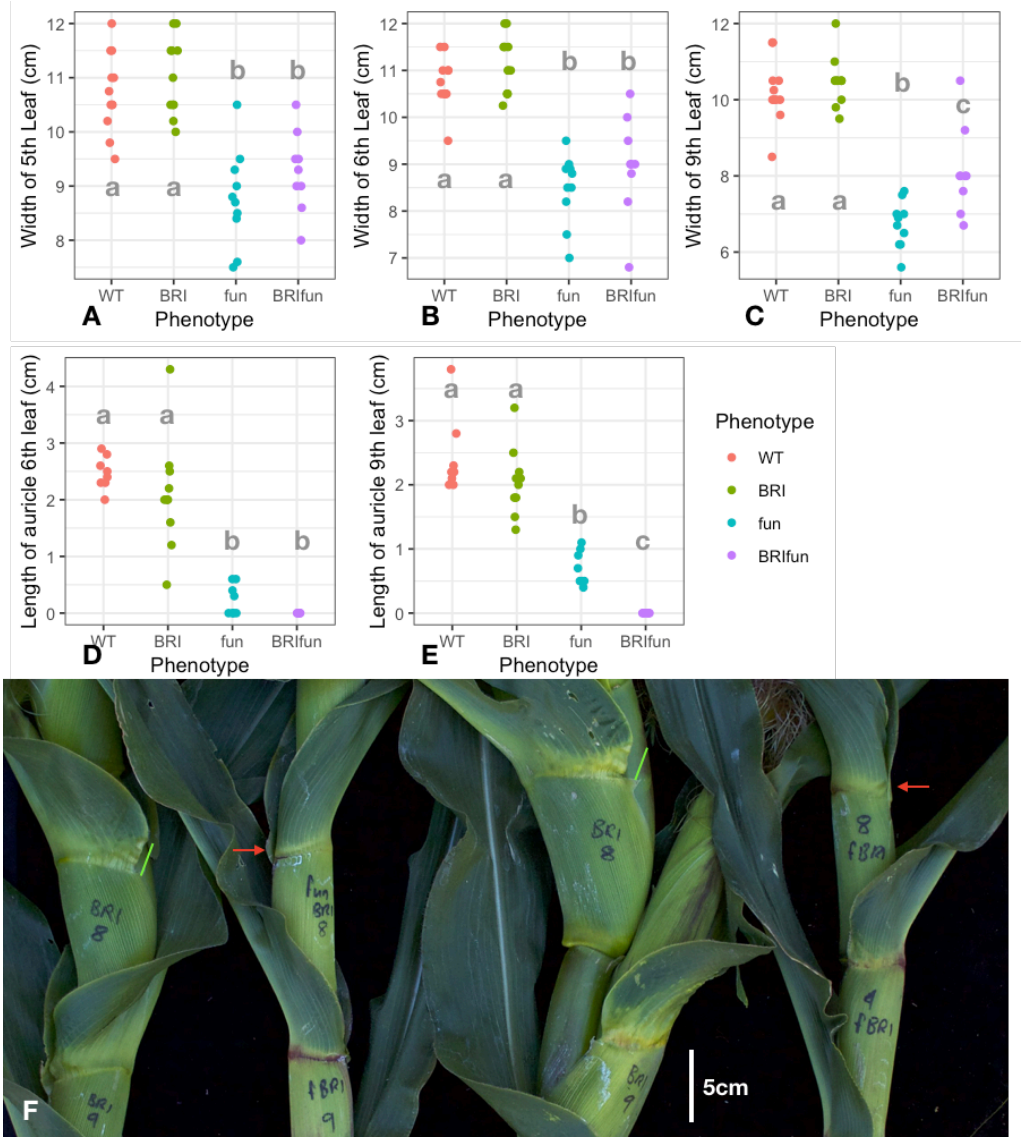

Figure 4-6: Leaf Phenotype of *bri1::RNAi*, *fun* and double "mutant" plants. Graphs show width of 5th, 6th and 9th leaf as counted down from the flag leaf as number "1" (A, B, C, respectively). Length of auricle is measured at the leaf margin as highlighted in green (F) and shown graphically in D and E for the 6th and 9th leaf from the top. F shows 8th and 9th leaves from the top of two *bri1::RNAi* plants and two *bri1::RNAi;fun* plants as labelled. Red arrows highlight the lack of auricle in *bri1::RNAi;fun* plants. Statistical analysis was done in R using ggpubr. A Wilcoxon method was used, and p values of lower than 0.05 were considered significant.

severe when combined with *bri1*::*RNAi* than feminisation in the single *fun* mutant. A few instances of feminisation may be observed in *bri1*::*RNAi* plants (Figure 4-5D, red arrows), but this is rare and was only observed in a couple individuals (Figure 4-5C) and has not been observed in previous publications of the *bri1*::*RNAi* phenotype[75].

Leaf width is not affected in *bri1*::*RNAi* plants as compared to normal siblings, and *bri1*::*RNAi*;*fun* plants mimic *fun* plants in leaves 5 and 6 and are of an

intermediate width in leaf 9 (Figure 4-6A-C). While no difference was detected in auricle size between *bri1*::*RNAi* and normal siblings, auricle size of *bri1*::*RNAi*;*fun* mimicked that of *fun* mutants in the 6th leaf, and the auricle was completely abolished in leaf 9 (Figure 4-6D-F). In family AV802, *bri1*::*RNAi* and *fun* plants were not significantly different in height from each other, and were shorter than normal siblings. *bri1*::*RNAi*;*fun* individuals were significantly shorter than the single mutants (see Figure 4-7). The *bri1::RNAi* phenotype was observed in family AV802, and progeny from a cross between *bri1*::*RNAi* plants from family AV802 and B73 showed the *bri1*::*RNAi* phenotype, confirming that the transgene had not been silenced.

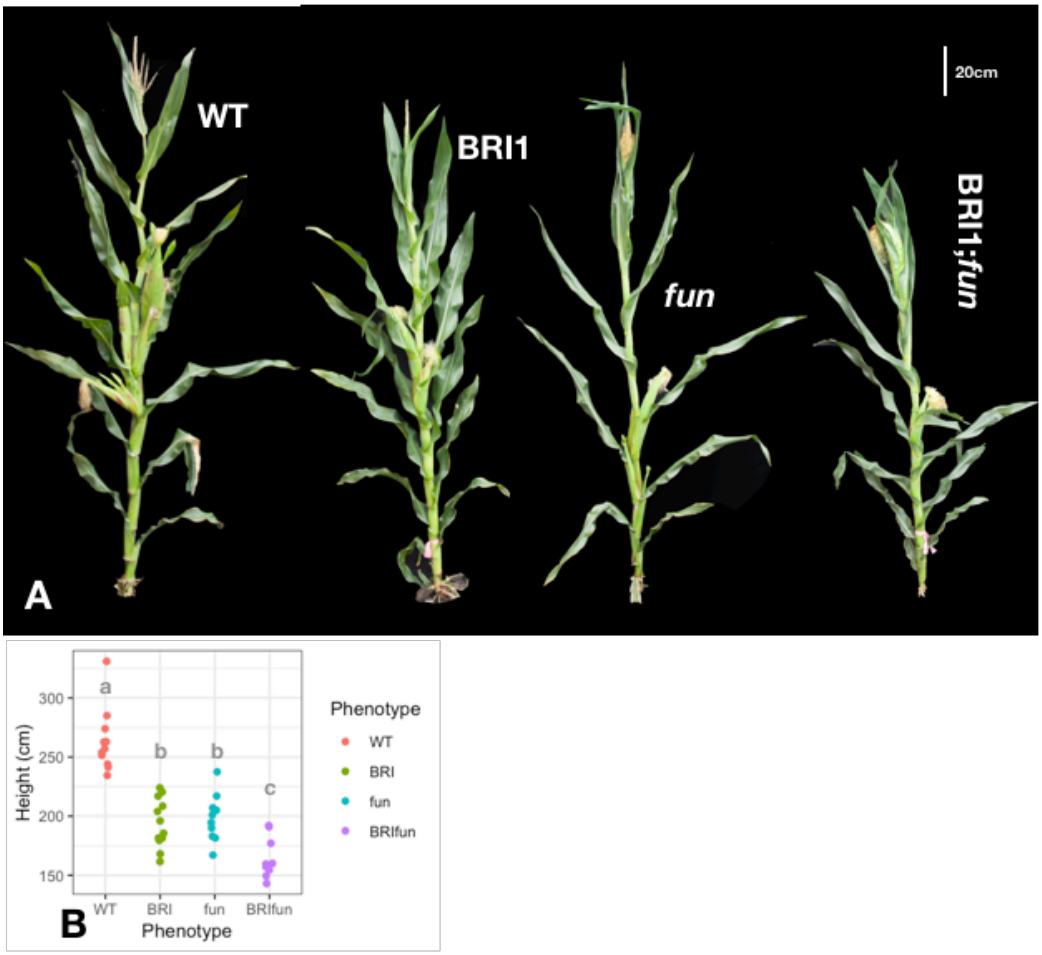

Figure 4-7: Whole plant phenotype of *bri1::RNAi*, *fun* and double "mutant" plants. The height phenotype of both *bri1::RNAi* and *fun* is clearly noticeable in panel A, along with the additive height phenotype of *bri1::RNAi*;*fun* plants. Heights of the plants are graphed in panel B. Statistical analysis was done in R using ggpubr. A Wilcoxon method was used, and p values of lower than 0.05 were considered significant.

Leaf width is reported to be wider than normal siblings in *bin2*::*RNAi* plants[83]. This difference was captured statistically in the 4th leaf from the top of the plant in family AV529, but was not found in the 5th leaf of family AV529, nor in any leaf measured in family AV804. Nevertheless, it was consistently observed in both families measured that combining *bin2*::*RNAi* with *fun* gave leaves of the same width as *fun* (Figure 4-8A-C). Similarly, the increased angle of *bin2*::*RNAi* plants as compared to normal siblings was not captured in

measurements, though it is clear that combining *bin2*::*RNAi* with *fun* gave leaves with a steeper angle (Figure 4-8E-F). The epistasis of the *fun* auricle phenotype and the wide angle of *bin2*::*RNAi* plants is most visible in photographs (Figure 4-8D; Figure 4-9C) rather than any of the quantitative measurements made. The distinctive crenulations of *bin2*::*RNAi* blades were observed on 23 of 25 *bin2*::*RNAi*;*fun* plants and 0 of 11 *fun* plants in family AV804 (images not shown).

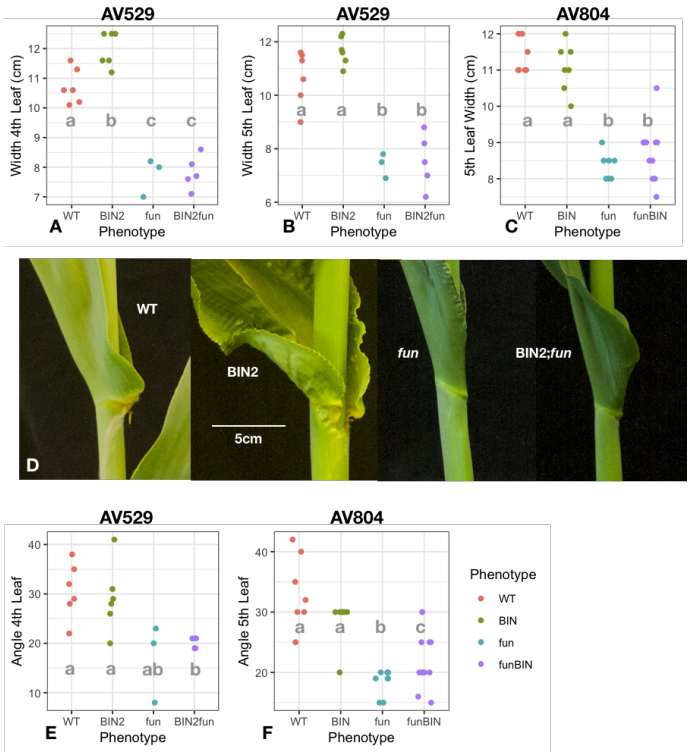

Figure 4-8: Leaf phenotype of bin2::RNAi, fun, and double "mutant" plants. Leaf width as measured at the midpoint is graphed in panels A-C, using the 4th leaf from the top in family AV529 (A), 5th leaf family AV529 (B) and 5th leaf family (AV804). Panel D shows the 5th leaf from the top of each genotype from family AV529. Panels E and F show the angle of the 4th and 5th leaves from the top of families AV529 and AV804 respectively. Statistical analysis was done in R using ggpubr. A Wilcoxon method was used, and p values of lower than 0.05 were considered significant.

bin2::*RNAi* plants are significantly shorter than normal siblings, and are statistically the same as *fun* plants. *bin2*::*RNAi*;*fun* plants are significantly shorter than *bin2*::*RNAi* plants, but not shorter than *fun* plants (Figure 4-9A). When the tassel is removed from the height measurements, *bin2*::*RNAi*, *fun* and *bin2*::*RNAi*;*fun* are not significantly different from each other, though significantly shorter than normal siblings (Figure 4-9B). This result suggests that differences in tassel size contribute to overall height differences seen between the genotypes. Measurements of internode length for each genotype show a similar pattern for all four genotypes (Figure 4-9D), suggesting that the height differences are not due to specific internodes.

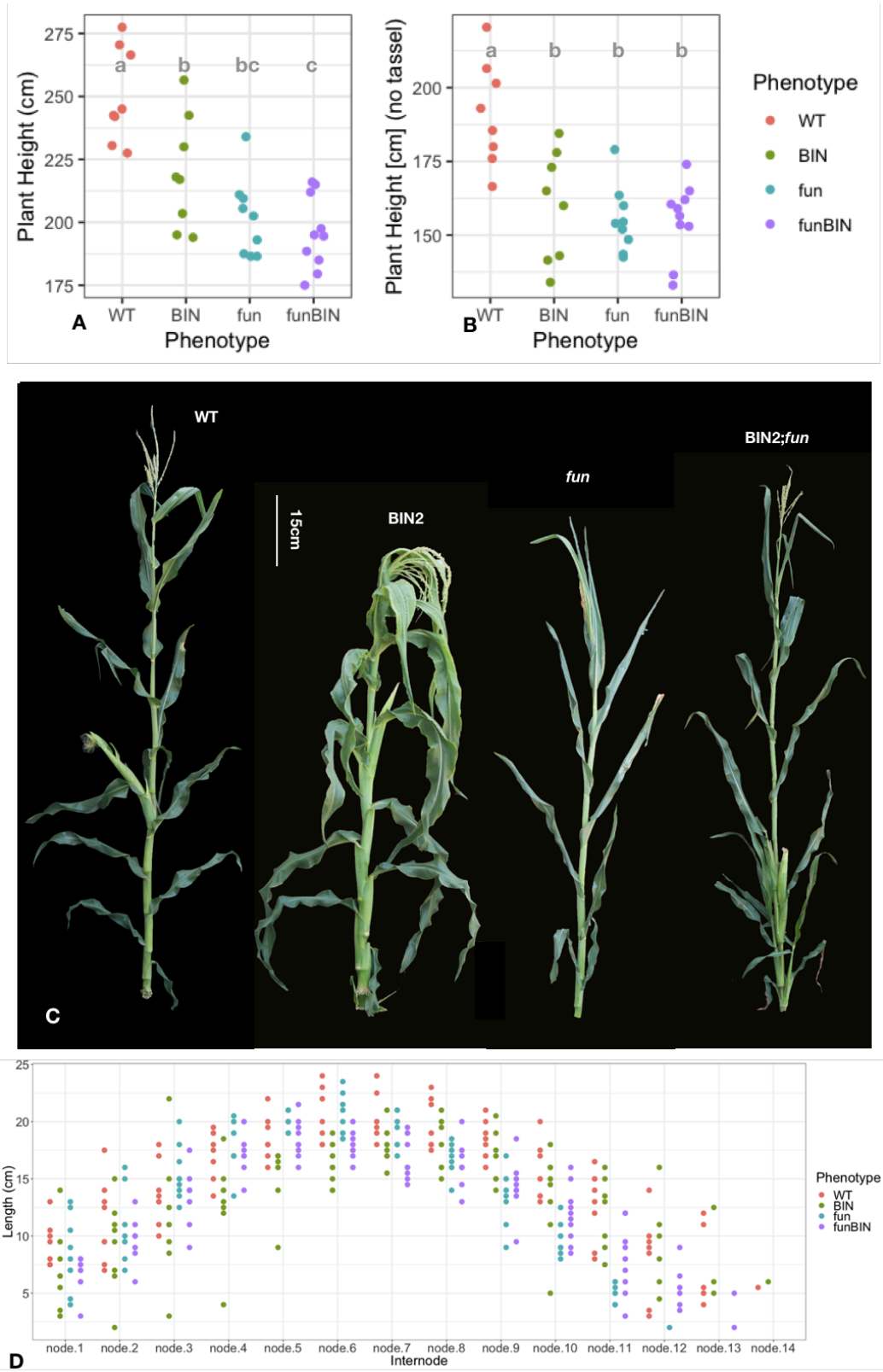

Figure 4-9: Whole plant phenotype of *bin2*::*RNAi*, *fun*, and double "mutant" plants. Panel A graphs the heights of each genotype, while panel B graphs the heights of each genotype excluding the tassel. Panel C shows the whole plant of each genotype to highlight the gross phenotype of *bin2*::*RNAi* and the abolishment of this phenotype in the *bin2*::*RNAi*;*fun* double. Panel D shows internode lengths. Statistical analysis was done in R using ggpubr. A Wilcoxon method was used, and p values of lower than 0.05 were considered significant.

No feminisation is observed in *bin2*::*RNAi* tassels, as might be expected from a constitutive BR responding plant. Combining *fun* with *bin2*::*RNAi* renders the tassels feminised on all metrics measured. Tassel length and branch number are both reduced to match the *fun* single mutant, and most branches are feminised (Figure 4-10A-D).

Discussion

When considering mutants with pleiotropic phenotypes, it is difficult to ascertain whether we are observing epistasis, additivity, or synergy simply because there may be epistasis for one phenotype, but not for another. Thus it is important to take into account all metrics when evaluating the mutant interactions. Taking each organ in isolation before coming to a synthesis can be a helpful approach. The *fun* and *na2* mutants interact both additively and synergistically in different tissues. The *fun* mutant acts additively with *na2* to reduce the overall height of the plant by further affecting the tassel and internodes. Since the *d5;na2* double mutant also showed additive effects for height[31], this could point to a role for FUN in the GA pathway. On the other hand, the synergistic interaction between *fun* and *na2* at the auricle would point to FUN's involvement in the BR pathway. These two data need not be in contradiction – Best *et al*.'s work clearly showed that the BR and GA pathways impinge on one another[31], and the FUN protein itself may be involved in this crosstalk.

Though there is very mild feminisation in the *bri1*::*RNAi* tassel, this is not an originally described phenotype of the *bri1*::*RNAi* line[75], nor is it common in family AV802 (Figure 4-5D). Further, the metric of branch number does not indicate feminisation in the *bri1*::*RNAi* tassel, though *bri1*::*RNAi* is slightly shorter which can be considered a feminine inflorescence trait. Lack of feminisation in the *bri1*::*RNAi* tassel is surprising since removing BR causes feminisation in the tassel in the *na1* and *na2* mutants. Combining the *bri1*::*RNAi* line with *fun* leads to more feminisation than *fun* alone, implying not simple epistasis by the feminised tassel of *fun*, but rather an enhancement of the very mild feminisation caused by *bri1*::*RNAi*. Similarly, the reduced height phenotype is enhanced in the double mutant (Figure 4-7).

Phenotype enhancement, or additivity, is also observed at the auricle. Though auricle size was not found to be smaller in *bri1*::*RNAi* plants in family AV802, a smaller auricle in *bri1*::*RNAi* plants has been reported[75]. Thus we can consider the completely absent auricle phenotype observed in *bri1*::*RNAi*;*fun* plants in family AV802, as compared to the *bri1::RNAi* and *fun* single mutants of AV802, as an enhancement of the reduced auricle associated with *fun*. No leaf width phenotype has been reported for *bri1*::*RNAi* plants, and *fun* appears to have simple epistasis of the leaf width phenotype.

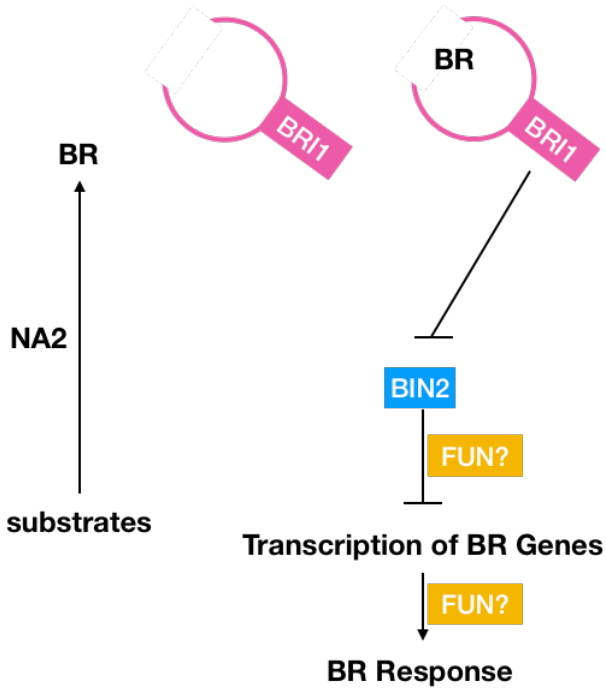

Figure 4-11: Possible locations of FUN in BR pathway. BRI1 and BIN2 locations based on review [74]. FUN predicted to be downstream of BIN2 perhaps in the transduction of signal to transcription, or downstream of transcription of relevant genes.

According to almost all metrics measured, *fun* is epistatic to *bin2*::*RNAi*. The oversized auricle of *bin2*::*RNAi* is completely abolished in the double mutant. Since increased leaf angle has been linked to BR hypersensitivity in rice[76] as well as appearing in this *bin2*::*RNAi* line, it is reasonable to assume that this monstrous auricle is a product of BR hypersensitivity, and by extension, auricle growth is promoted by BR. The fact that the *fun* mutation abolishes this auricle growth is strong support for the function of FUN in the BR pathway, downstream of *bin2*::*RNAi*. On the other hand, the retention of leaf blade margin crenulations in the double mutant does not fit into this explanation, unless FUN is simply not expressed along the margin, which would be consistent with the *Wab1*;*fun* double mutant (see Chapter 2).

The strong feminisation seen in the double mutant is further support for the placement of *fun* downstream of *bin2*::*RNAi* in the BR signalling pathway. BR is known to accumulate in developing anthers[31], and hence is a hormone associated with masculinity in maize. The fact that loss of normal FUN produces feminisation in the *bin2*::*RNAi* background also supports the hypothesis that FUN is in the BR pathway, downstream of BIN2.

Taking together these phenotypes and interactions, this analysis supports the hypothesis that *fun* functions late in BR pathway, perhaps at its intersection with GA. Additivity with *na2* for height is observed as with the *d5* GA

knockout mutant. At the same time *fun* enhances the feminisation phenotype of BR deficient *na2* and acts additively with the BR insensitive *bri1:RNAi* while abolishing the phenotypes of the hyper-responder *bin2:RNAi*. Figure 4-11 shows FUN's tentative placement in the BR pathway.

Jasmonic Acid

Classical mutants *tasselseed1* (*ts1*) and *ts2* were first described by Emerson in 1920 following the "freak" class exhibition of the Annual Corn Show in Lincoln, Nebraska 1913-14[87]. Together with the classical mutant *silkless1*, described by Jones in 1925[88], these mutants have elucidated the role of JA in sex determination in *Zea mays*. The *ts* mutants bear tassels that are heavy with seeds, so that they bend over from their own weight at maturity. All or most flowers will be female, but the tassel retains a normal degree of branching that is not seen in the ear or *fun* mutant tassels[87]. Upon cloning, *ts1* was found to be a lipoxygenase that catalyses a step in the JA biosynthetic pathway[35]. While the function of the alcohol dehydrogenase encoded by *ts2*[36] has not been definitively shown, the similarity of the *ts1* and *ts2* phenotype, the lack of any interaction in the *ts1*, *ts2* double mutant[89], and rescue of the *ts2* phenotype by JA application[35] supports the hypothesis that it is also in the JA pathway.

The *sk1* mutant is described as developing normal cobs but failing to produce any silks such that even stripping back the husk leaves and pollinating directly onto the ear failed to produce any kernels. No differences in the tassel nor the vegetative parts of the plant were originally noted[88] but it was later observed that *sk1* has less tassel branches than normal siblings[90]. Combining *sk1* with the mutants *ts1* and *ts2* put *sk1* in the same pathway, (*i.e.* the JA pathway). Though in the first generations of the double mutant *sk1* and *ts2*, partial epistasis was observed[89,91], two further rounds of self pollinations of these double mutants revealed complete epistasis by *ts2*[92]. That is, both the tassel and the ear bear silks. From this it was concluded that *sk1* in some way inhibits the silk killing product of *ts2*[92], supposedly, JA[35,36]. This has been supported by the cloning of SK1 as a uridine diphosphate (UDP)-glycosyltransferase, the overexpression of which resulted in very low JA accumulation in developing tassels and a feminised tassel phenotype[37]. In summary: SK1 breaks down JA that would otherwise lead to pistil abortion. In a normal tassel, JA accumulates in the pistils and they abort; in a normal ear, SK1 degrades the JA and prevents silk abortion.

Methods

Two families were planted in the greenhouse at the same time, one segregating for *ts1* (AV720), and the other segregating for *fun*. *ts1* plants were identified by genotyping (see Appendix 3), and *fun* plants were identified by their leaf phenotype at 4 weeks. Dissection of SAMs of normal siblings allowed staging of the mutant plants in each family and when SAMs transitioned to

inflorescence meristems (4-5 weeks after sowing) JA applications were begun. Every 2 days for 4 weeks, 1ml of 1mM JA in 0.016% tween was applied by pipette into the whorl of *ts1* and *fun* plants.

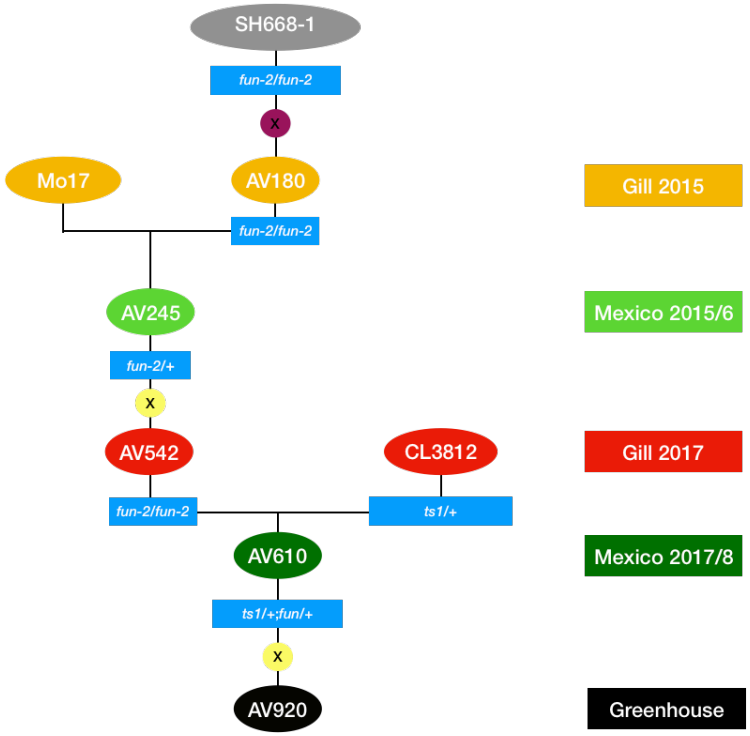

Figure 4-12: Genealogy of families used in JA treatment and construction of *ts1*;*fun* double mutant. Note that the second allele *fun-2* (see Chapter 4) was used for this analysis.

A family segregating for both *ts1* and *fun* was constructed according to the genealogy detailed in Figure 4-12. Note that the second allele *fun-2* was used for this experiment. Family AV920 was planted in the greenhouse in December 2018. The family was genotyped for *ts1* according to Appendix 3, and phenotyped for *fun*. At 4 weeks, JA applications were begun as detailed above. These plants were grown to maturity and phenotyped.

Family AV846 was generated by crossing a *fun*/*fun*;*sk1*/+ plant from family AV369 with a *fun*/+;*sk1*/*sk1* sibling. The family segregated normal:*sk1*:*fun*:double 14:19:13:11 which is close to the expected 14:14:14:14 (rounded down to nearest whole). The *sk1* plants were identified by their distinctive lack of silks in the ear, while *fun* plants were identified by their leaf phenotype since the double possessed a novel tassel phenotype.

Results

The first treatment of *ts1* and *fun* plants with JA was successful at rescuing the *ts1* plants, but not the *fun* plants. The treated *fun* plants bore female flowers that produced silks on tassels that were short and had few branches. There was very little visible difference between treated and untreated *fun* tassels. Conversely, treated *ts1* plants bore only male flowers and their tassels were longer than the untreated *ts1* plants (Figure 4-13).

The second JA treatment using family AV920 segregating for both *ts1* and *fun* (Figure 4-14, 4-15) also showed rescue of *ts1* plants by JA application, but the results of JA application on *fun* plants were more ambiguous. JA application rescued tassel length in *fun* plants but did not rescue branch number (Figure 4-14, 3.15). Although feminisation was observed in some *fun* plants treated with JA, there was much less feminisation observed in treated *fun* plants than untreated *fun* plants. Treated *ts1* plants did not show any feminisation of the tassel (Figure 4-14, 3.15) while untreated *ts1* plants showed some.

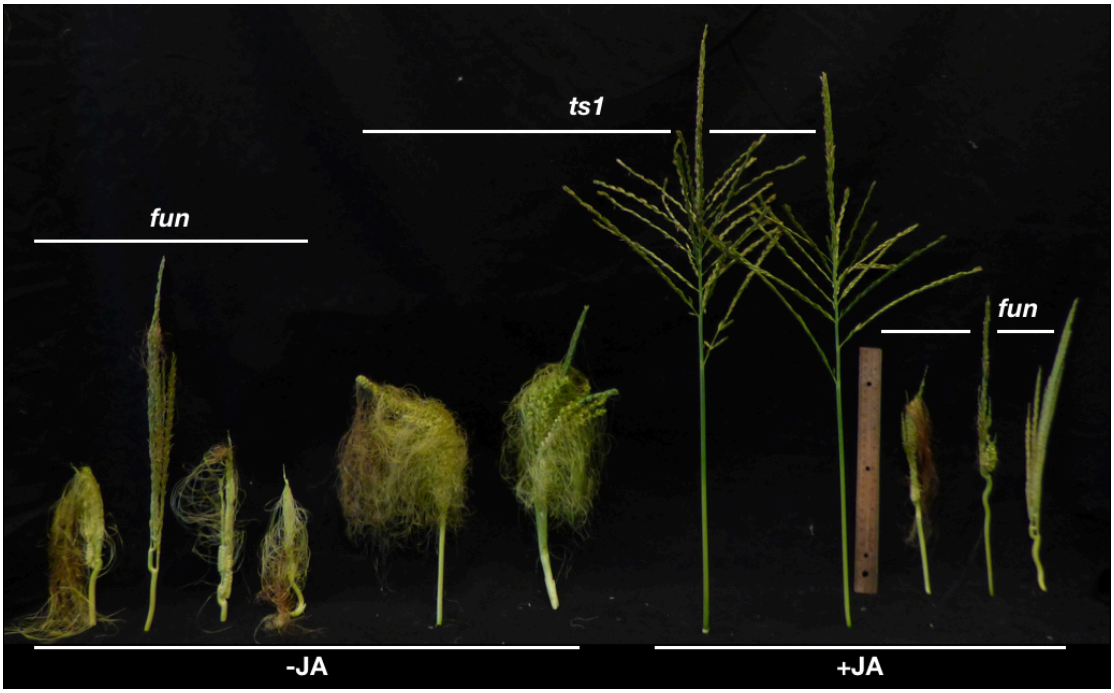

Figure 4-13: JA treatment pilot experiment. JA completely rescues *ts1* mutant plants, but application of JA does not affect the phenotype of *fun* plants.

Family AV920 also contained *ts1*;*fun* individuals. These plants bore very short tassels, with few branches, that were completely feminised (Figure 4-14, 4-15). Lack of abortion of the lower spikelet was frequently observed in feminised tassel flowers in *ts1*, and *ts1*;*fun* plants, while this was not observed in *fun* plants (Figure 4-16). One *ts1*;*fun* plant was also treated with JA, this plant bore a long tassel with very few tassel branches (Figure 4-15G). The flowers of the *ts1*;*fun* plant treated with JA could not be definitively characterised as male or female. They bore neither silks nor anthers, and were fatter than normal male spikelets as well as being glabrous (Figure 4-16). They resembled half-way feminised spikelets observed on a *sk1*;*fun* from family AV152 (Figure 4-17). Further, the JA treated *fun* tassels resembled the *sk1*;*fun* double mutant tassels.

sk1 mutants are the same height as non-mutant siblings and the *sk1*;*fun* double mutant was the same height as *fun* (Figure 4-18A). *sk1* mutants do not differ from non-mutant siblings for tassel length and combining *sk1* with *fun* rescued

the tassel length, except for two very short outliers. As observed by Zhao *et al*., *sk1* plants in families AV152 and AV846 had fewer tassel branches than normal siblings[90] (Figure 4-18C). The double mutant had significantly fewer than *fun* or *sk1*, with some double mutant tassels having no tassel branches at all (Figure 4-18E,C). Combining *sk1* and *fun* abolished silks from the tassel, though glabrous, thickened glumes remained on some spikelets (Figure 4-17A, 3.18E).

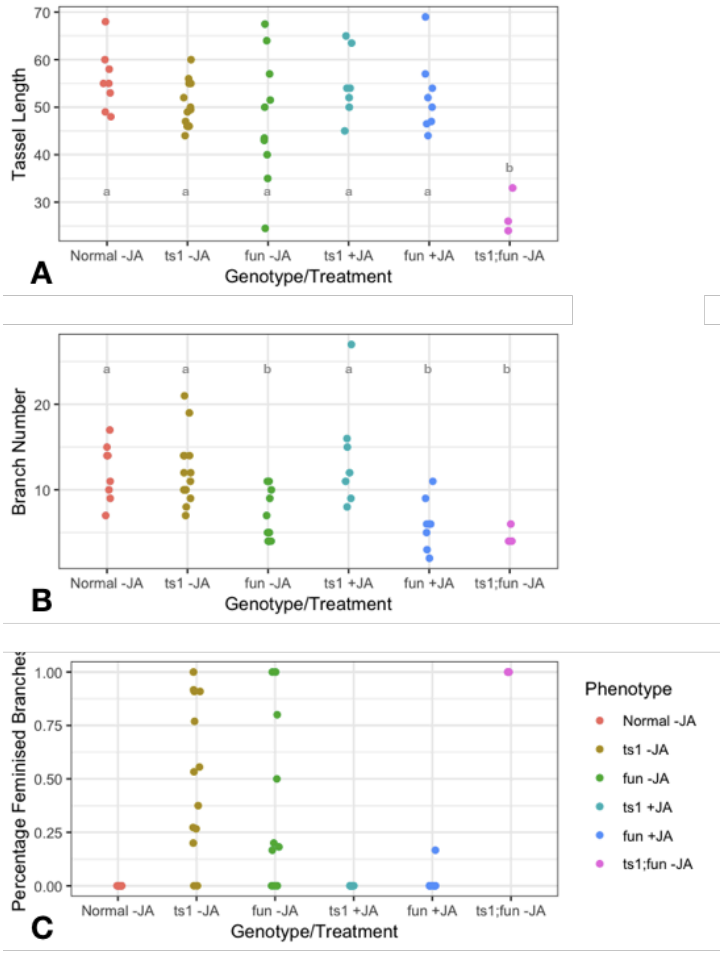

Figure 4-14: Tassel measurements from JA treated and untreated plants family AV920. Tassel length (A) is same as normal in *ts1* treated and untreated plants. *fun* plants have more variable (but not significantly different) tassel lengths than normal in this family, and are known to have shorter tassels (Chapter 2), but this appears rescued by JA. Combining the *fun* and *ts1* mutations leads to very short tassels. Branch number (B) is not affected in the *ts1* background, with or without JA treatment as compared to normal siblings. As previously described (Chapter 2), branch number is reduced in *fun*, and this is not rescued by JA application; in the *ts1*;*fun* double mutant, the branch number is reduced to *fun* levels. No feminised branches (C) are seen in JA treated *ts1* tassels, nor normal tassels, while untreated *ts1* tassels are heavily feminised. JA treatment reduces the degree of feminisation in family AV920. Statistical analysis was done in R using ggpubr. A Wilcoxon method was used, and p values of lower than 0.05 were considered significant.

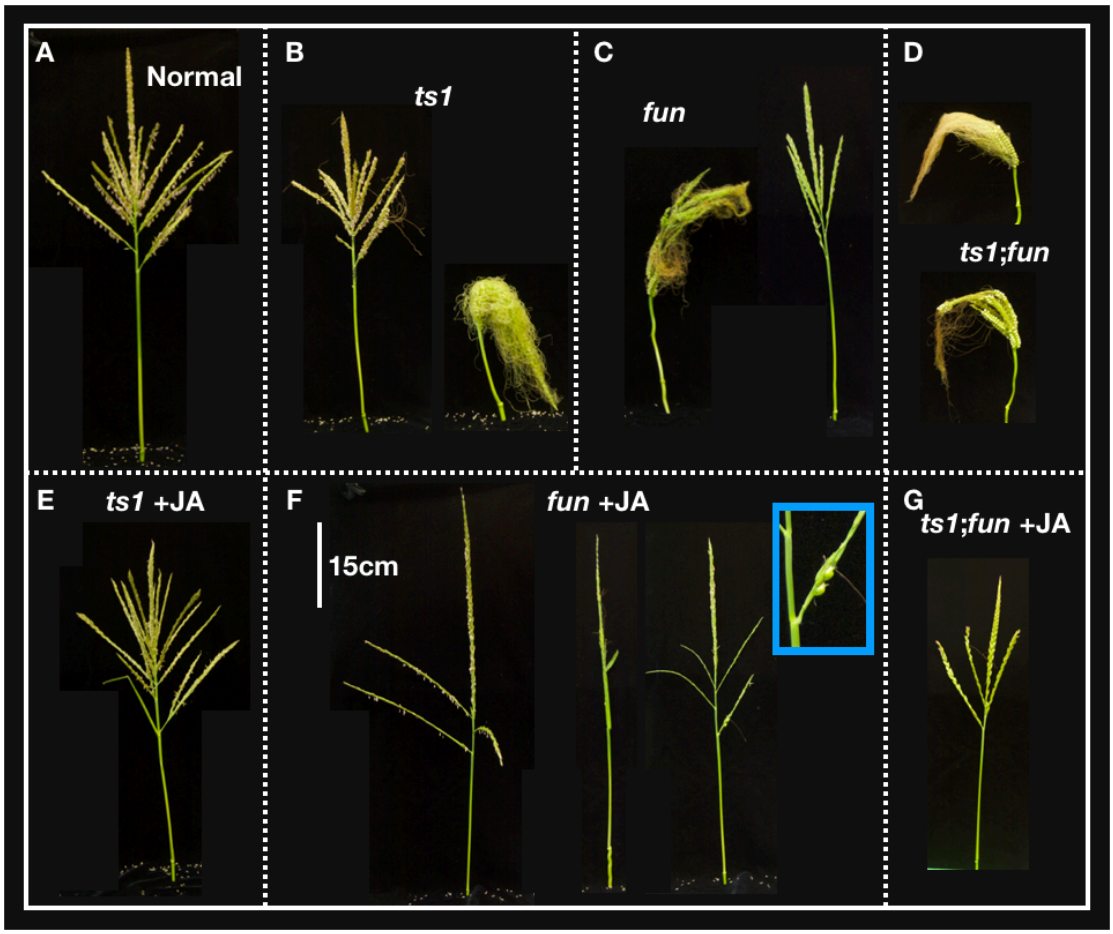

Figure 4-15: Normal, *ts1*, *fun*, *ts1*;*fun* tassels (A-D) and *ts1*, *fun* and *ts1*;*fun* tassels treated with JA (E-G) of family AV920 (Figure 4-12). B and C show the extremes of most masculine and most feminine of each phenotypic class. A range of phenotypes of JA treated *fun* is shown in panel F, with a close up of a feminised branch of the extreme right tassel (inset). All tassels to scale.

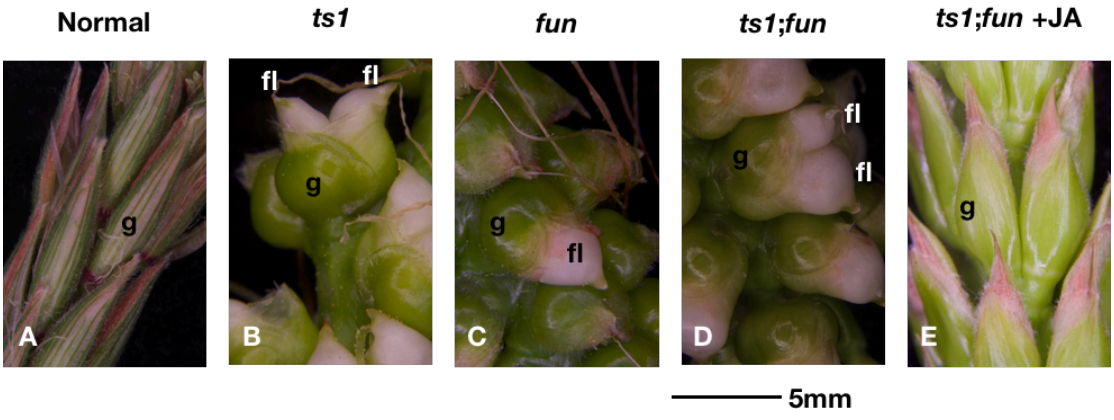

Figure 4-16: Tassel flower feminisation. Normal siblings with masculine flowers, g marks a glume (A). *ts1* spikelet with two florets (marked fl) and glabrous glumes (B). *fun* spikelet with glabrous glumes and single floret (C). *ts1*;*fun* spikelet with glabrous glumes and two florets (E). *ts1*;*fun* flowers treated with JA showing glabrous glume, but no outgrowth of florets (E).

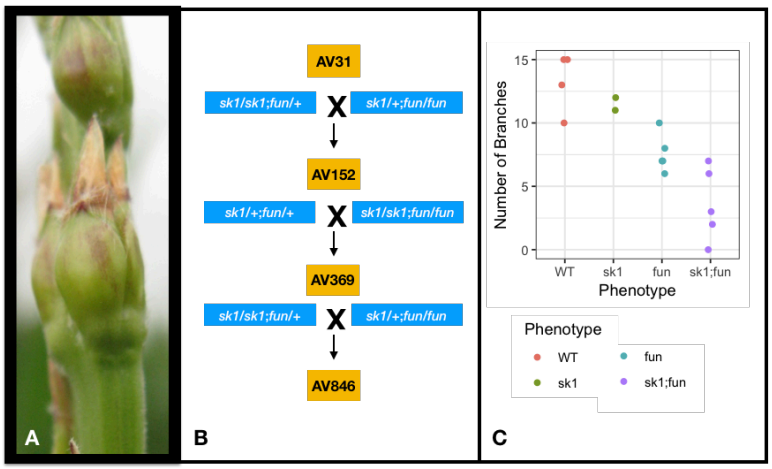

Figure 4-17: Family AV152 and genealogy of *sk1* families used in this study. Panel A shows a partially feminised spikelet pair found on a *fun*;*sk1* tassel in family AV152. Panel B shows the genealogy of *sk1* families. Panel C shows tassel branch numbers of the different genotypes of family AV152 for which there were not enough data points to create confident statistical tests, but is shown here for completeness.

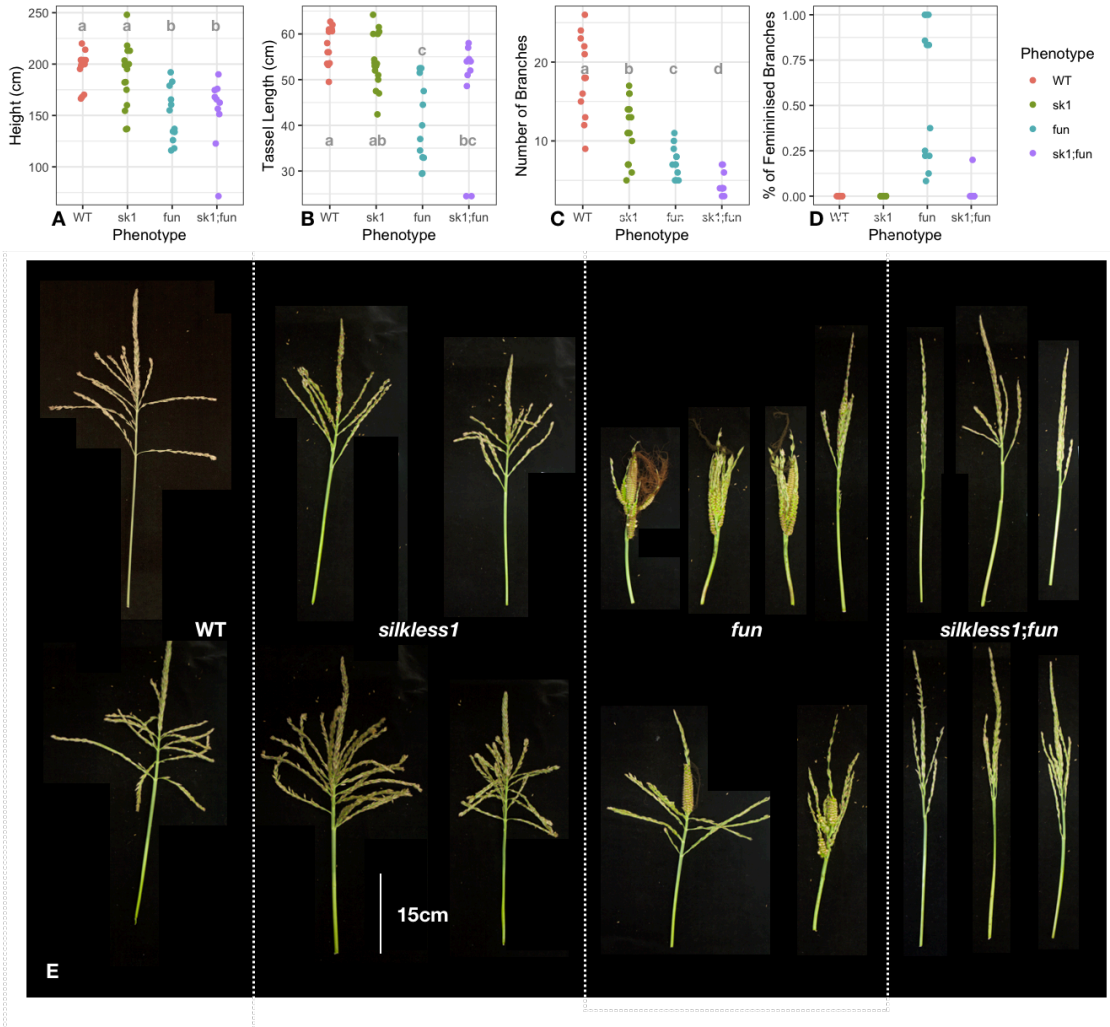

Figure 4-18: Tassel and height phenotypes of normal, *sk1*, *fun* and double mutant genotypes from family AV846. Panels A-D graph height, tassel length, branch number and percentage of feminised branches, respectively. Statistical analysis was done in R using ggpubr. A Wilcoxon method was used, and p values of lower than 0.05 were considered significant. Panel E shows representative examples of each genotype's tassels.

Discussion

Since addition of JA was unable to fully rescue the feminised tassel of *fun* plants, FUN is unlikely to be deficient in JA. Though failure to correct the feminised phenotype was more obvious in the first application of JA (Figure 4-13) family AV920 still showed a failure to rescue by JA application when branch number is considered. AV920 was not ideal for this experiment because the *fun* plants in this family were not heavily feminised. This could have been due to the fact that they were grown in the winter greenhouse – greenhouse grown *fun* plants have been observed to be less feminised than those grown in the field, and the winter greenhouse is particularly sub-optimal for growing corn. Further these plants were the *fun-2* allele, which has not been adequately characterised, but may have lower feminisation severity than the original *fun-1* allele. Finally, the genealogy of these plants contains a recent cross to Mo17, which may have reduced the severity of the phenotype (Figure 4-12), as well as the fact that some of the *fun* plants were heterozygous for *ts1* (though higher masculinisation due to heterozygosity for *ts1* is counterintuitive). Nevertheless, JA application to *fun* and *ts1* plants in family AV920 did not refute the original experiment showing that JA is unable to fully rescue the feminised tassel phenotype of *fun* plants.

ts1 and *fun* can be considered additive in their effects on feminisation of the tassel. Double mutant tassels were more heavily feminised than either double mutant, supporting the hypothesis that *ts1* and *fun* are in different pathways. The lack of lower floret abortion in the tassel of *ts1* and *ts1*;*fun* plants compared to successful lower floret abortion in *fun* plants (Figure 4-16) further supports the hypothesis that *fun* is not deficient in JA since JA is required for lower floret abortion in the ear[36].

The loss of silks in the *sk1*;*fun* further refutes the hypothesis that FUN is involved in the production of JA. A JA biosynthetic mutant would be expected to retain silks in combination with *sk1*, as previously shown with *ts1* and *ts2*[89]. The retention of feminised traits in the form of glabrous, thickened glumes in the double mutant (Figure 4-17A) implies an additive interaction – the *fun* mutation is still causing aspects of feminisation in the tassel, though the lack of functional SK1 cannot protect the silk from abortion by the action of JA. Branch loss in both *sk1* and *fun*, and the additivity in the double is a complex set of observations. Though branch loss is a feminine trait since the ear is branchless and tassels are branched, the *sk1* mutant also has branch loss. *sk1* is presumably high in JA due to the loss of the SK1 gene that is responsible for JA degradation. This high JA allows silk abortion, and so would seem to be a masculine characteristic. Paradoxically, this loss of functional SK1 is also associated with the feminine trait of less branching in the tassel, implying a role for JA in branch inhibition during tassel development. Since there is an additive interaction between the *sk1* and *fun* mutations, and addition of JA to developing *fun* tassels lead to tassels that resembled the *sk1*;*fun* double mutant tassels, the hypothesis of FUN being outside of the JA pathway is supported.

The *D9/fun* double mutant

If we consider JA and BR as masculinising hormones in *Zea mays*, GA can be thought of as a feminising hormone. In the 50s, Nickerson showed that application of GA directly to the whorl during tassel development was sufficient to induce feminisation of the terminal inflorescence[27]. In the early 80s it was shown that developing ears have GA levels two orders of magnitude higher than in developing tassels[66]. The *d1* mutant in maize was shown to block steps in the GA biosynthesis pathway[65,93,94] and when the gene was cloned it was found to be a GA_3 oxidase that catalyses the final step in bioactive GA synthesis[63]. While the most striking phenotype of *d1* is its tiny stature, more pertinent to this discussion is its ear phenotype, dubbed "anther ear". Without the presence of GA, the anthers of the ear do not arrest and instead grow out to produce bisexual flowers in the ear while the flowers of the tassel are normal[63]. As such it is perhaps erroneous to call GA a simple feminising hormone – rather it is a male killer hormone. The mRNA coding for D1 protein was shown by *in situ* to accumulate in stamen primordia of the developing ear[63] which undergo cell cycle arrest and ceases growth early in its development[67]. *d1* mutant plants do not undergo this stamen primordia arrest in the ear[63]. Since the *fun* mutant was feminised in the tassel, we made crosses to GA mutants and applied paclobutrazol (PBZ) which is an antagonist of the GA pathway and has applications as a plant growth retardant and fungicide[95]. PBZ blocks the ent-kaurene oxidation step of GA biosynthesis, and thus plants treated with this compound are unable to produce GA[95]. PBZ has been used to investigate the role of GA in maize, and to elucidate the nature of dwarf mutants in the GA pathway[96].

The dominant *D9* mutant was obtained from the maize stock centre and is similar to the *D8* maize mutant[96], which both bear similarities to the biosynthetic *d1* mutant. *D8* and *D9* are both dwarf, have increased tillering, and display varying degrees of anther ear. All the *D8* alleles described have anther ear, while *D9* displays full anther ear in some backgrounds, but in others it develops anthers up to the point that they are visible with a magnifying glass[96]. The D8 locus on chromosome 1 encodes a DELLA protein, and D9 has been shown to encode a duplicate of this protein[96,97] located on chromosome 5. DELLA proteins are part of the Gibberellic Acid (GA) signalling pathway, and act to repress the GA response[98] . Many DELLA mutants are constitutive repressors of the GA response and they have been made famous by the so-called "Green Revolution" which included wheat and rice plants that were dwarfed by their inability to respond to GA[99]. Both *D8* and *D9* maize mutants do not respond to application of GA_3 that causes an increase in height in normal siblings[65,96]. Neither *D8* nor *D9* are as short as plants treated with PBZ, nor as short as GA biosynthetic mutants like *d1*, which suggests there are other GA receptor pathways in addition to D8 or D9 in maize[96].

Methods

Crosses were made to both *D8* and *D9*, unfortunately, none of the *D8*;*fun* double mutant families I attempted to create were successful, so instead the *D9* family was used with its less obvious anther ear phenotype. Stock from the Maize Genetics Cooperative (502C) were used to plant family AV274 segregating for *D9*. A *D9* plant from AV274 was backcrossed to B73 to produce AV353. From family AV353, a *D9* plant was crossed to a *fun* plant from AV360 to produce family AV618. A *D9*/+;*fun*/+ plant was then crossed to a *fun*/+ sib to create AV807. Family AV807 segregating for both *D9* and *fun* was grown in the Gill Tract field in the summer of 2018. Family AV807 segregated 15:16:8:5 for normal:D9:*fun*:D9;*fun,* as compared to the expected 18:18:6:6 (rounded up to nearest whole). *D9* plants were first identified by their consistently shorter stature, which was confirmed by co-segregation with a short tassel phenotype (Figure 4-19A), and *fun* by the missing auricle and feminised tassel phenotype. The double was identified as having a combination of these phenotypes – very short stature accompanied by auricleless leaves and feminised tassels.

PBZ treatment was used to test the effects of no GA on *fun* mutant plants. A family of maize segregating for *fun* was grown in the greenhouse for 4 weeks until the *fun* phenotype was apparent. 5 *fun* plants and 5 normal siblings were treated every 2 days with 1 litre of 90μM PBZ applied to the pot. Five of each phenotypic class were treated with 1 litre of water every 2 days as controls.

Results

Combining *D9* with *fun* made plants shorter than either single mutant alone (Figure 4-20A,C). These double mutant plants continued to show the leaf phenotype of *fun* plants (Figure 4-20B). Despite variation in the degree of feminisation in both *fun* and D9;*fun* plants in family AV809 (Figure 4-19C,D), feminisation of the double mutant was clear and associated with fewer branches in the tassel. No feminised tassel flowers were observed in the D9

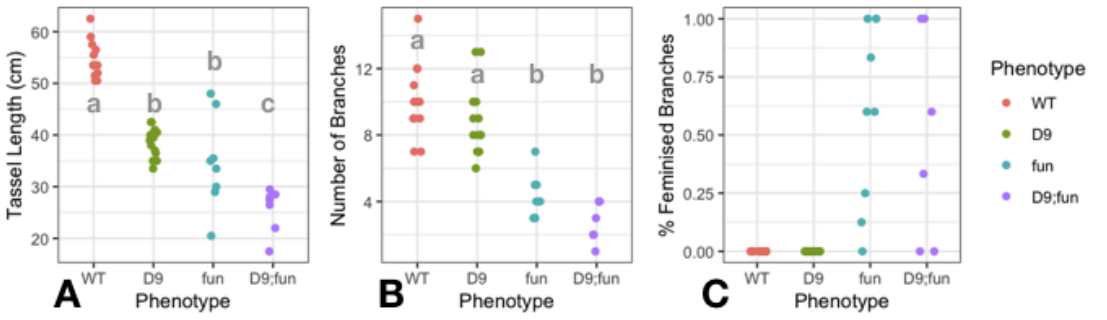

Figure 4-19: Tassel phenotypes of normal *D9*, *fun* and *D9*;*fun* plants. Panels A-C graph the tassel length, number of branches, and percentage of feminised branches, respectively. Statistical analysis was done in R using ggpubr. A Wilcoxon method was used, and p values of lower than 0.05 were considered significant. Panel D shows the tassels of *D9* and *D9*;*fun* plants from Figure 4-20A stripped of their leaves. These tassels are photographed together with the bases of the plants on the ground, so the differences in height are real. As can be seen, there is a range of feminisation in the double mutants of this family, but reference to panel C shows that this range of feminisation is seen in both *fun* and *D9*;*fun* plants in this family.

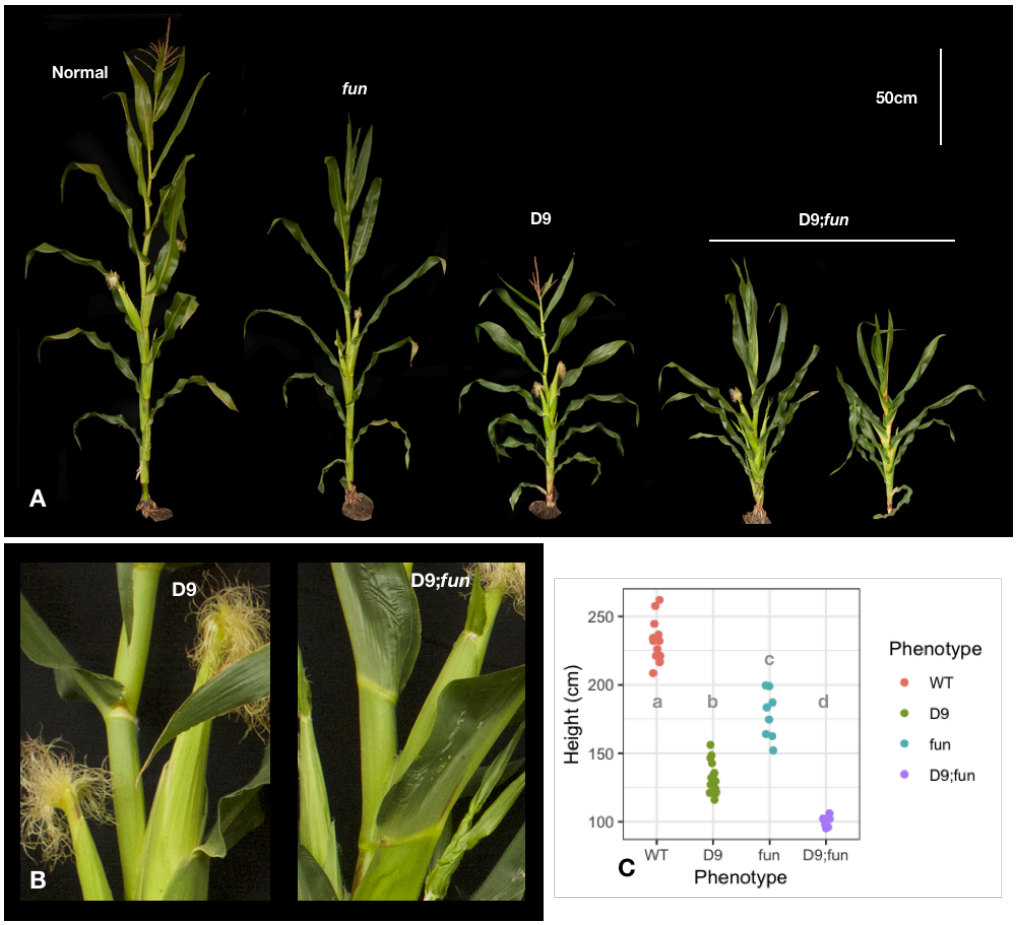

Figure 4-20: Leaf and whole plant phenotypes of *fun*, *D9* and double mutants. Panel A shows representative whole plant pictures of each phenotype, as labelled. Panel A makes the differing height phenotypes of *fun* and *D9* obvious, and the additive nature of these phenotypes is especially obvious in the *D9*;*fun* plant on the far right. Panel B shows the auricle above the ear of a *D9* and *D9*;*fun* plant to show that the *fun* auricle is epistatic to the normal *D9* auricle. Panel C graphs the heights of all plants in family AV807. Statistical analysis was done in R using ggpubr. A Wilcoxon method was used, and p values of lower than 0.05 were considered significant.

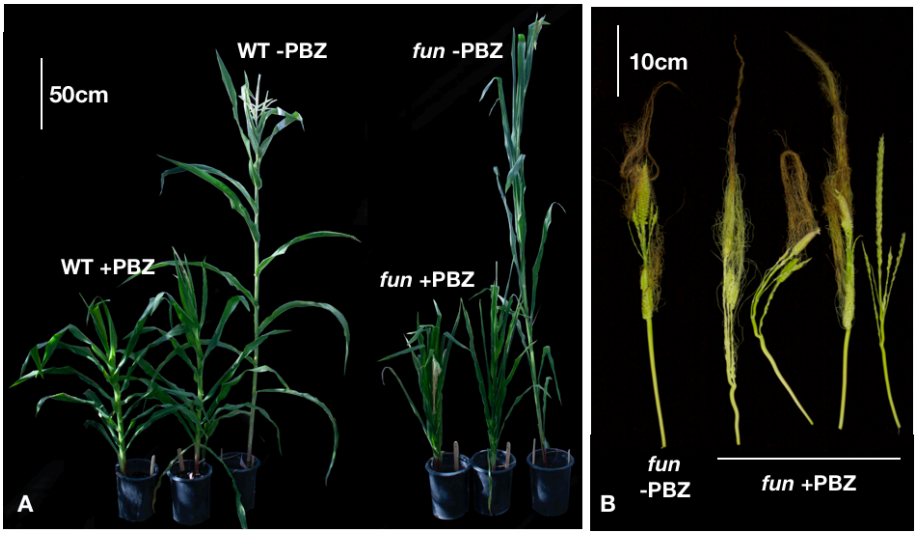

Figure 4-21: Paclobutrazol treatment of normal and *fun* plants. Panel A shows the effects of PBZ on the heights of normal (WT, left) and *fun* (right) plants. Panel B shows that treatment with PBZ does not affect the feminisation of *fun* tassels, with PBZ treated tassels displaying feminisation like untreated.

single mutant (Figure 4-20B). Tassel length, though usually a helpful proxy for feminisation, is not appropriate to use here because of the non-feminised shortening of the tassel observable in *D9*. The short tassel phenotype of *D9* translated to the double mutant displaying even shorter tassels than either of the single mutants (Figure 4-20A).

Both normal and *fun* plants were affected by the PBZ treatment as compared to untreated siblings. Once treatment was started, the plants barely grew any taller, while untreated plants grew to full size (Figure 4-21A). PBZ treatment did not affect the feminisation phenotype of *fun* mutants (Figure 4-21B), nor did it affect the leaf phenotype.

Discussion

The additivity of reduced height in the D9;*fun* plants points to *fun* being outside of the DELLA GA response pathway. Since blocking GA biosynthesis with PBZ also had an additive effect on height of *fun* plants, the reduced height phenotype of *fun* is unlikely to be due to defects in GA biosynthesis or perception in the *fun* mutant. The feminisation of *D9*;*fun* tassels, as well as the epistasis of the *fun* leaf phenotype support the hypothesis that the *fun* phenotype is not due to defects in the GA pathway. Similarly, since blocking GA with PBZ did not affect the feminisation of the tassel, nor did it affect the leaf phenotype, GA itself is not required for *fun* feminisation nor the leaf phenotype.

Hormone Control of Sex Determination in Maize

- summary and conclusions -

FUN clearly operates at some point in the sex determination pathway of *Zea mays* since the loss of function mutant is feminised in the tassel. This observation leads to the hypothesis that FUN has some role in the masculinisation of maize inflorescences. A pictorial summary of the double mutant tassel phenotypes is given in Figure 4-22, and a textual summary and interpretations of observations of the fun double mutants follow.

One observation is that *fun* mutants consistently have fewer branches than siblings with a wild-type copy of FUN. This is also true for double mutants with JA biosynthetic mutant *ts1* (Figure 4-14), JA elimination mutant *sk1* (Figure 4-12), BR perception mutant *bri1::RNAi* (Figure 4-5), BR hyper-responding mutant *bin2::RNAi* (Figure 4-10) and GA perception mutant *D9* (Figure 4-19). The loss of FUN causes reduction in tassel branches in all of these mutant backgrounds.

Branches are one of the earliest visible sex specific characters of a maize inflorescence. Branches occur at the base of the inflorescence and due to the

basipetal development of a maize inflorescence must therefore make the decision on how to develop long before the spikelet pair meristem develops. Since both *na2* and *sk1* have less branching in the tassel, it would appear that BR promotes tassel branching while JA inhibits it – this is surprising since although BR is associated with maleness, JA is also associated with maleness and branching is a male trait. This observation also prompts further study, since although we have some understanding of how the various hormones work at the floral level to define sex in maize (see Figure 4-126), the link between hormones, tassel branching and inflorescence sex has not been examined. *fun*, with both branch number and sex determination defects, could be operating at this stage of development. A cross to the ramosa branching mutants[100–102] might help explore this link.

Another sex trait that is feminised in *fun* mutants is tassel length. Though there is variability, *fun* mutants on average have shorter tassels than normal siblings. This is also true for double mutants with *ts1* (Figure 4-14, *bri1::RNAi* (Figure 4-5), *bin2::RNAi* (Figure 4-10) and *D9* (Figure 4-19). However, in the *sk1* background, tassel length is not consistently shorter in combination with the *fun* mutation (Figure 4-12). Further, addition of JA may rescue tassel length in *fun* plants (Figure 4-14B). Thus the presence of JA can limit the reduction of tassel length associated with the *fun* mutation, in this way FUN may be linked to the JA pathway.

While the BR pathway double mutants point to involvement in the BR pathway, it is not yet possible to rule out involvement in the GA pathway for FUN. A GA biosynthetic mutant (*i.e. d5*) abolish a BR biosynthetic mutant's (*i.e. na2*) ability to feminise a tassel[31], but chemical blocking of GA by PBZ did not disrupt the feminisation of the *fun* tassel (Figure 4-21). Further *fun*'s additivity with *na2* for height mirrors the additive height phenotype of the *d5*;*na2* double[31]. In summary, I believe FUN sits at an intersection between all of these discussed hormones and may function to regulate maize development at an early stage.

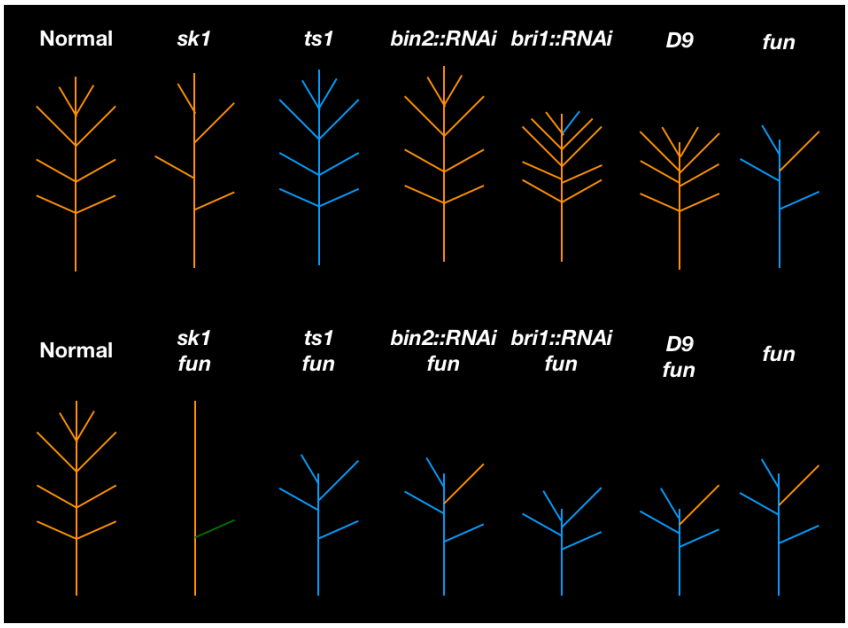

Figure 4-22: Summary of tassel phenotypes. Orange showing masculine inflorescence and/or branches; blue showing feminine; green showing intermediate (*sk1*;*fun* double). Normal tassel shown here with 8 branches; *sk1* has fewer branches than normal, but is same length; *ts1* is same length and has same branch number, but is femininsed; *bin2::RNAi* is same as normal tassel; *bri1::RNAi* is slightly shorter than normal, has more branches, and can show mild feminisation; *D9* is shorter than normal, but with the same number of branches; *fun* is shorter than normal, less branches and mostly feminised. The *sk1*;*fun* double mutant is as long as normal tassels, but has fewer branches than either the *sk1* or *fun* double mutant, further though the tassel is mostly masculine, there is evidence of intermediate sexual phenotypes in this double; the *ts1*;*fun* double mutant resembles a *fun* tassel, but is fully feminised; the *bin2::RNAi*;*fun* tassel resembles a *fun* tassel; the *bri1::RNAi*;*fun* tassel is shorter than either the *bri1::RNAi* or the *fun* tassel, has a similar number of branches to the *fun* tassel and is fully feminised; the *D9*;*fun* double tassel resembles a *fun* tassel but is shorter.

Chapter V

Characterising the FUN Gene by Bioinformatic and Molecular Approaches

Introduction

Genes of unknown function abound in many genomes. One of these genes has been called GRMZM2G323353 and *Zm*00001d039435, and has tentatively been assigned the name of FUN, as it will be referred to in the remainder of this work. FUN is homologous to an *Arabidopsis thaliana* gene known as AT3G58770, also of unknown function.

Methods

Publically Available Datasets and Computational Work

Datasets available for *Zea mays* at maizeGDB were used to ascertain if FUN RNA or protein was enriched in any genotypes, backgrounds or tissues in these plants. The FUN protein amino acid sequence* was entered into various online prediction tools to predict structure, localisation and function.

PSI-BLAST against the entire non-redundant database was used to collect divergent homologues of the FUN protein. In order to collect homologues from *Amborealla trichopoda*, the FUN protein was directly BLASTed against the *A. trichopoda* genome. In order to find similar proteins from *Arabidopsis thaliana*, the *Carica papaya* homologue (the only Brassicale to return a hit from the PSI-BLAST method starting with *Zm*FUN) was BLASTed against the *A. thaliana* genome. After collecting these protein sequences, a tree was built using MAFFT (available at https://mafft.cbrc.jp/alignment/server). A progressive method, G-INS-1, was used. In order to forgive gaps, the "unalign level" was put to 0.8 and the box "leave gappy regions" was selected.

RNA-seq and Y2H

Four-week-old shoot apices of *fun* homozygous plants and B73 plants were harvested from the greenhouse. Two pools of ten from each genotype were prepared for RNA-seq under the supervision of Katsutoshi Tsuda. The RNA-seq data was run through the TopHat pipeline[103] and viewed in IGV for SNP discovery. PCR was carried out using GoTaq or Phusion and Illumina sequencing was carried out by Quintara Bio. A full list of primers can be found in Appendix 2.

A pENTR clone containing the third and largest exon of FUN (or, GRMZM2G323353) was sent to Hybrigenics and used to carry out a yeast 2 hybrid (Y2H) assay against a library built from the cDNA of developing *Zea mays* tassels and ears. The results were run through the AgriGO GO term analysis, and were also converted to *A. thaliana* homologues (where available)

and put through the STRING interactome portal (https://string-db.org) to find known clusters of interacting genes in the dataset.

Protein localisation by YFP fusion

The FUN transcript, including all three exons, was cloned from B73 shoot tissue cDNA by Phusion using primers AV235 and AV239. This reaction used an annealing temperature of 60°C, an extension time of 1 minute 30 seconds, and 40 cycles. This PCR fragment was incubated with the pENTR mix provided by Thermo Fisher Scientific in a 3:1 insert:vector ratio for 5 minutes, before this mixture was used to transform *Escherichia coli* C3040 cells which were plated on LB agar + Kanamycin.

The resulting purified plasmid was sequenced using flanking primers and the FUN insert was found to be in the correct orientation and without mutations. 2000ng of plasmid was then cut using restriction enzyme *MluI* and gel purified. The cut plasmid was then used in an LR clonase reaction with an empty pEARLEYGATE-104 plasmid in a 3:1 insert:vector ratio and the entire reaction was used to transform *Escherichia coli* C3040 cells which were plated on LB agar + Kanamycin.

The resulting purified plasmid was sequenced using flanking primers and the FUN insert was found to be in the correct orientation. The plasmid was then transformed into *Agrobacterium* GV3103 cells which were plated on LB agar + Kanamycin + Gentamycin. 3ml cultures were grown overnight from resulting colonies. These cultures were spun down and the pellet resuspended in 3ml MES Competency Media (see Appendix 1). After shaking at room temperature for 3 hours, this suspension was diluted to 0.05 at OD_{600nm}. The diluted suspension was then infiltrated into young *N. benthamiana* leaves and the plants allowed to recover for 3 days.

The bacteria-infiltrated leaves were then infiltrated with a 300nM DAPI solution. The abaxial sides of the leaves were examined using a Leica DM4000B on the bright field, and 405nm and 514nm fluorescence channels (for DAPI and YFP visualisation, respectively). ImageJ was used to merge the resulting photos to line up YFP expression and DAPI stain in order to confirm nuclear expression.

Protein detection by antibody

The 3rd exon of FUN was cloned into pENTR and recombined using LR clonase into pDEST15, which encodes an Nterm 6xHis tag. FUN-pDEST17 was then used to transform Rosetta cells and a one-litre culture was grown, induced with IPTG and grown for 6 hours. The culture was then spun down and the pellet collected. Nickel beads were used to purify protein from the lysed cells and the protein was resuspended in 6M urea. This protein suspension was sent to Cocalico Biologicals where it was injected into guinea

pigs to produce antibody-containing sera. Concurrently, a FUN-pDEST17 plasmid was produced to create a GST-fusion of the FUN protein and antigenic FUN protein fragments. This was also transformed into Rosetta cells and the resulting protein was run over an anti-GST column to purify. Agarose beads were bound to the GST-fusion proteins and these were used to make columns to purify the guinea pig sera. The purified sera was used in a immunoblot on 12mm normal and *fun* tassels as well as for Western Blot on crude, nuclear and cytoplasmic extracts run on acrylamide gels.

Results

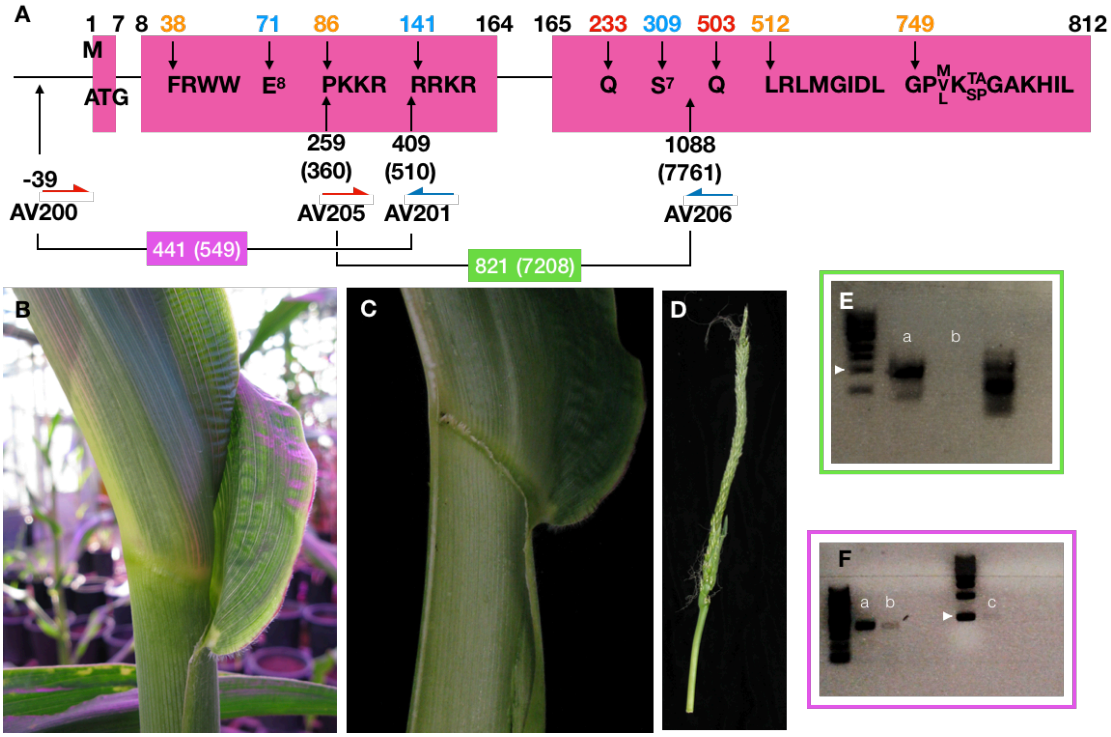

Figure 5-1: Gene Model of FUN.
FUN has 3 exons (A) and 812 amino acids. Sequences numbered in orange show the sequence as conserved in grasses and are also largely conserved across the Plant Kingdom (see also Figure 5-4B). Sequences numbered in blue highlight interesting features of the *Zm*FUN such as the predicted nuclear localisation sequence (141, see also Figure 5-5A), a string of 8 glutamic acids (71) and a string of 7 serines (309). Residues numbered in red show the glutamines that have been mutated to STOP codons in the two mutant alleles *fun-1* (233) and *fun-2* (503). Along the bottom of the gene sketch are shown primers used to amplify over the introns with their nucleotide numbers for coding sequence using the starting A of the sequence as number "1", genomic nucleotide numbers given in parentheses, length of fragment given in boxes. The *fun-2* allele has reduced auricle and expanded midrib (B) but retains the ligule (C) and shows feminisation in the tassel (D). E: Amplification using primers AV205 and AV206 spanning the first intron is possible in cDNA samples (a) but not gDNA (b); white arrow shows 1kb on ladder. F: Amplification using primers AV200 and AV201 spanning the second intron is possible in cDNA samples (a,b) and produces a larger fragment in gDNA (c); white arrow shows 500bp on ladder.

Cloning the Gene

At the beginning of my project, FUN had already been mapped to a 638,541bp region on chromosome 3S containing 22 gene models (v3) by Thant Niang under the supervision of George Chuck. RNA-seq was carried out on two pools of ten 4-week-old SAMs collected from B73 and fun homozygotes grown in the greenhouse. The RNA-seq data for this region was examined in IGV and a C>T transition in GRMZM2G323353 was revealed. This mutation results in 233Q>STOP[1] in the translated amino acid sequence (Figure 5-1A). This mutation was confirmed by PCR amplification and sequencing of this region by Illumina-seq. The only other mutation detected in this region was a C>T transition in an intron of the zinc-finger protein *Zm*DDB3 (GRMZM5G834596; Zm00001d039437).

A similar phenotype to *fun* was found in an EMS screen in the A619 inbred background (Figure 5-1B-D). Sequencing of GRMZM2G323353 in these individuals showed a C>T transition which would result in 503Q>STOP[**] (Figure 5-1A). An allelism test showed no rescue of the *fun* phenotype. This second allele was thus designated *fun-2*.

Updating of the MaizeGDB database to version 4 (v4) of the maize genome renamed GRMZM2G323353 as *Zm*00001d039435. *Zm*00001d039435 contains two more exons upstream of the single exon gene GRMZM2G323353 detailed in v3 of the maize genome. PCR of cDNA confirmed that these exons are present in the mRNA transcript (Figure 5-1E,F).

Publically Available Datasets and Computational Work

BLASTing the non-redundant maize genome with the FUN protein found partial homology to a region on chromosome 6, where chromosome 3 is known to have duplicates[104]. This region does not translate into a continuous peptide chain, which could mean that duplicates of this gene are punished by selection. BLAST retrieved closely conserved homologues to FUN across the grasses. With PSI-BLAST it was possible to collect homologues of FUN throughout the Plant Kingdom, including *Amborella trichopoda*, Rosids, Asterids and non-grass monocots. The resulting tree assembled by MAFFT from these proteins fell into the same distribution as the APG IV phylogeny[105], and is therefore assumed to be reliable (Figure 5- 2A). Alignment of the diverse family of FUN proteins revealed conserved regions (Figure 5-2B), including one of the regions predicted by NucPred to be involved in nuclear localisation, which may be important to the function of FUN. The conservation of FUN makes it likely to be an important gene in plant development in general. Though BLASTing of *Zm*FUN only found one hit in the Brassicales (*C. papaya*), using the *C. papaya* gene as a BLAST query returned more Brassicale hits, allowing the retrieval of

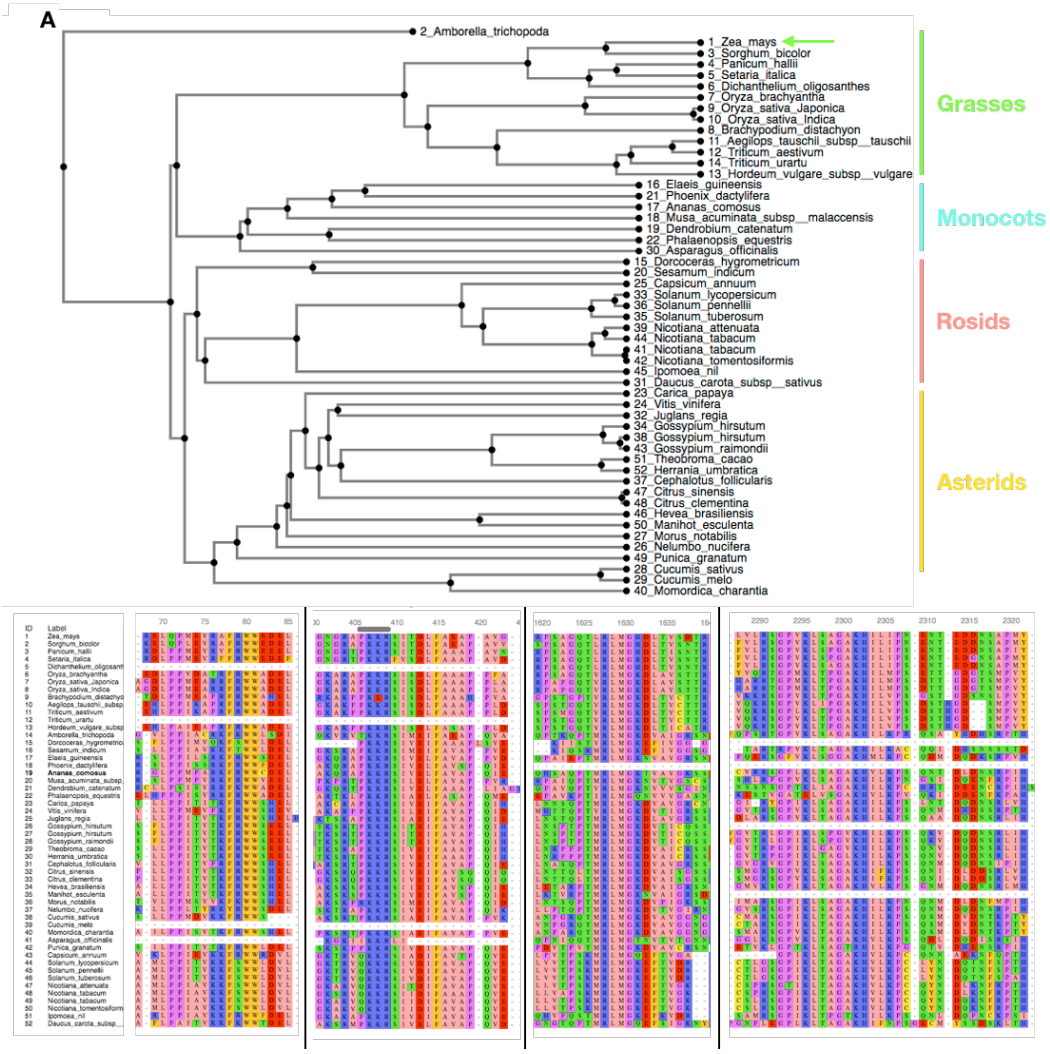

Figure 5-2. Tree from alignment of diverse FUN homologues across plants.
Amborella trichopoda as root (A), *Zm*FUN highlighted by green arrow. Highly conserved regions of the FUN protein as shown across plants coloured using the Zappo colour scheme (B), for summary see Figure 5-1A.

an *Arabidopsis thaliana* homologue. The Brassicales were found to have retained the FRWW, MRLM and KKR motifs, but not the GAKHIL motif (Figure 5-3).

RNA-seq datasets published by Stelpflug *et al*. tracking different stages of maize development[106] showed that the FUN transcript is highly expressed in the developing seed and endosperm. The next highest peaks (although dwarfed by the high expression detected in endosperm) were: developing leaves, especially the base; immature and meiotic tassels; and the immature and pre-pollination cob. FUN transcript was detected in all samples examined in Stelpflug *et al*.'s dataset (Figure 5-4A). Walley *et al*. collected transcript and protein from 23 developing maize tissues and mapped them to the v4 genome[107]. FUN was also examined in this data set, where the highest transcript reads were found in

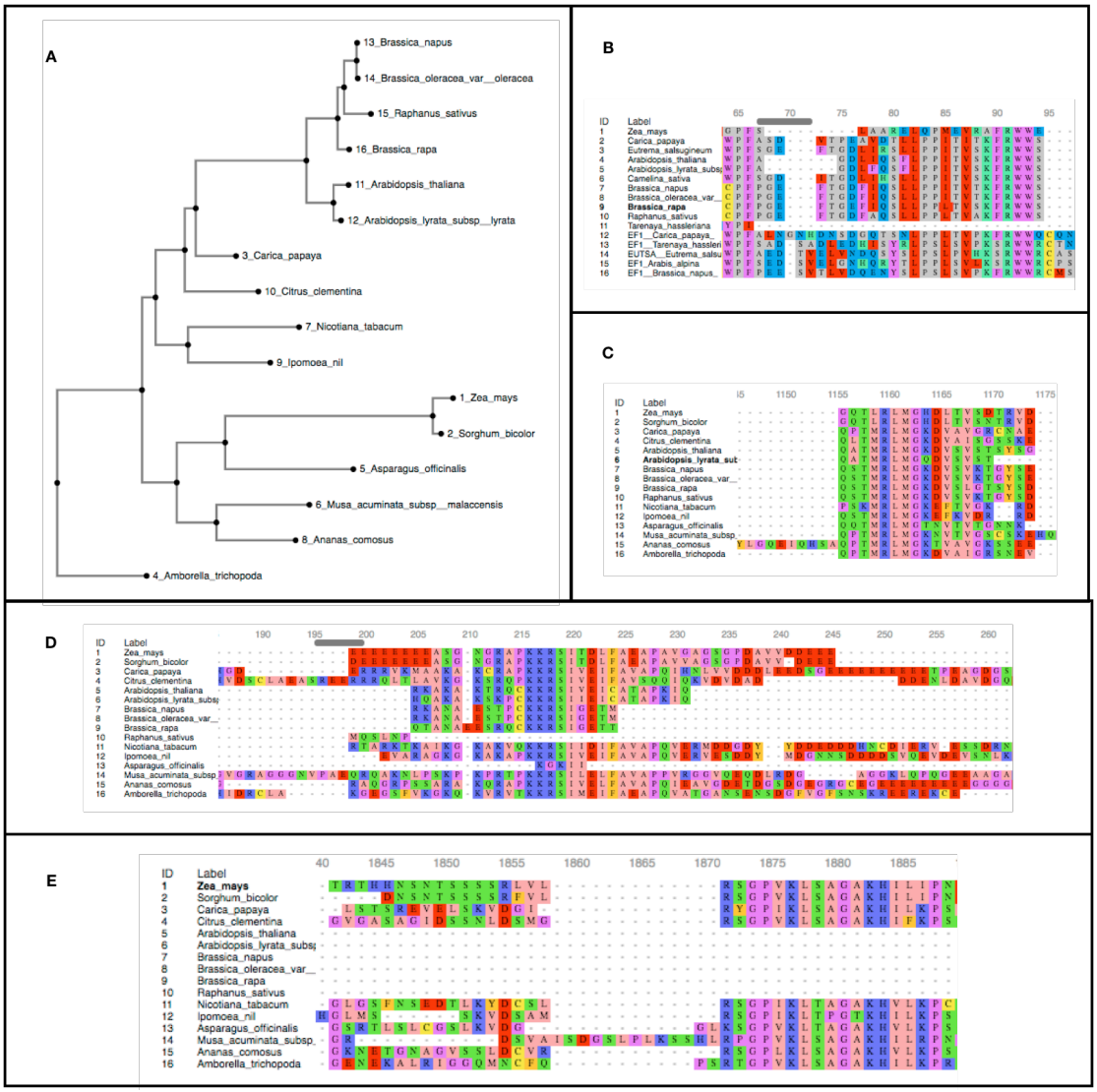

Figure 5-3: Tree and MSA including Brassicales. Tree (A) shows split between monocots and dicots, with *Amborella trichopoda* as an outgroup. FRWW motif (B), MLRM motif (C) and KKR motif (D) are all conserved in the Brassicales, while the GAKHIL domain (E) is found in grasses, monocots and dicots but not in the Brassicales (*Arabidopsis ssp*., *Brassica spp*. and *Raphanus sativus*).

developing leaves, and were much lower in mature leaves. Endosperm levels were still high, but not as extreme as seen in the dataset of Stelpflug *et al*. Unfortunately, immature tassels were not sampled, but strikingly, no FUN transcript was detected in mature pollen, unlike all other tissues sampled. Relatively high levels of FUN transcript were found in the female spikelet, as well as some in the silk (Figure 5-4B). The proteomic data mapped to v4 did not return anything for FUN, but mapped to v3, high levels of protein were found in the endosperm and the developing leaves, but not the mature leaf, nor any other tissues sampled (Figure 5-4C). No phosphorylated peptides were detected in any tissue sampled. Since these datasets were highly generalised, a dataset created specifically to query auricle development in maize was also used.

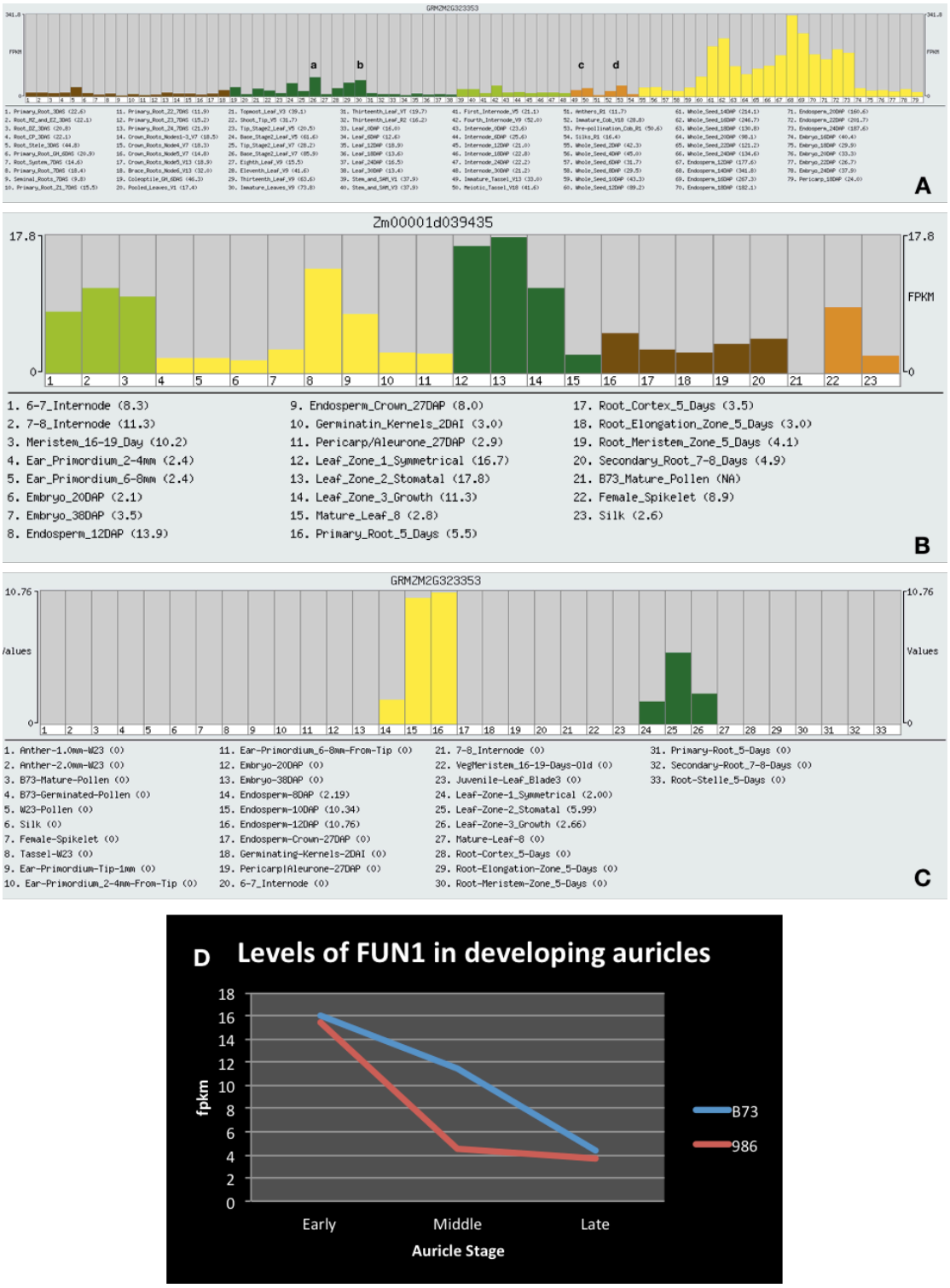

Figure 5-4: Publically available RNA-seq and proteomic data quantifying FUN
(A) Stelpflug *et al*. (2016) quantified transcript levels in 79 tissues. Base of stage 2 leaf at V7 is marked "a", immature leaves "b", immature tassel and meiotic tassel are marked "c", and immature cob and pre-pollination cob are marked "d". Yellow bars show various whole seed and endosperm samples these data are available at https://www.maizegdb.org/gene_center/gene/GRMZM2G323353. Walley *et al*. (2016) quantified transcript levels (B) and protein levels (C) in 23 tissues; these data are available at https://www.maizegdb.org/gene_center/gene/Zm00001d039435. Data provided by Gang Li show that transcript levels of FUN are found in young auricles and drop off faster in inbred 986 than in B73 (D).

A dataset created by Kong *et al*. compares developing B73 auricles with those of the inbred 986[108]. B73 has what can be considered normal auricles, while the auricles of 986 are much smaller (see Figure 5-4E). Developing auricle tissue was collected at three stages and RNA-seq libraries were made. According to Kong *et al*.'s dataset, FUN is found at equal levels in the early auricle of both B73 and 986. At mid auricle development, both B73 and 986 drop, but 986 is lower than B73. Both have dropped to low levels by late auricle development (Figure 5-2D). Thus, various RNA-seq datasets were used to give indications of where FUN localised at the macro level. Next, various software were used to predict where FUN localised at the subcellular level.

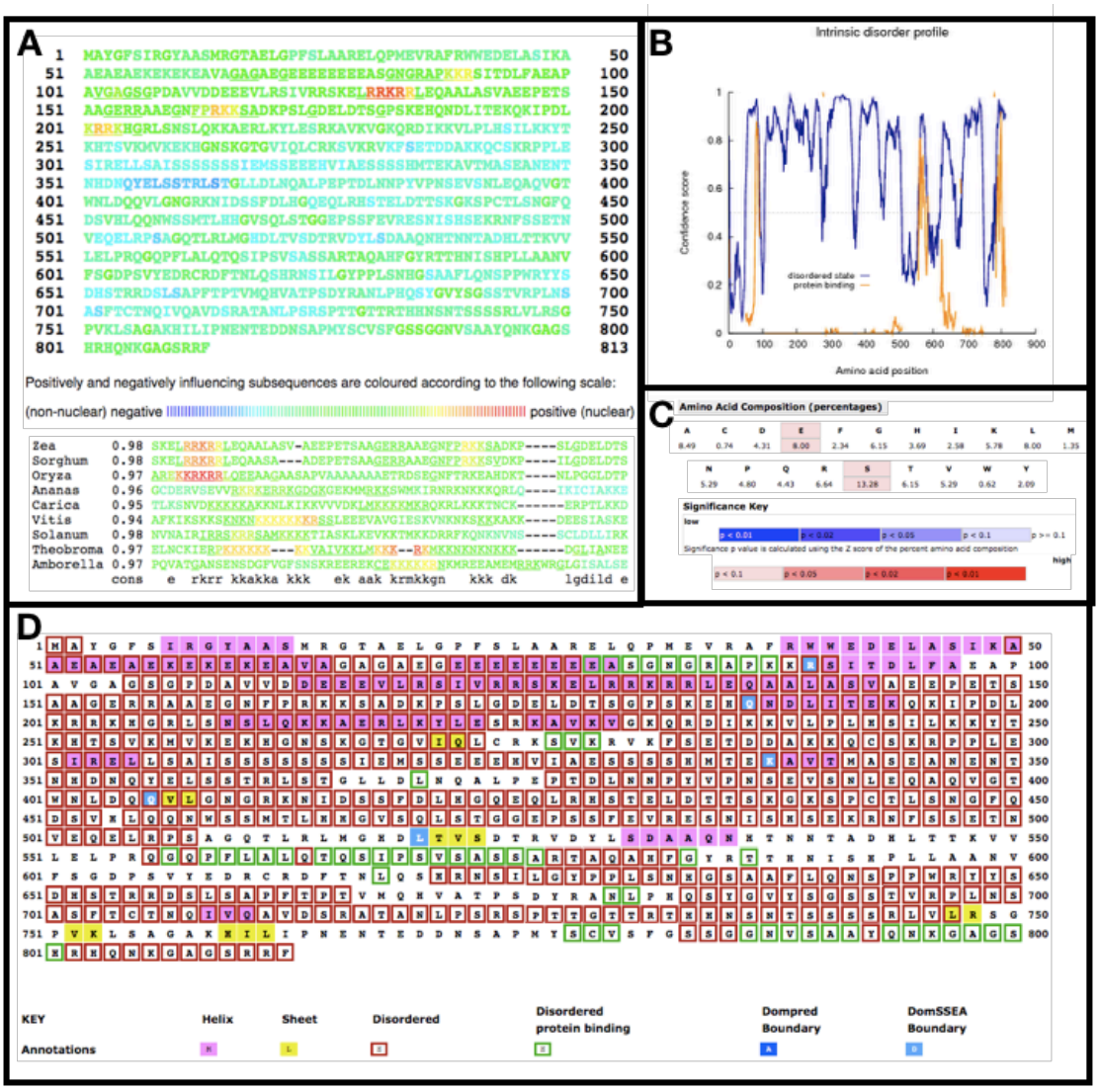

Figure 5-5: Bioinformatic protein predictions.
NucPred predicts that FUN is nuclear localised, largely due to a RRKR motif that is conserved in sorghum and rice (position 180) as well as a more highly conserved motif at position 86 (see also Figure 1A). Most of FUN is above the threshold (0.5 on *y* axis) for DISOPRED2 to predict it as disordered, and there are also parts that are likely to bind to proteins (B). Glutamic acid and serine are over represented in FUN (C), as shown by FFPred. A summary of the information generated by PSIPRED package is shown in D.

The entire FUN protein amino acid sequence was entered into NucPred, an online tool for prediction of nuclear proteins as well as PSORT, which predicts subcellular localisation given a protein sequence. The entire FUN protein sequence was entered into the PSIPRED prediction tool (available at http://bioinf.cs.ucl.ac.uk/psipred_new/), which runs multiple protein folding and interaction predictions to come to a synthetic prediction for the structure and function of a given protein sequence.

NucPred gave the FUN amino acid sequence a score of 0.98 on a scale of 0.1-1, with a score of 1 indicating certainty that the protein is nuclear (Figure 5-5A). The *k*-NN Prediction provided by the online program PSORT lists FUN as 91.3% likely to be nuclear and 8.7% likely to mitochondrial. FFPred, part of the PSIPRED package, also agreed that FUN is likely to nuclear.

FFPred also predicted that FUN is likely to be involved in DNA and RNA interactions, is likely to be involved in cytoskeletal and DNA binding, and has a high percentage of serines (13%) and glutmamic acid (8%; Figure 5-5C). DISOPRED, also part of the PSIPRED package, predicted that most of the FUN sequence can be defined as disordered, though the first 50 amino acids of FUN are not predicted to be disordered (Figure 5-5B,D).

In sum, FUN transcript is found in developing leaves and tassels, which fits with the phenotype of the mutant. FUN transcript is also found in developing ears, which is surprising since an ear phenotype was not observed. Higher levels of FUN during leaf development are associated with larger auricles. FUN is predicted to be a disordered protein that localises to the nucleus. Attempts were then made to validate these predictions.

Y2H, using the FUN protein as bait, and a cDNA library of immature ears and tassels as prey, retrieved a list of 234 possible interactors. Using the *A. thaliana* homologues of these proteins in a GO term biological process analysis found enrichment for proteins involved in negative regulation organ, specifically flower, development; and proteins involved in negative regulation of nucleic acid metabolic processes (Figure 5-6A). The *A. thaliana* homologues were enriched in transcription factor activity and hydrolase activity according to a GO term analysis based on molecular function (Figure 5-6B), and most of these predicted interacting partners were nuclear or cytosol localised. The GRMZM numbers were also run through the GO term analysis prediction software provided by AgriGO and were found to be enriched in GTP and GTPase binding (Figure 5-7B). A table of selected genes returned by the Y2H can be seen in Figure 5-7A. One such gene is *Zm*DWF1, (AKA: NANA2). This brassinosteroid synthesis protein was found to have a synergistic interaction in double mutant analysis with *fun* (Chapter 3). Another gene implicated in the brassinosteroids pathway was BSL1 that is known as an inhibitor of BRI1. The strongest confidence hit for the Y2H as an interactor for FUN was tubulin, but

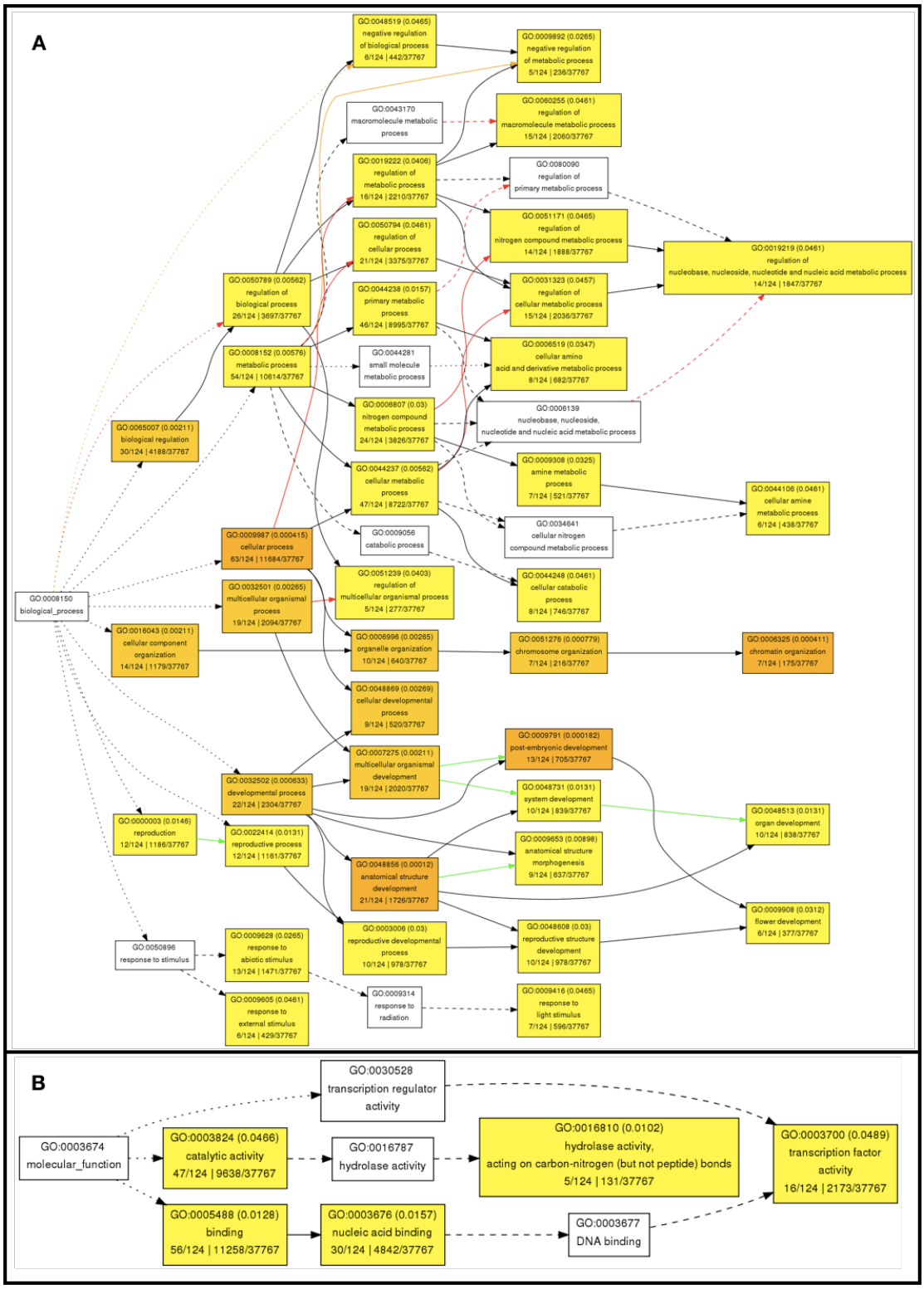

Figure 5-6: GO Term analysis using *Arabidopsis thaliana* homologues.
A: Biological processes. B: Molecular function. For key: see Figure 5-7C.

A

NCBI ID	GRMZM number	Descriptor	Protein Expression Zones				Arabidopsis Homologue
			Endosperm	Leaf Zone 1	Tassel	Other (Most Abundant)	
541827	GRMZM2G025592	DNA methyl transferase2	yes	yes	yes	Leaf Zone 2	AT1G69770.1
542129	GRMZM2G529859	yabby15	no	yes	yes	Immature Tasssel	AT2G45190.1
542549	GRMZM2G057000	nana plant2	yes	yes	yes	Root	AT3G19820.1
10019321(	GRMZM2G015861	actin-related protein like7	yes	yes	yes	Ear	AT3G60830.1
10019277	GRMZM2G028700	BRI1 suppressor 1 (BSU1)-like 2	yes	yes	yes	Vegetative Meristem	AT1G08420.1
10364060	GRMZM2G081158	ARF-transcription factor 34	yes	yes	no	Secondary Root	AT1G30330.2
10364830(	GRMZM2G146688	AP2-EREBP-transcription factor	no data	no data	no data	no data	AT4G37750.1
10365044	GRMZM2G074742	Aux/IAA-transcription factor 9	no data	no data	no data	no data	AT3G17600.1
542509	GRMZM2G321753	defective kernel1	no data	no data	no data	no data	AT1G55350.1
10027631(	GRMZM2G124288	Development and Cell Death domain	yes	yes	yes	Vegetative Meristem	AT2G32910.1
10027350	GRMZM2G116557	ARF-transcription factor 25	yes	no	no	Embryo	AT5G62000.1

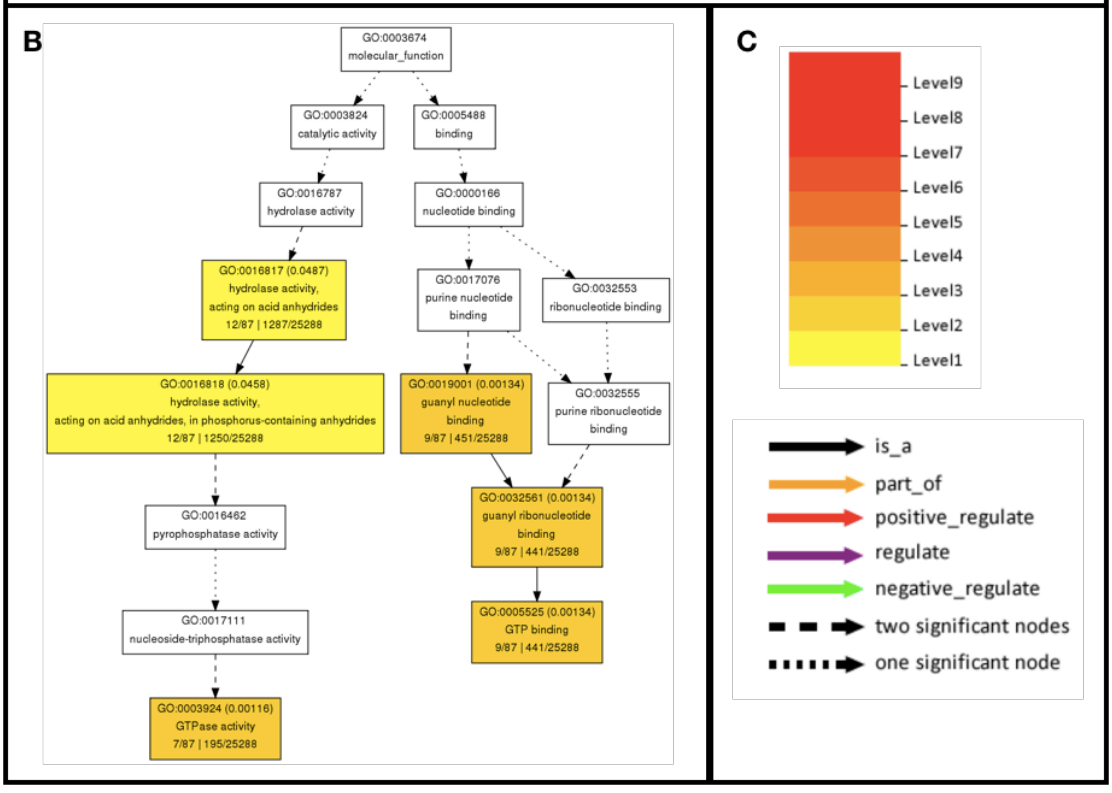

Figure 5-7
Selected predicted interaction partners for FUN by Y2H (A). GO term analysis for GRMZM numbers (B). Key for GO term analysis (C).

this may be a false positive due to the high concentration of this protein in a cell.

Wet Lab Validation

In order to test the idea that FUN is nuclear-localized, I carried out a transformation experiment using *Nicotiana benthamiana*. The entire FUN protein (*Zm*00001d039435) was fused to an N terminus YFP as described in Methods. The FUN-YFP fusion was found to localise to the nucleus in transformed *N. benthamiana* pavement cells. This result was observed in two separate transformations. Though not all nuclei in the samples were found to fluoresce under YFP excitation, this is likely due to imperfect transformation efficiency and is normal in this kind of experiment[109]. 25 nuclei expressing YFP were photographed and many more observed (Figure 5-8G,H) during the course of this experiment; YFP expression was not observed in any other subcellular regions.

In order to confirm that the YFP expression was nuclear, the leaves were also examined under 405nm excitation. Since the leaves had been infiltrated with DAPI prior to examination, this caused the DNA to fluoresce. YFP fluorescence was shown to overlap with this DAPI fluorescence (Figure 5-8B). As further confirmation, the sample was also examined under bright field and the YFP fluorescence was thus seen to overlap with clearly visible nuclei (Figure 5-8C). This was observed at the microscope, as well as by overlapping micrographs using ImageJ. Close inspection of individual transformed nuclei revealed a nuclear speckle pattern (Figure 5-8F).

In order to make an antibody to the FUN protein, the purified protein has to be injected into a living animal and the antibody produced must then be purified. To this end, the third exon of FUN (which at the time was thought to be the entirety of the protein) was amplified by primers 53xF/R (see Figure 5-9A) and cloned into pENTR. Recombining with pDEST17 was unsuccessful. I hypothesised that FUN may be toxic, which would explain why the expression plasmid would not grow, though pENTR would grow, so bacteria were grown at lower temperatures. This was also unsuccessful, so a smaller fragment (600bp) out of the exon was used, amplified from cDNA with primers An2F/R (see Figure 5-9A and Appendix 2). This 600bp fragment was successfully cloned into pDEST17. Interestingly, the other fragments attempted that contained the conserved GAKHIL motif did not clone into pDEST17 under the conditions used, which could imply a toxicity of this domain, since all fragments that did not contain the GAKHIL motif were successfully cloned.

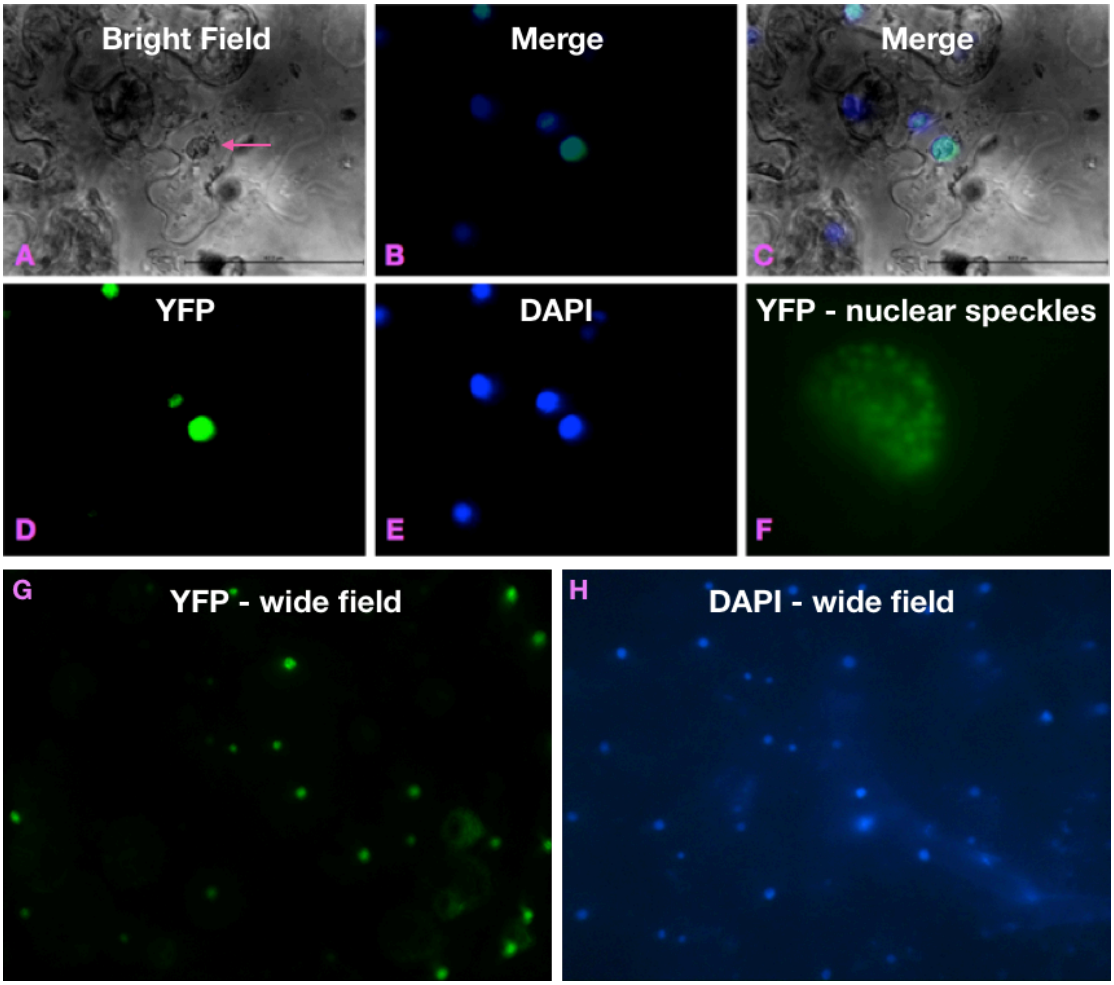

Figure 5-8: YFP expression in *Nicotiana benthamiana*.
Nuclei transiently expressing FUN-YFP fusion protein - A-E show the same field of view, scale bar is 62.2µm. A: *N. benthamiana* pavement cell under bright field (BF). D: 514nm fluorescent excitation (YFP excitation channel). E: 405nm fluorescent excitation (DAPI excitation channel). B: merge of images D and E. C: merge of images A and B. F: close up of nucleus under 514nm excitation. G and H show the same field of view under 514nm excitation (G) and 405nm excitation (H).

The newly made plasmid pDEST17-An2F/R was then cloned into Rosetta cells and grown into a 100ml culture overnight. This culture was used to spike 1 litre of fresh LB. After 4 hours of growth at 37°C this culture reached 0.42 OD_{600nm} and 200µl of 1M IPTG were added. This culture was then shaken at room temperature for 5 hours and spun at 8000 RCF for 15 minutes at 4°C. The resulting pellet was resuspended in 75ml of lysis buffer (see Appendix 1). This was spun at 12000 RCF for 15 minutes and the supernatant co-incubated with 2.5ml of 50% Ni++ beads in EtOH slurry. The beads were spun and washed several times using wash buffer (see Appendix 1) and were finally eluted using elution buffers (wash buffer equilibrated to given pH) at pH 4.4, 3.8 and 3

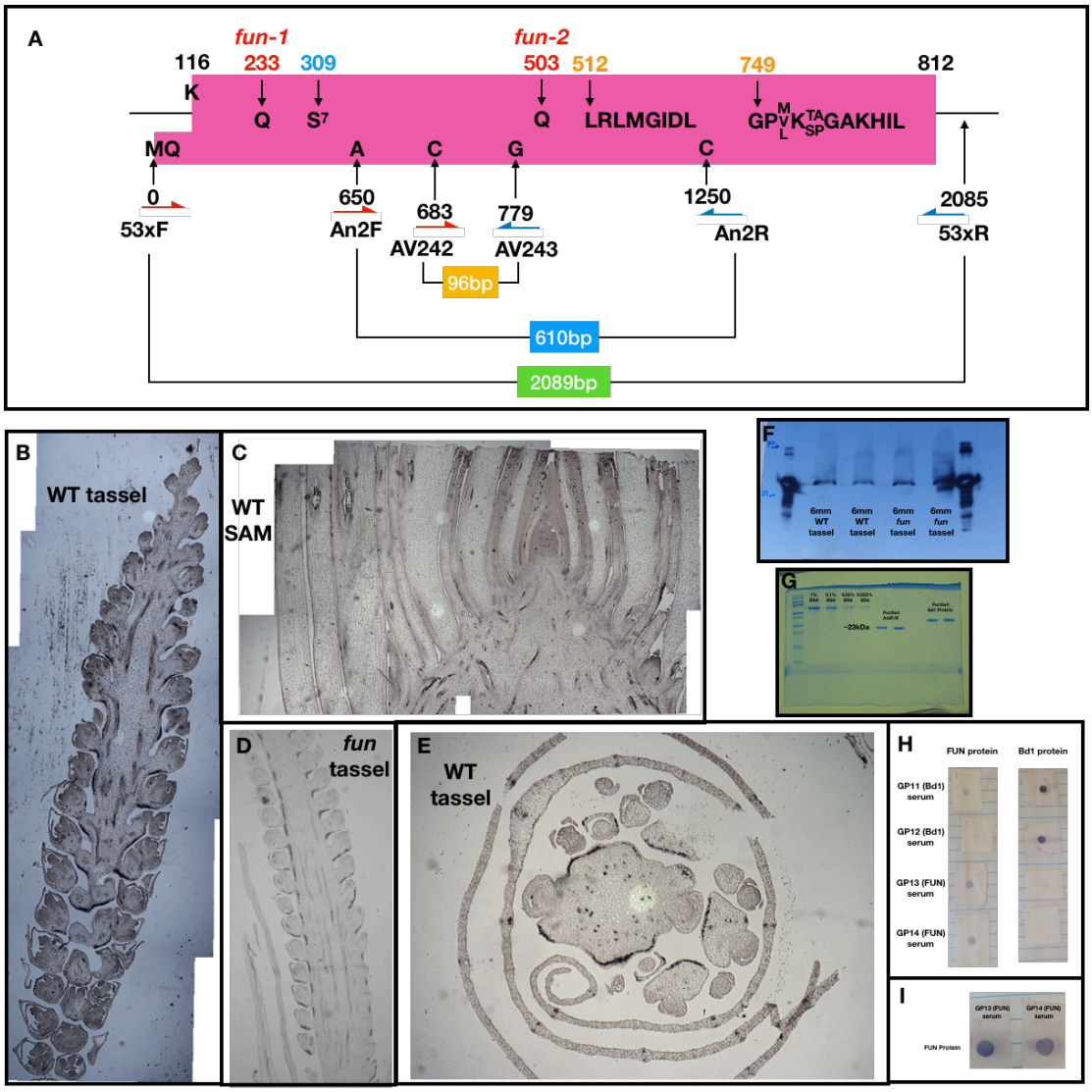

Figure 5-9: Antibody Creation and Application
A: Sketch of third exon of FUN (*cf.* Figure 5-1A). Nucleotides numbered according to GRMZM2G323353 (as opposed to full protein *Zm*00001d039435; see Figure 5-1), primers used for antibody creation and purification listed and marked. 12mm WT tassel (B), 4wk WT SAM (C), 12mm *fun* tassel (D), and 12mm WT tassel (E) stained with antibody purified from GP14. F: western using tassel protein and antibody GP14. G: acrylamide gel loaded with BSA, protein produced by An2F/R, An1F/R, and BD1. H: dot plot of recombinant FUN and BD1 protein probed by FUN and BD1 antibodies. I: FUN recombinant protein probed by primary bleeds of GP13 and GP14.

twice each. Most protein was recovered from the second pH 4.4 and first 3.8 elutions as measured by nanodrop. These samples were then run on an SDS gel (Figure 5-9G) and the correct size band was observed for An2F/R samples, but nothing was observed for An1F/R. Thus the protein produced by plasmid pDEST17-An2F/R was purified. It was then resuspended in 6M urea by dialysis in a side-A-lyser cassette and sent to Cocalico for injection into guinea pigs.

Test-bleeds and pre-bleeds were returned from the company. The pDEST17-An2F/R protein product was blotted onto nitrocellulose and incubated in 2ml of PBS with 2µl of test-bleed or 2µl of pre-bleed (as control) for 2 hours before

washing and incubating in PBS and anti-Guinea Pig Alkaline Phosphotase fusion antibody. Finally this was incubated in NETN (see Appendix 1) and NBT/BCIP to give an output of purple colour if the antibody is reacting to the protein (Figure 5-9I). Later, second bleeds were returned by the company, and this dot-blot process was repeated, along with the sera from another antibody (BD1) as a control (Figure 5-9H). Thus, it was confirmed that the guinea pigs were producing appropriate antibody.

In order to purify the terminal bleeds, a GST-tagged version of the protein was made. The pENTR-An2F/R was therefore combined with pDEST-15, transformed into Rosetta cells and induced and spun down as for the pDEST17-An2F/R purification step. This pellet was resuspended in NETN (see Appendix 1) and put through a French press twice at ~1000lbs of pressure before 2x 20s of sonication to shear DNA. Triton X-100 was then added to 0.5%. This cell lysate was then spun at 12,000 RCF for 15mins and the supernatant was added to 2ml of 50% glutathione-sepharose beads equilibrated in 10ml NETN. After co-incubation during which the GST-tagged protein should bind to the beads, the beads are spun down and washed several times with 0.2M Borate pH8. The washed beads are then transferred to a column and cross-linked to the beads using DMP solution (see Appendix 1) before washing with 0.1M glycine-Cl pH2.5 to remove non-covalently linked molecules and a final wash with 1xTBS (see Appendix 1).

The terminal bleeds were thawed and 1/10 volume 10xTBS (see Appendix 1) was added. This TBS-serum was then incubated in a column containing beads bound to GST for 30min at 4°C. Thus any antigens specific to GST that might be in the guinea pig sera would bind to these beads and the eluate from this column should be free of such contaminants. This eluate was incubated in the column described in the preceding paragraph and incubated at 4°C for 1 hour. Thus any antibodies specific to the FUN fragment should bind to these beads. The column was washed several times with TBS and 0.1 x TBS to remove any unbound molecules. Finally the column was eluted with 0.1M glycine-Cl pH2.5. 6ml of this 0.1M glycine-Cl pH2.5 was added to the column, and each sequential 800µl was collected separately. There were two guinea pigs (GP) murdered for this experiment designated 13 and 14. The 2nd elution for GP13 and the 3rd elution for GP14 had the highest concentrations of protein as measured by nanodrop.

Purified antibody GP14-3 was then used for immunoblots on a transverse section of normal immature tassel, cross section of normal immature tassel and on normal SAM tissue. Tissue was sectioned from wax using a microtome. Sections were laid on a slide, and the wax dissolved with Histoclear. Histoclear was then washed off with 100% EtOH and then the tissue was slowly rehydrated step-wise with lower concentrations of EtOH until finally pure water. The slides were then boiled in citrate buffer and left to stand for 10min. Slides were then incubated in PBS (see Appendix 1) and then blocking solution (see Appendix 1). Next, the slides were incubated in 2ml of blocking solution

and 2µl of antibody overnight, before incubating with the secondary antibody GP-AP, washing, and finally NETN (see Appendix 1) and NBT/BCIP. Slides were examined under a light microscope and signal was observed at the base of the pedicel in the longitudinal section (Figure 5-9B), and in the L2 in the transverse section (Figure 5-9E), of the tassel. A similar localisation pattern was observed by *in situ* for TS1 RNA[35]. No signal was observed in the longitudinal section of the SAM, though it is possible that there is signal at the base of the axillary meristem (Figure 5-9C). As a control, a longtitudinal section of a *fun* tassel was also used for an immunoblot (Figure 5-9D). A similar localisation pattern was observed in this mutant control as was seen in the normal tassel casting doubt on the reliability of the wild-type localisation patterns since the *fun* mutation causes a truncation of the protein before the region that the antibody was designed to (Figure 5-1A).

This apparent non-specificity prompted a western blot using antibody GP14-3. No band was observed at the predicted size of 90kDa, and a 30kDa band was observed in both mutant and normal samples (Figure 5-9F). Due to this lack of specificity, it was decided to make another antibody, using the entire third exon of FUN. The pENTR clone containing the 53xF/R insert was amplified by Phusion with primers AV53 and AV54 (see Appendix 2) to create a DNA fragment containing the third exon of FUN flanked by appropriate restriction sites. The fragment was then cut with XhoI and BamHI, purified by phenol:choloroform extraction and ligated into the His-tagged expression vector pet21. After verification by sequencing, this plasmid was transformed into Rosetta cells, grown in a 1L culture and induced with IPTG and purified with Ni++ beads as described above. This time, most protein was eluted at the 3rd pH3 elution. As before, this was dialysed into 6M urea and sent to Cocalico for injection into Guinea Pigs 15 and 16.

In a dot plot, the test bleeds from GP15 and 16 showed strong reactivity against the antigens sent to Cocalico, no reactivity with control purified Tru1 protein, and a little reactivity with purified Bd1 protein, possibly due to the His tag on this protein. The secondary bleeds showed similar results. Recombination of pENTR-53xF/R and pDEST15 was unsuccessful, so pgex5x-2, a GST-fusion expression plasmid, was used instead. pENTR-53xF/R was amplified by Phusion with primers AV63 and AV64 (see Appendix 1) for blunt end cloning. This PCR fragment was incubated with Polynucleotide Kinase (PNK) to remove phosphoryl groups at the 3' end and phosphorylate the 5' end. pgex5x-2 was cut with SmaI and incubated with Shrimp Alkaline Phosphotase to remove both 5' and 3' phosphate groups. The cut plasmid was then ligated to the PCR product with T4 ligase at 16°C overnight. Sequencing showed successful recombination, so the pgex5x-2-53xF/R plasmid was transformed into Rosetta cells and grown in a 1litre culture. This culture was induced with IPTG and made into a column, as described above. The pellet and supernatant of this Rosetta-pgex5x-2-53xF/R were used in a dot plot against an anti-GST antibody to test if the protein made was soluble, which it was (Figure 5-10C).

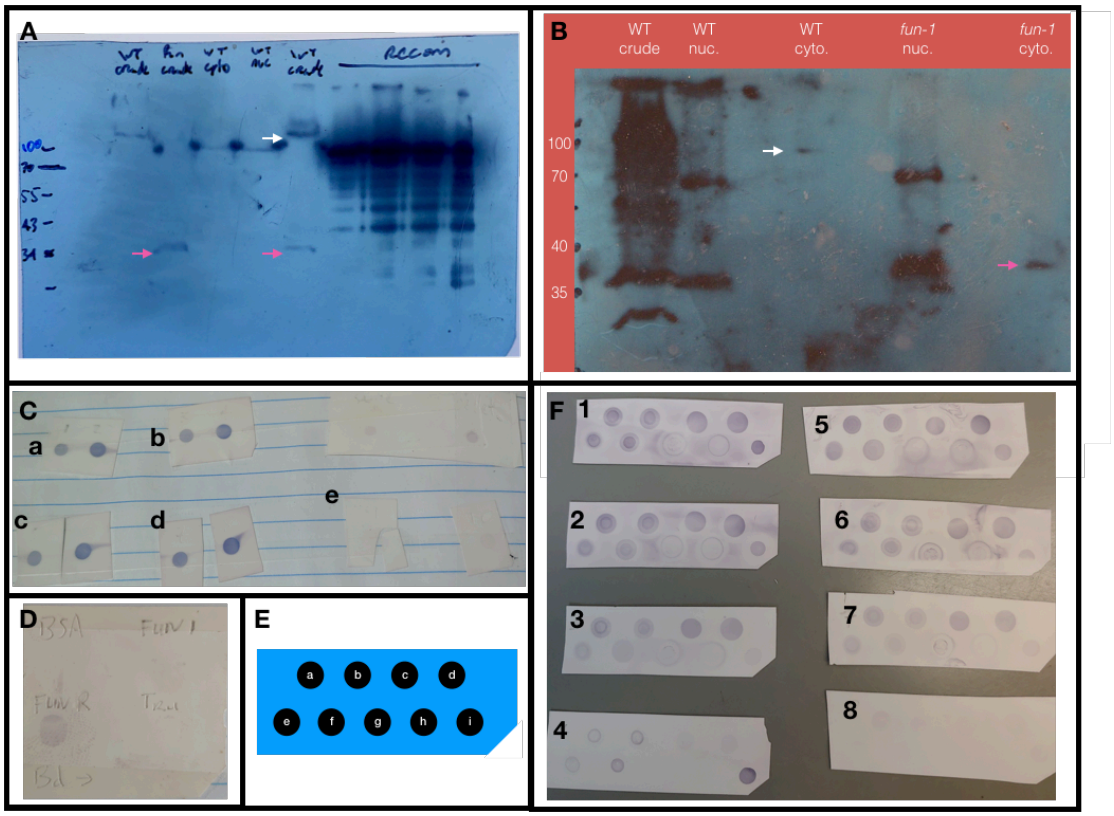

Figure 5-10: Testing GP15 and GP16 antibodies
Western with tassel extracts against purified GP16 serum (A), white arrow ~100kDa band in WT, pink arrow, ~34kDa band in *fun* and WT. Purified GP15 serum against nuclear and cytoplasmic extracts, WT cytoplasmic shows 90kDa band (white arrow), *fun* cytoplasmic shows 37kDa band (pink arrow) (B). C: solubility test for pgex5-2-xF/R recombinant protein (exon 3 + GST), each pair shows (left) supernatant and (right) pellet; probed with GP13 (a), probed with GP14 (b), probed with GP15 (c), probed with GP16 (d), probed with GP32 as negative control (e). FUN recomb protein and controls probed by dot plot with 3500 purified GP16 (D). E: key for panel F; two cultures of Rosetta with pDEST15-3500 prepared (1: a,e,c,g; 2:b,f,d,h) and were extracted with (a,b,c,d) and without (e,f,g,h) DTT; the pellet (a,b,e,f) and supernatant (c,d,g,h) were plotted along with GST (i) as a control. F: dotplots of pDEST15-3500 preps probed with GP13 serum (1), GP14 serum (2), 3500-purified GP16 (3), GP11 test bleed as negative control (4), purified GP13 elute 2 (5), purified GP14 elute 3 (6), 53xF/R purified GP16 (7), anti-GST (8).

The pgex5x-2-53xF/R column was then used to purify sera from GP15 and GP16 (to recap, this is entire 3rd exon serum purified against entire 3rd exon GST fusion). The purified serum was used in a western blot where it reacted strongly with recombinant FUN protein. This western also found a >100kDa band in WT crude extract which was not present in *fun* crude extract, and a ~34kDa band that was present in both WT and *fun* crude extract (Figure 5-10A). Crude extract of protein was carried out by grinding 2g of tissue in liquid nitrogen and adding 1ml of loading buffer (see Appendix 1), which was centrifuged before loading into gel. Nuclei and cytoplasmic extractions were carried out as follows. 2g of tissue was ground in liquid nitrogen and mixed with 1xNIB buffer with DTT; the mixture was filtered through microcloth and the filtrate centrifuged at 1260g at 4°C for 10 minutes. The supernatant was decanted and reserved as the cytoplasmic fraction. The pellet was resuspended in 2ml 1xNIB buffer with 10ul of 10% triton x-100 and protease inhibitors

before centrifuging at 1200g at 4°C for 10 minutes. The supernatant was discarded and the pellet resuspended in 0.5ml of JAJ-Extraction Buffer (Jazmin Juarez; see Appendix 1). This suspension was sonicated and centrifuged at 3000g at 4°C for 10 minutes – the resulting supernatant was reserved as the nuclear fraction.

Nuclear and cytoplasmic fractions were then run on an acrylamide gel and a western blot was carried out using the purified GP16 serum. A ~90kDa band was observed in the WT cytoplasmic fraction which is the correct size for full length FUN protein, and a ~37kDa band was observed in the *fun* cytoplasmic fraction. Both WT and *fun* nuclear fractions displayed a ~70kDa and ~37kDa band (Figure 5-10B). Western blots were then attempted using crude, nuclear and cytoplasmic fractions of protein extracted from *fun-2* plants, but none of these gels showed any bands (not shown) despite confirmation of protein presence in sample by probing with KN1 antibody (not shown). Other extraction procedures were carried out using triton, SDS, dodecyl maltosidase and IGEPAL detergents, but none of these westerns showed any bands (not shown).

In order to further purify the serum, primers AV242 and AV243 (see Appendix 2) were designed to a highly antigenic region of the protein predicted by antigen prediction software (Figure 5-9A). This 96bp product (PCR3500) was cloned into pENTR and recombined into pDEST15 using C3040 cells, which greatly improved transformation efficiency. pDEST15-3500 was cloned into Rosetta cells to purify protein and create a column as described above. This column was used to purify GP15 serum; the purified serum was found to react weakly to FUN-recombinant protein in a dot plot, but none of the controls (Figure 5-10D). 15 western blots were attempted using this purified serum, but none showed bands, or had high background such that any bands present would be obscured (not shown). Solubilising the 3500-GST construct before creating a column may help – a dot plot based on extractions solubilised with DDT showed that solubilisation greatly improved 3500-GST construct recovery from culture (Figure 5-10F).

Discussion

In summary, we can say that FUN is a conserved, universally expressed, disordered protein that localises to the nucleus. Cytoskeletal binding has been implied by both bioinformatic prediction programs and Y2H, as has involvement in nucleotide binding, especially RNA and GTPases.

The highly conserved nature of FUN across the grasses, and significant conservation across the Plant Kingdom, along with the mutant study presented in Chapter 1, make a compelling case for the importance of this protein in general plant growth and development. The nuclear localisation of FUN, along with its synergistic interaction with the transcription factor WAB1 (Chapter 2),

and its interactions with various hormone mutants (Chapter 3) suggest that FUN is involved at some stage in a signal transduction pathway between the hormones and downstream gene expression. The universal expression of FUN makes it unlikely that FUN can be considered a signalling molecule *per se*; instead it strengthens the hypothesis that FUN is involved in the transduction of these signals. On the other hand, there is evidence of variance in transcript levels (Figure 5-2) so there could be some merit to the idea that FUN is a real signal. Using Gene Ontology (GO) term analysis, it has been shown that disordered proteins are heavily biased toward signalling, regulation and control[110], strengthening the signalling network hypothesis. The disorder of FUN may also have contributed to the difficulty in creating a specific antibody. Many disordered proteins are thought to undergo conformational changes in order to transduce signals[110] and the high concentration of serines that could be phosphorylated (Figure 5-5C), as well as a serine repeat chain in FUN (Figure 5-1A), could allow these conformational change.

Despite the fact that the antibody was shown to be non-specific, and the same immunoblot pattern was produced in both normal and *fun* tassels (Figure 5-9B,D), the pattern of expression in the normal tassel fits the feminised tassel phenotype. Additionally, the expression pattern agrees with the nuclear localisation shown by YFP-fusion (Figure 5-8) and bioinformatic prediction (Figure 5-5). Thus the expression pattern could indeed be real.

Since both GO term analysis by FFPred agrees with the Y2H that tubulin interacts with FUN, and that nucleotide binding is likely for FUN, these avenues should not be ignored. While it is difficult to imagine how cytoskeletal binding could be important to the FUN protein's function in a signal transduction pathway, the importance of nucleotide binding in signalling needs no explanation. Intriguingly, one of the Y2H predictions is ricin, a protein that binds to ribosomes, which are of course rich in RNA. Though ricin is a deadly poison to animals, its presence in low levels in plant cells could indicate that it works as a regulator of ribosome function in plants, and has been co-opted by the infamous *Ricinus communis* that accumulates it in high concentrations in its beans, presumably as a defence mechanism.

Bibliography

1. Lewis, D. The Evolution of Sex in Flowering Plants. *Biol. Rev.* **17**, 46–67 (1942).

2. Jong, T. J. de, Shmida, A. & Thuijsman, F. Sex allocation in plants and the evolution of monoecy. *Evol. Ecol. Res.* **10**, 1087–1109 (2008).

3. MACHADO, I. C., LOPES, A. V. & SAZIMA, M. Plant Sexual Systems and a Review of the Breeding System Studies in the Caatinga, a Brazilian Tropical Dry Forest. *Ann. Bot.* **97**, 277–287 (2006).

4. Renner, S. S. The relative and absolute frequencies of angiosperm sexual systems: Dioecy, monoecy, gynodioecy, and an updated online database. *Am. J. Bot.* **101**, 1588–1596 (2014).

5. Bertin, R. I. Incidence of Monoecy and Dichogamy in Relation to Self-Fertilization in Angiosperms. *Am. J. Bot.* **80**, 557–560 (1993).

6. Bawa, K. S. Evolution of Dioecy in Flowering Plants. *Annu. Rev. Ecol. Syst.* **11**, 15–39 (1980).

7. Dinnetz, P. Male sterility, protogyny, and pollen-pistil interference in Plantago maritima (Plantaginaceae), a wind-pollinated, self-incompatible perennial. *Am. J. Bot.* **84**, 1588 (1997).

8. Rodríguez-Riaño, T. & Dafni, A. Pollen–Stigma Interference in Two Gynodioecious Species of Lamiaceae with Intermediate Individuals. *Ann. Bot.* **100**, 423–431 (2007).

9. Charlesworth, D. & Charlesworth, B. Population genetics of partial male-sterility and the evolution of monoecy and dioecy. *Heredity* **41**, 137–153 (1978).

10. Schlessmann, M. A. Major events in the evolution of sexual systems in Apiales: ancestral andromonoecy abandoned. *Plant Divers. Evol.* 233–245 (2010). doi:10.1127/1869-6155/2010/0128-0011

11. Reuther, K. & Claßen-Bockhoff, R. Andromonoecy and developmental plasticity in Chaerophyllum bulbosum (Apiaceae–Apioideae). *Ann. Bot.* **112**, 1495–1503 (2013).

12. Dorken, M. E. & Pannell, J. R. Hermaphroditic Sex Allocation Evolves When Mating Opportunities Change. *Curr. Biol.* **19**, 514–517 (2009).

13. Bertin, R. I. & Gwisc, G. M. Floral sex ratios and gynomonoecy in Solidago (Asteraceae). *Biol. J. Linn. Soc.* **77**, 413–422 (2002).

14. Onodera, Y., Yonaha, I., Niikura, S., Yamazaki, S. & Mikami, T. Monoecy and gynomonoecy in Spinacia oleracea L.: Morphological and genetic analyses. *Sci. Hortic.* **118**, 266–269 (2008).

15. Spigler, R. B. & Ashman, T.-L. Gynodioecy to dioecy: are we there yet? *Ann. Bot.* **109**, 531–543 (2012).

16. Barrett, S. C. H. Gender variation and the evolution of dioecy in Wurmbea dioica (Liliaceae). *J. Evol. Biol.* **5**, 423–444 (1992).

17. Poppendieck, H.-H. Monoecy and Sex Changes in Freycinetia (Pandanaceae). *Ann. Mo. Bot. Gard.* **74**, 314–320 (1987).

18. Interactions between tassel seed genes and other sex determining genes in maize - Irish - 1994 - Developmental Genetics - Wiley Online Library. Available at: https://onlinelibrary.wiley.com/doi/abs/10.1002/dvg.1020150206. (Accessed: 28th April 2019)

19. Martin, A. *et al.* A transposon-induced epigenetic change leads to sex determination in melon. *Nature* **461**, 1135–1138 (2009).

20. Geraldes, A. *et al.* Recent Y chromosome divergence despite ancient origin of dioecy in poplars (Populus). *Mol. Ecol.* **24**, 3243–3256 (2015).

21. Bräutigam, K. *et al.* Sexual epigenetics: gender-specific methylation of a gene in the sex determining region of Populus balsamifera. *Sci. Rep.* **7**, (2017).

22. Divashuk, M. G., Alexandrov, O. S., Razumova, O. V., Kirov, I. V. & Karlov, G. I. Molecular Cytogenetic Characterization of the Dioecious

Cannabis sativa with an XY Chromosome Sex Determination System. *PLOS ONE* **9**, e85118 (2014).

23. Hirata, K. Sex determination in hemp (Cannabis sativa L.). *J. Genet.* **19**, 65–79 (1927).

24. Feminized Seeds: What they are and the top methods used to produce them. *Ed Rosenthal* Available at: https://www.edrosenthal.com/the-guru-of-ganja-blog/feminized-seeds-the-top-methods-used-to-produce-them. (Accessed: 26th April 2019)

25. Jong, T. J. de, Nell, H. W. & Glawe, G. A. Heritable Variation in Seed Sex Ratio of the Stinging Nettle (Urtica dioica). *Plant Biol.* **7**, 190–194 (2005).

26. Glawe, G. A. & de Jong, T. J. Complex sex determination in the stinging nettle Urtica dioica. *Evol. Ecol.* **23**, 635 (2008).

27. Nickerson, N. H. Sustained Treatment with Gibberellic Acid of Five Different Kinds of Maize. *Ann. Mo. Bot. Gard.* **46**, 19–37 (1959).

28. Boualem, A. *et al.* A conserved mutation in an ethylene biosynthesis enzyme leads to andromonoecy in melons. *Science* **321**, 836–838 (2008).

29. Chailakhyan, M. K. & Timiriazev, K. A. Genetic and Hormonal Regulation of Growth, Flowering, and Sex Expression in Plants. *Am. J. Bot.* **66**, 717–736 (1979).

30. Manzano, S. *et al*. The role of ethylene and brassinosteroids in the control of sex expression and flower development in Cucurbita pepo. *Plant Growth Regul*. **65**, 213–221 (2011).

31. Best, N. B. *et al*. nana plant2 Encodes a Maize Ortholog of the Arabidopsis Brassinosteroid Biosynthesis Gene DWARF1, Identifying Developmental Interactions between Brassinosteroids and Gibberellins1[OPEN]. *Plant Physiol*. **171**, 2633–2647 (2016).

32. Minato, N. *et al*. The phytoplasmal virulence factor TENGU causes plant sterility by downregulating of the jasmonic acid and auxin pathways. *Sci. Rep*. **4**, 7399 (2014).

33. Liu, G. *et al*. Alterations of Mitochondrial Protein Assembly and Jasmonic Acid Biosynthesis Pathway in Honglian (HL)-type Cytoplasmic Male Sterility Rice. *J. Biol. Chem*. **287**, 40051–40060 (2012).

34. Lunde, C., Kimberlin, A., Leiboff, S., Koo, A. J. & Hake, S. Tasselseed5 overexpresses a wound-inducible enzyme, ZmCYP94B1 , that affects jasmonate catabolism, sex determination, and plant architecture in maize. *Commun. Biol*. **2**, 114 (2019).

35. Acosta, I. F. *et al*. tasselseed1 is a lipoxygenase affecting jasmonic acid signaling in sex determination of maize. *Science* **323**, 262–265 (2009).

36. DeLong, A., Calderon-Urrea, A. & Dellaporta, S. L. Sex determination gene TASSELSEED2 of maize encodes a short-chain alcohol

dehydrogenase required for stage-specific floral organ abortion. *Cell* **74**, 757–768 (1993).

37. Hayward, A. P. *et al*. Control of sexuality by the sk1-encoded UDP-glycosyltransferase of maize. *Sci. Adv.* **2**, e1600991 (2016).

38. Tsuchisaka, A. & Theologis, A. Unique and overlapping expression patterns among the Arabidopsis 1-amino-cyclopropane-1-carboxylate synthase gene family members. *Plant Physiol.* **136**, 2982–3000 (2004).

39. Silencing Gene Expression of the Ethylene-Forming Enzyme Results in a Reversible Inhibition of Ovule Development in Transgenic Tobacco Plants | Plant Cell. Available at: http://www.plantcell.org/content/11/6/1061. (Accessed: 26th April 2019)

40. Malepszy, S. & Niemirowicz-Szczytt, K. Sex determination in cucumber (Cucumis sativus) as a model system for molecular biology. *Plant Sci.* **80**, 39–47 (1991).

41. Rudich, J. & Halevy, A. H. Involvement of abscisic acid in the regulation of sex expression in the cucumber. *Plant Cell Physiol.* **15**, 635–642 (1974).

42. McAdam, S. A. M. *et al*. Abscisic acid controlled sex before transpiration in vascular plants. *Proc. Natl. Acad. Sci.* **113**, 12862–12867 (2016).

43. (PDF) The involvement of phytohormones in the plant sex regulation. Available at: https://www.researchgate.net/publication/271905900_The_involvement_of_phytohormones_in_the_plant_sex_regulation. (Accessed: 28th April 2019)

44. Transgenic Studies on the Involvement of Cytokinin and Gibberellin in Male Development. Available at: https://www.ncbi.nlm.nih.gov/pmc/articles/PMC166887/. (Accessed: 28th April 2019)

45. Gupta, R. & Chakrabarty, S. K. Gibberellic acid in plant. *Plant Signal. Behav.* **8**, (2013).

46. Saini, S., Sharma, I. & Pati, P. K. Versatile roles of brassinosteroid in plants in the context of its homoeostasis, signaling and crosstalks. *Front. Plant Sci.* **6**, (2015).

47. Reinbothe, C., Springer, A., Samol, I. & Reinbothe, S. Plant oxylipins: role of jasmonic acid during programmed cell death, defence and leaf senescence. *FEBS J.* **276**, 4666–4681 (2009).

48. Johnston, R. *et al.* Transcriptomic analyses indicate that maize ligule development recapitulates gene expression patterns that occur during lateral organ initiation. *Plant Cell* **26**, 4718–4732 (2014).

49. ORGAN INITIATION AND THE DEVELOPMENT OF UNISEXUAL FLOWERS IN THE TASSEL AND EAR OF ZEA MAYS - Cheng - 1983 - American Journal of Botany - Wiley Online Library. Available at: https://onlinelibrary.wiley.com/doi/abs/10.1002/j.1537-2197.1983.tb06411.x. (Accessed: 4th December 2018)

50. Dellaporta, S. L. & Calderon-Urrea, A. Sex determination in flowering plants. *Plant Cell* **5**, 1241–1251 (1993).

51. Sharman, B. C. Development of the Ligule in *Zea Mays* L. *Nature* **147**, 641 (1941).

52. Sylvester, A. W., Cande, W. Z. & Freeling, M. Division and differentiation during normal and liguleless-1 maize leaf development. *Development* **110**, 985–1000 (1990).

53. Walsh, J., Waters, C. A. & Freeling, M. The maize gene liguleless2 encodes a basic leucine zipper protein involved in the establishment of the leaf blade–sheath boundary. *Genes Dev*. **12**, 208–218 (1998).

54. Moreno, M. A., Harper, L. C., Krueger, R. W., Dellaporta, S. L. & Freeling, M. liguleless1 encodes a nuclear-localized protein required for induction of ligules and auricles during maize leaf organogenesis. *Genes Dev*. **11**, 616–628 (1997).

55. Becraft, P. W., Bongard-Pierce, D. K., Sylvester, A. W., Poethig, R. S. & Freeling, M. The liguleless-1 gene acts tissue specifically in maize leaf development. *Dev. Biol.* **141**, 220–232 (1990).

56. Foster, T., Hay, A., Johnston, R. & Hake, S. The establishment of axial patterning in the maize leaf. *Development* **131**, 3921–3929 (2004).

57. Lewis, M. W. *et al.* Gene regulatory interactions at lateral organ boundaries in maize. *Dev. Camb. Engl.* **141**, 4590–4597 (2014).

58. Walsh, J. & Freeling, M. The liguleless2 gene of maize functions during the transition from the vegetative to the reproductive shoot apex. *Plant J. Cell Mol. Biol.* **19**, 489–495 (1999).

59. Hay, A. & Hake, S. The Dominant Mutant Wavy auricle in blade1 Disrupts Patterning in a Lateral Domain of the Maize Leaf. *Plant Physiol.* **135**, 300–308 (2004).

60. Harper, L. & Freeling, M. Interactions of Liguleless1 and Liguleless2 Function during Ligule Induction in Maize. *Genetics* **144**, 1871–1882 (1996).

61. Osmont, K. S., Jesaitis, L. A. & Freeling, M. The extended auricle1 (eta1) Gene Is Essential for the Genetic Network Controlling Postinitiation Maize Leaf Development. *Genetics* **165**, 1507–1519 (2003).

62. Hartwig, T. *et al*. Brassinosteroid control of sex determination in maize. *Proc. Natl. Acad. Sci.* **108**, 19814–19819 (2011).

63. Chen, Y. *et al*. The Maize DWARF1 Encodes a Gibberellin 3-Oxidase and Is Dual-Localized to the Nucleus and Cytosol. *Plant Physiol.* pp.114.247486 (2014). doi:10.1104/pp.114.247486

64. Lunde Shaw, C. *Ts5 is due to an overexpression of a JA degrading enzyme*.

65. Phinney, B. O. GROWTH RESPONSE OF SINGLE-GENE DWARF MUTANTS IN MAIZE TO GIBBERELLIC ACID*. *Proc. Natl. Acad. Sci. U. S. A.* **42**, 185–189 (1956).

66. Rood, S. B., Pharis, R. P. & Major, D. J. Changes of Endogenous Gibberellin-like Substances with Sex Reversal of the Apical Inflorescence of Corn. *Plant Physiol.* **66**, 793–796 (1980).

67. Dellaporta, S. L. & Calderon-Urrea, A. The sex determination process in maize. *Science* **266**, 1501–1505 (1994).

68. Li, J., Biswas, M. G., Chao, A., Russell, D. W. & Chory, J. Conservation of function between mammalian and plant steroid 5alpha-reductases. *Proc. Natl. Acad. Sci. U. S. A.* **94**, 3554–3559 (1997).

69. Fujioka, S. *et al*. The Arabidopsis deetiolated2 mutant is blocked early in brassinosteroid biosynthesis. *Plant Cell* **9**, 1951–1962 (1997).

70. Li, J., Nagpal, P., Vitart, V., McMorris, T. C. & Chory, J. A role for brassinosteroids in light-dependent development of Arabidopsis. *Science* **272**, 398–401 (1996).

71. Chory, J., Nagpal, P. & Peto, C. A. Phenotypic and Genetic Analysis of det2, a New Mutant That Affects Light-Regulated Seedling Development in Arabidopsis. *Plant Cell* **3**, 445–459 (1991).

72. Klahre, U. *et al*. The Arabidopsis DIMINUTO/DWARF1 gene encodes a protein involved in steroid synthesis. *Plant Cell* **10**, 1677–1690 (1998).

73. Choe, S. *et al*. The Arabidopsis dwarf1 mutant is defective in the conversion of 24-methylenecholesterol to campesterol in brassinosteroid biosynthesis. *Plant Physiol*. **119**, 897–907 (1999).

74. Zhu, J.-Y., Sae-Seaw, J. & Wang, Z.-Y. Brassinosteroid signalling. *Dev. Camb. Engl*. **140**, 1615–1620 (2013).

75. Kir, G. *et al*. RNA Interference Knockdown of BRASSINOSTEROID INSENSITIVE1 in Maize Reveals Novel Functions for Brassinosteroid Signaling in Controlling Plant Architecture. *Plant Physiol*. **169**, 826–839 (2015).

76. Yamamuro, C. *et al*. Loss of function of a rice brassinosteroid insensitive1 homolog prevents internode elongation and bending of the lamina joint. *Plant Cell* **12**, 1591–1606 (2000).

77. Li, D. *et al*. Engineering OsBAK1 gene as a molecular tool to improve rice architecture for high yield. *Plant Biotechnol. J.* **7**, 791–806 (2009).

78. Morinaka, Y. *et al*. Morphological alteration caused by brassinosteroid insensitivity increases the biomass and grain production of rice. *Plant Physiol.* **141**, 924–931 (2006).

79. Li, J. & Nam, K. H. Regulation of brassinosteroid signaling by a GSK3/SHAGGY-like kinase. *Science* **295**, 1299–1301 (2002).

80. BIN2, a New Brassinosteroid-Insensitive Locus in Arabidopsis | Plant Physiology. Available at: http://www.plantphysiol.org/content/127/1/14.long. (Accessed: 5th February 2019)

81. Clouse, S. D., Langford, M. & McMorris, T. C. A Brassinosteroid-Insensitive Mutant in Arabidopsis thaliana Exhibits Multiple Defects in Growth and Development. *Plant Physiol.* **111**, 671–678 (1996).

82. Yan, Z., Zhao, J., Peng, P., Chihara, R. K. & Li, J. BIN2 functions redundantly with other Arabidopsis GSK3-like kinases to regulate brassinosteroid signaling. *Plant Physiol.* **150**, 710–721 (2009).

83. Kir, G. Regulation of shoot development in maize via brassinosteroid signaling. *Grad. Theses Diss.* (2015). doi:https://doi.org/10.31274/etd-180810-3931

84. Tong, H. *et al*. DWARF AND LOW-TILLERING acts as a direct downstream target of a GSK3/SHAGGY-like kinase to mediate brassinosteroid responses in rice. *Plant Cell* **24**, 2562–2577 (2012).

85. Emerson, R. A. (Rollins A. *et al*. summary of linkage studies in maize. (1935).

86. Sharman, B. C. Developmental Anatomy of the Shoot of Zea mays L. *Ann. Bot.* **6**, 245–282 (1942).

87. Emerson, R. Heritable Characters of Maize II.-Pistillate Flowered Maize Plants. *Agron. Hortic. -- Fac. Publ.* (1920).

88. Jones, D. F. HERITABLE CHARACTERS OF MAIZE. 4

89. Irish, E. E., Langdale, J. A. & Nelson, T. M. Interactions between tassel seed genes and other sex determining genes in maize. *Dev. Genet.* **15**, 155–171 (1994).

90. Zhao, Y. *et al*. Mapping and Functional Analysis of a Maize Silkless Mutant sk-A7110. *Front. Plant Sci.* **9**, (2018).

91. Jones, D. F. Unisexual Maize Plants and Their Bearing on Sex Differentiation in Other Plants and in Animals. *Genetics* **19**, 552–567 (1934).

92. Calderon-Urrea, A. & Dellaporta, S. L. Cell death and cell protection genes determine the fate of pistils in maize. *Development* **126**, 435–441 (1999).

93. Fujioka, S. *et al*. Qualitative and Quantitative Analyses of Gibberellins in Vegetative Shoots of Normal, dwarf-1, dwarf-2, dwarf-3, and dwarf-5 Seedlings of Zea mays L. 1. *Plant Physiol*. **88**, 1367–1372 (1988).

94. Spray, C. R. *et al*. The dwarf-1 (dt) Mutant of Zea mays blocks three steps in the gibberellin-biosynthetic pathway. *Proc. Natl. Acad. Sci. U. S. A.* **93**, 10515–10518 (1996).

95. Rademacher, W. Inhibitors of Gibberellin Biosynthesis: Applications in Agriculture and Horticulture. in *Gibberellins* (eds. Takahashi, N., Phinney, B. O. & MacMillan, J.) 296–310 (Springer New York, 1991).

96. Winkler, R. G. & Freeling, M. Physiological genetics of the dominant gibberellin-nonresponsive maize dwarfs, Dwarf8 and Dwarf9. *Planta* **193**, 341–348 (1994).

97. Lawit, S. J., Wych, H. M., Xu, D., Kundu, S. & Tomes, D. T. Maize DELLA Proteins dwarf plant8 and dwarf plant9 as Modulators of Plant Development. *Plant Cell Physiol*. **51**, 1854–1868 (2010).

98. Sun, T. Gibberellin-GID1-DELLA: A Pivotal Regulatory Module for Plant Growth and Development1. *Plant Physiol*. **154**, 567–570 (2010).

99. Hedden, P. The genes of the Green Revolution. *Trends Genet. TIG* **19**, 5–9 (2003).

100. McSteen, P. Branching Out: The ramosa Pathway and the Evolution of Grass Inflorescence Morphology. *Plant Cell* **18**, 518–522 (2006).

101. Gallavotti, A. *et al*. The control of axillary meristem fate in the maize ramosa pathway. *Development* **137**, 2849–2856 (2010).

102. RAMOSA Gene Network Influences Grain Architecture And Yield In Maize. *ScienceDaily* Available at: https://www.sciencedaily.com/releases/2008/06/080627163206.htm. (Accessed: 6th May 2019)

103. Trapnell, C. *et al*. Differential gene and transcript expression analysis of RNA-seq experiments with TopHat and Cufflinks. *Nat. Protoc.* **7**, 562–578 (2012).

104. Gaut, B. S. Patterns of Chromosomal Duplication in Maize and Their Implications for Comparative Maps of the Grasses. *Genome Res.* **11**, 55–66 (2001).

105. Chase, M. W. *et al*. An update of the Angiosperm Phylogeny Group classification for the orders and families of flowering plants: APG IV. *Bot. J. Linn. Soc.* **181**, 1–20 (2016).

106. Stelpflug, S. C. *et al*. An Expanded Maize Gene Expression Atlas based on RNA Sequencing and its Use to Explore Root Development. *Plant Genome* **9**, (2016).

107. Walley, J. W. *et al*. Integration of omic networks in a developmental atlas of maize. *Science* **353**, 814–818 (2016).

108. Li, G. *Personal Communication*. (2017).

109. Juarez, J. A. *Personal Communication*. (2017).

110. Oldfield, C. J. & Dunker, A. K. Intrinsically Disordered Proteins and Intrinsically Disordered Protein Regions. *Annu. Rev. Biochem.* **83**, 553–584 (2014).

Appendix 1 - Solutions

MES competency media

MES	10mM
MgCl2	10mM
Acetosyringone	200µM

DMP

Triethanolamine solution (Sigma T1377)	0.27ml
water	9ml
pH	to 8.3
dimethylpimelimidate-Cl	16mg

10x TBS

Tris base	12.114g
NaCl	43.83g
water	to 500ml
pH	to 7.5

Wash Buffer

NaH2PO4:H2O	2.1g
Tris base	0.18g
Urea	72g
water	to 150mls
pH	to 6.5

Lysis Buffer

NaH2PO4:H2O	0.7g
Tris base	0.06g
Guanidine hydrochloride	28.7g
water	to 50ml
pH	to 8.0

NETN

1M Tris HCl pH 7.5	5ml

4M NaCl	9.35ml
0.5M EDTA	0.5ml
water	to 250ml

JAJ Extraction Buffer

50mM Tris HCl pH 7.5	100ul
150mM NaCl	60ul
1% NP40	400ul
0.5% deoxychlorate	200ul
1x protease inhibitor	80ul
water	to 2ml

Appendix 2 - Primers

F Primer Name	F Primer Seq	R Primer Name	R Primer Seq	Length of WT product	PCR Notes	Lab Book Ref	Purpose
AV219	ATCAGGAACTAC TACCACGA	AV220	tgcaatgacaagggtattc atgtg	283bp	55 annеal, 2.5min extention, add 0.5% BSA to reaction	Book 4 pg 170	genotyping *nu2*
AV273	cacaggagattctgtactgt gaccaa	AV274	tgcaatgacaagggtattc atgtg	600bp	50 annеal, 1 min extension	Book 4 pg 168	genotyping *ts1*
AV63	CAGAAATCAGCT GACAAACC	AV64	TCAGAACCTACG GGAACC	1.5-2kb	Phusion; 66 annеal, 1 min extention	Book 3 pg 179	antibody (blunt cloning)
An2F	caccatgACCAGAT TGTCCACCg	An2R	tcaGGAAAGGCT GACCTTGTCGT	610bp	Phusion; 60 annеal, 1 min extention	Book 2 pg 75	antibody fragment
53xF	CACcATGCAGAA ATCAGCTGACAA ACCAAGTTTGG	53xR	TTCCTTCAAAAC ATGCAGCCTCTT GCCCAGCAGCT	2kb	Phusion; 69 annеal, 1:30 min extension	Book 2 pg 17	antibody fragment
AV235	CACCATGGCGTA CGGCTTCTC	AV239	TGCAGGCCACA AAACAAAACC	3kb	Phusion 60 annеal	Book 4 pg 114	Full length FUN for pENTR
AV53	attggatcccaagtttggg agatgaattgg	AV54	taactcgaggaacctacg ggaacctgctcct	2kb	Phusion 60 annеal	Book 3 pg 108	antibody fragment (pet21)
AV200	ATGGCGTACGGC TTCTCCAT C	AV201	GCTCCAGACGC CTCTTTCTT	409bp	55 annеal, 1min extention	Book 4 pg 57	Exon Validation
AV205	CCGAAGAAACG CTCCATCAC	AV206	ATCAAGCAAAC CGGTGGACA	849bp	60 annеal	Book 4 pg 57	Exon Validation

Appendix 3 – Mutant Identification

Mutant	Method of Detection	Phenotype	Primer F	Primer R	Length of Mutant Product	Length of WT Product	Restriction Enzyme	Mutant RE products	WT RE products
fun	rhAmp	feminised tassel, no auricle, narrow leaves	n/a	n/a	n/a	n/a	n/a	n/a	n/a
na2	PCR	feminised tassel, very short stature	AV219	AV220	2kb	283bp	n/a	n/a	n/a
ts1	Restriction Digest	feminised tassel	AV273	AV274	600bp	600bp	MluCI (Tsp509I)	600bp	400; 200 bp
Bri1	BASTA test	short stature, twisted leaves	n/a	n/a	n/a	n/a	n/a	n/a	n/a
Bin2	BASTA test	short stature, large auricle, long tassel, crenulated leaf margin	n/a	n/a	n/a	n/a	n/a	n/a	n/a
lg1	by phenotype	complete loss of ligule, partial ligule recovery on upper leaves	n/a	n/a	n/a	n/a	n/a	n/a	n/a
lg2	by phenotype	no ligule on lower leaves, partial recovery of ligule at margins, few tassel branches	n/a	n/a	n/a	n/a	n/a	n/a	n/a
Wab-1	by phenotype	large auricle, narrow leaves, ectopic auricle in blade	n/a	n/a	n/a	n/a	n/a	n/a	n/a
D9	by phenotype	short stature	n/a	n/a	n/a	n/a	n/a	n/a	n/a
eto	by phenotype	large auricle, short stature	n/a	n/a	n/a	n/a	n/a	n/a	n/a
sk1	by phenotype	loss of silks, increased tassel branching	n/a	n/a	n/a	n/a	n/a	n/a	n/a

BASTA test

20µl of Finale (containing 11.3% glufosinate-ammonium) and 1µl of 10% Tween were added to 1ml water. This solution was applied to a 1cm wide patch on a young maize leaf and circled with Sharpie. 5-7 days later the leaves were scored for response. Localised cell death visible by browning and dessication indicated non-resistance (*i.e.* does not contain the resistance gene/insert/transgene), while no response (area stays green and healthy) indicates resistance (*i.e.* contains the resistance gene/insert/transgene).

rhAmp

The *fun-1* and WT sequences were submitted to Integrated DNA Technologies (IDT; www.idtdna.com) for design of rhAmp primers. rhAmp primers bind different flourophores based on the SNP in question. The protocol provided by IDT was followed and qPCR machine was used to read the plates.